RESEARCH LABORATORIES FOR THE ENGINEERING SCIENCES

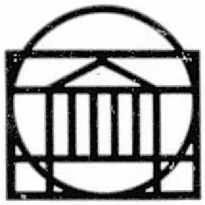

SCHOOL OF ENGINEERING AND APPLIED SCIENCE

University of Virginia

Charlottesville, Virginia 22901

EFFECTS OF SIMULATED TURBULENCE ON AIRCRAFT HANDLING QUALITIES

Technical Report

Grant No. NGR 47-005-208(4)

Submitted to:

National Aeronautics and Space Administration
Scientific and Technical Information Facility
P. O. Box 8757
Baltimore/Washington International Airport
Baltimore, Maryland 21240

Submitted by:

Ira D. Jacobson

and

Dinesh S. Joshi

Report No. UVA/528066/ESS77/106

March 1977

EFFECTS OF SIMULATED TURBULENCE ON AIRCRAFT HANDLING QUALITIES

Technical Report

Grant No. NGR 47-005-208(4)

Submitted to:

National Aeronautics and Space Administration
Scientific and Technical Information Facility
P. O. Box 8757
Baltimore/Washington International Airport
Baltimore, Maryland 21240

Submitted by:

Ira D. Jacobson

and

Dinesh S. Joshi

Department of Engineering Science and Systems
RESEARCH LABORATORIES FOR THE ENGINEERING SCIENCES
SCHOOL OF ENGINEERING AND APPLIED SCIENCE
UNIVERSITY OF VIRGINIA
CHARLOTTESVILLE, VIRGINIA

Report No. UVA/528066/ESS77/106

March 1977

Copy No. 1

ABSTRACT

The results of an investigation of the influence of simulated turbulence on aircraft handling qualities is presented. Pilot opinions of the handling qualities of a light general aviation aircraft were evaluated in a motion-base simulator using a simulated turbulence environment. A realistic representation of turbulence disturbances is described in terms of rms intensity and scale length and their random variations with time. The time histories generated by the proposed turbulence models showed characteristics which appear to be more similar to real turbulence than the frequently-used Gaussian turbulence model. In addition, the proposed turbulence models can flexibly accommodate changes in atmospheric conditions and be easily implemented in flight simulator studies.

Six turbulence time histories, including the conventional Gaussian model, were used in an IFR-tracking and a landing approach task. The realism of each of the turbulence models and the handling qualities of the simulated airplane were evaluated. Analyses of pilot opinions show that at approximately the same rms intensities of turbulence, the handling quality ratings transit from the satisfactory level, for the simple Gaussian model, to an unacceptable level for more realistic and compositely structured turbulence models.

TABLE OF CONTENTS

LIST OF TABLES

LIST OF FIGURES

NOMENCLATURE

$a(t)$	Gaussian random process
$b(t)$	Gaussian random process
b	wing span
c	Rayleigh distribution parameter
$c(t)$	modified Bessel process
$d(t)$	Gaussian random process
f	frequency in cps
G_i	filter transfer function of i^{th} component (i = u, v, w)
h	altitude
I_x, I_y, I_z	moment of intertia in body axes
L_i	turbulence scale length in i^{th} direction (i = u, v, w)
m	mean
m_n	n^{th} normalized central moment
R_{ij}	cross correlation function
R_{ii}	autocorrelation function
R	standard deviation ratio
s	standard deviation
S	wing area
T	time period
u	longitudinal gust velocity
v	lateral gust velocity
w	vertical gust velocity
$\dot{w}$	derivative of vertical gust velocity
$\bar{u}$	mean of u

σ_i	variance of i = u, v, w
ϕ_{ij}	cross spectral density
ϕ_{ii}	power spectral density
ϕ_0	white noise
ω	frequency in rad/sec

SECTION I

INTRODUCTION

Simulated time histories of aircraft motion in a turbulence environment are required in a variety of engineering applications, and their use appears to be increasing as more intricate and sophisticated design studies are attempted. As an example, the use of flight simulators for the study of airplane handling and ride quality has proven to be more valuable when disturbances in the form of artificially simulated turbulence are introduced into the system. Several methods have been used to generate turbulence signals; each one aimed at realizing the actual atmosphere as closely as possible. A realistic representation of turbulence becomes especially important in the simulation of future aircraft with high sensitivity to turbulence, as even light to moderate turbulence may seriously degrade their controllability and ride quality. Low altitude atmospheric turbulence critically affects the evaluation of vehicle handling qualities, pilot work load, ride quality, and other design factors. Several empirical studies (1,2,3) have shown that low altitude, clear air atmospheric turbulence is only locally isotropic, i.e., isotropic over a finite range of scale lengths. The proposed gust model accounts for the anisotropy of typical low altitude clear air turbulence by randomly varying the rms velocities and scale length of the gust field. The scale lengths predicted by either the Von Karman or the Dryden models (4) are large compared to real atmospheric turbulence and hence the scale length distribution is modified to achieve compatibility.

With a suitable combination of scale length and intensity distribution, the proposed model will simulate various atmospheric conditions characterized by altitude, stability, and terrain. This new model is mechanized to be included in a flight simulator experiment in order to determine to what extent the pilots are sensitive to changes in atmospheric conditions and the realism of the model. The flight simulator experiment is conducted for two sets of landing conditions. The first requires the pilot to follow an IFR-tracking task with no out-the-window cues provided. In the second condition the simulator is equipped with a visual display which provides a realistic landing approach scene. The following chapters describe the proposed turbulence model and the flight simulator experiment in detail.

SECTION II

LITERATURE SURVEY

In this chapter statistical properties of atmospheric turbulence are reviewed and presently-used simulation techniques are discussed. A review of basic definitions in probability and statistics is included in Appendix A.

2.1 Properties of Atmospheric Turbulence

Simulations of aircraft flying through atmospheric turbulence require a realistic model of the physical environment. Therefore, simulation studies in general begin with a study of the real atmosphere. In references 1-3, atmospheric data have been reported characterizing various atmospheric conditions for variation in terrain, stability, altitude, temperature, time, season, and geographic location. This data has been suitably modified to establish a basis of comparison for the simulated turbulence field.

The following criteria are used as the bases of comparison:

a) Output Statistics

Mean and standard deviations of the gust velocities.

b) Probability Distribution

Cumulative probability

Probability density

Fourth and sixth normalized moments

c) Patchiness of the Field

d) Power Spectral Density

e) Element of Surprise

Each of these properties will be discussed from the standpoint of real atmospheric turbulence.

Mean: Analysis of several sets of data presented in Reference (1) indicates that the mean velocity of atmospheric turbulence is 0.0 ± 0.1 ft/sec (0 ± 0.03 m/sec).

Standard Deviation: The standard deviation of the velocity field for low altitude clear air turbulence is 3.0 ± 1.31 ft/sec (0.91 ± 0.4 m/sec). Typical values for various conditions are listed in Reference (4) as:

σ_u = 2 ft/sec (0.61 m/sec) for light turbulence

σ_u = 4 ft/sec (1.22 m/sec) for moderate turbulence

σ_u = 6 ft/sec (1.82 m/sec) for severe turbulence

where u is the longitudinal gust component.

Probability Distribution: The probability distribution of a random process provides information concerning the range of values assumed by that function and the frequency with which they occur. As there is little experimental data available which distinguishes between probability distributions of different gust components, no distinction will be made here.

Probability Density Distribution: Figure 1 presents data from Reference (5) showing a typical probability density distribution of atmospheric turbulence velocity. The departure from the Gaussian curve clearly indicates increased probabilities of large and small gusts.

Normalized Central Moments: The fourth and sixth moments of low altitude real atmospheric turbulence are $M_4 = 3.5$ and $M_6 = 21.7$, respectively. (5)

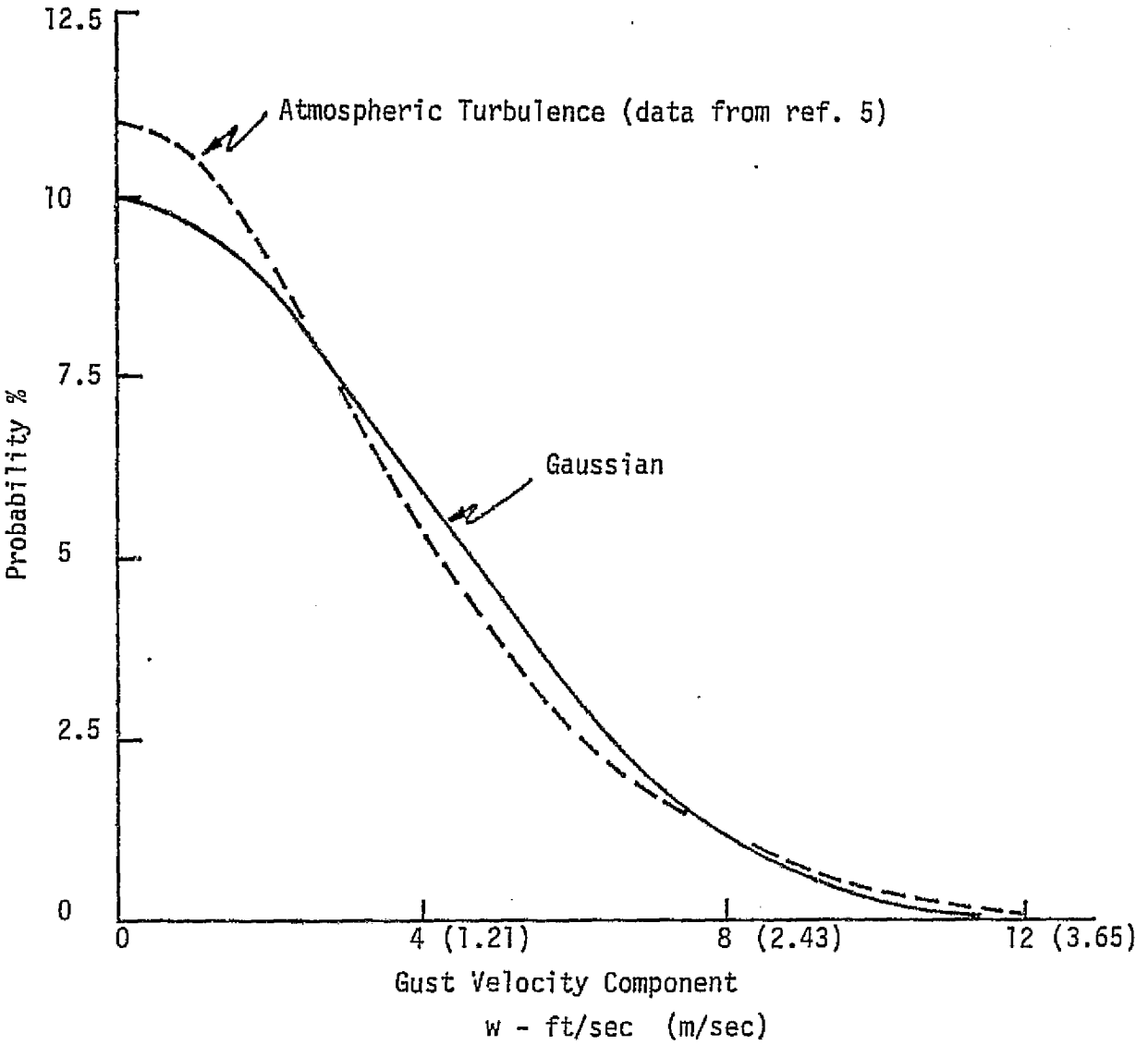

Figure 1 Typical Probability Density Function of Atmospheric Turbulence

Patchiness: It is known that turbulence has a non-Gaussian patchy structure which seems to occur in bursts of relatively intense motion separated by areas of relative calm. Figure 2 shows typical patchy characteristics for a 40-sec sample of real atmospheric turbulence.

Power Spectral Density (PSD): The PSD of a random process provides information on the average contribution to the process from the frequency components which make it up. Figure 3 presents a typical plot of PSD of low altitude clear air atmospheric turbulence. It may be observed that at high frequencies, the spectral density varies as inverse square of frequency (ω^{-2}). On the other hand, at low frequencies the PSD is characterized by a horizontal asymptote. Two convenient mathematical forms are used to represent the power spectra of atmospheric turbulence. These are:

a) Von Karman Spectra

$$\phi_u(\omega) = \frac{\sigma_u^2 L_u}{\pi u_0} \frac{2}{\left[1 + \left(1.339 \frac{L_u \omega}{u_0}\right)^2\right]^{5/6}} \tag{2.1.1}$$

$$\phi_v(\omega) = \frac{\sigma_v^2 L_v}{\pi u_0} \frac{1 + \frac{8}{3}\left(1.339\, L_v \omega/u_0\right)^2}{\left[1 + \left(1.339\, L_v \omega/u_0\right)^2\right]^{11/6}} \tag{2.1.2}$$

$$\phi_w(\omega) = \frac{\sigma_w^2 L_w}{\pi u_0} \frac{1 + \frac{8}{3}\left(1.339\, L_w \omega/u_0\right)^2}{\left[1 + \left(1.339\, L_w \omega/u_0\right)^2\right]^{11/6}} \tag{2.1.3}$$

and

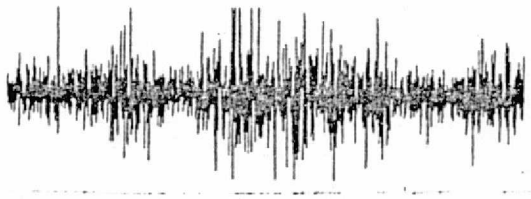

Figure 2 Typical Patchy Nature of Atmospheric Turbulence (6)

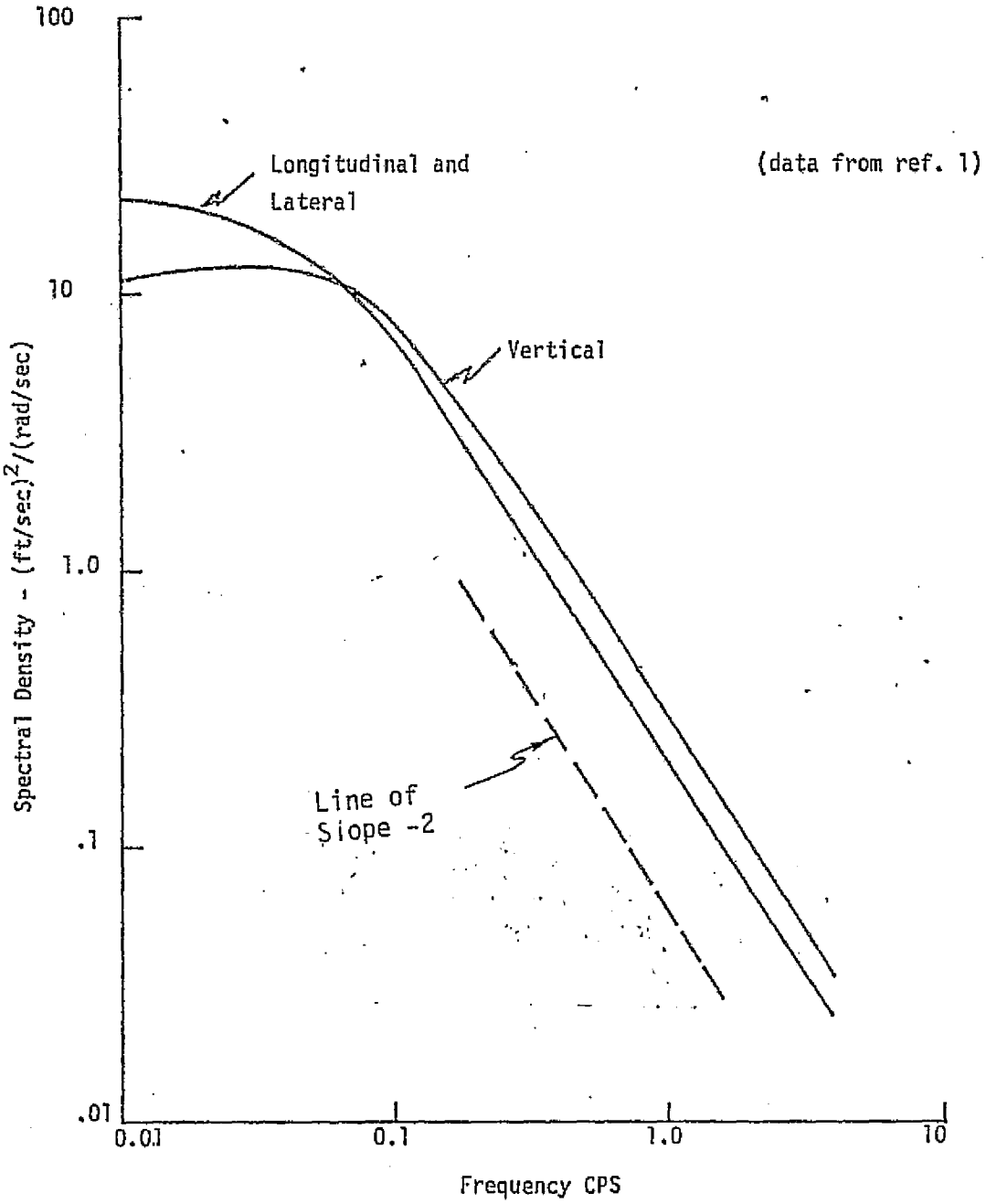

Figure 3 Typical Plot of PSD of Atmospheric Turbulence

b) Dryden Spectra

$$\phi_u(\omega) = \frac{\sigma_u^2 L_u}{\pi u_0}\left(\frac{2}{1 + \left(\frac{L_u\omega}{u_0}\right)^2}\right) \tag{2.1.4}$$

$$\phi_v(\omega) = \frac{\sigma_v^2 L_v}{\pi u_0}\left(\frac{1 + 3(L_v\omega/u_0)^2}{\left[1 + (L_v\omega/u_0)^2\right]^2}\right) \tag{2.1.6}$$

$$\phi_w(\omega) = \frac{\sigma_w^2 L_w}{\pi u_0}\left(\frac{1 + 3(L_w\omega/u_0)^2}{\left[1 + (L_w\omega/u_0)^2\right]^2}\right) \tag{2.1.6}$$

where

u_0 = initial total velocity

L_i = scale for i^{th} turbulence velocity

σ_i = rms gust intensities

ω = frequency

i = u, v, w gust components.

The Von Karman spectral shapes, although accurate, are not convenient for turbulence modelling work since they cannot be matched using linear filters. This is due to the noninteger power appearing in the denominators. Thus, in order to avoid computational complexity in this report, the Dryden form is adopted.

Element of Surprise: More often than not, real atmospheric turbulence, when encountered, presents an element of surprise. It is not easy to formulate a model of this phenomenon in terms applicable to flight simulator work. It seems that a measurement of "sudden jump" in the velocity field can be used as a possible criterion to describe this phenomenon. Relative frequency of "sudden jump" of atmospheric

turbulence can be compared to the simulated turbulence field. Changes in aircraft orientation angles can also be used to measure this phenomenon.

2.2 Presently-Used Simulation Techniques

In this section several presently-used simulation techniques are discussed from the standpoint of their statistical realism and suitability for use in flight simulators.

Measured Turbulence Field: Flight recordings of atmospheric turbulence is perhaps the most obvious method of producing a realistic simulation. There can be little argument as to whether or not these time histories are an accurate and realistic representation. However, it is difficult to adjust the measured time histories to allow for conditions other than those for which it was recorded. No allowances can be made for changes of altitude or different atmospheric conditions. Another serious drawback is that the recorded time histories are fixed in length. Extended run times, therefore, cannot be accommodated without repetition. From the simulation point of view, the pilots tend to recognize some of the characteristics of the turbulence field and develop an intuition for predicting the field. This defeats the purpose of an artificially simulated turbulence field, which is to provide unpredictable external disturbances. It can, therefore, be concluded that flight recordings of atmospheric turbulence are not suitable for the simulation of typical turbulence.

Sum of Sine Waves: Reference (5) describes this method in summary form. This technique involves superimposing several sinusoidal waves of different frequencies and amplitudes. The resultant is used to represent time histories of turbulence. One obvious disadvantage of

this method is that it contains only a finite range of frequencies whereas actual atmospheric turbulence consists of an infinite number of frequency components.

Results of this simulation are not available but the model can justifiably be discarded on the basis of its inadequacy in matching the frequency content.

Method of Orthogonal Functions: In this method (7), the recorded time histories of turbulence are decomposed into eigenfunctions of a covariance matrix. The probabilistic structure of the eigenfunction, and the coefficients of each of the time histories are studied. Simulated time histories are then regenerated by suitably modifying the distribution of the coefficients. The available preliminary results show that this technique adequately models the frequency contents and also presents an element of surprise. However, this model fails to show a patchy non-Gaussian characteristic which is typical of the real atmosphere. In addition to the mathematical complexity of the technique, its application is limited since recorded time histories are needed.

Gaussian Turbulence Model: The classical method, most widely used for turbulence simulation, is the linearly filtered white noise technique. Here the turbulence gust field is produced by passing white noise through a linear filter as shown in Figure 4a. The resultant signal is shaped so that the power spectrum and rms intensities match those of real turbulence. A Dryden or Von Karman form (6) are normally used to model the power spectrum. This model is remarkably easy to implement and can be adjusted for any general power spectrum. However,

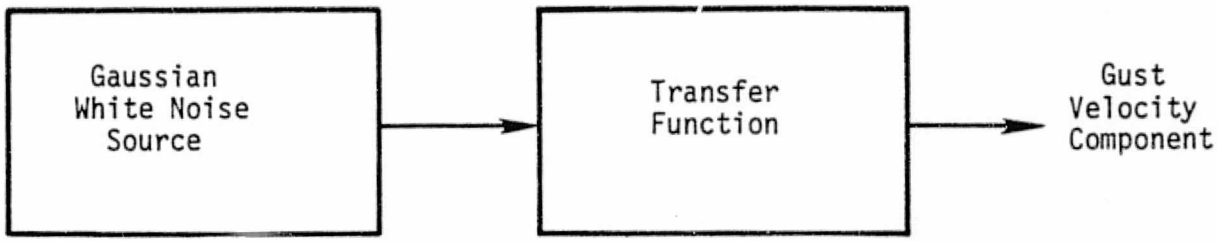

Figure 4a Gaussian Turbulence Simulation

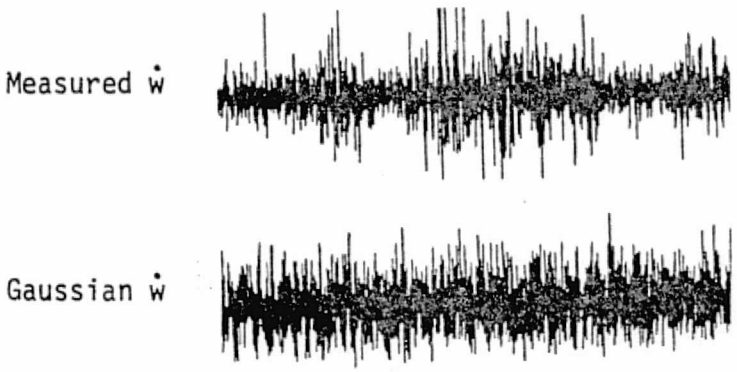

Figure 4b Derivative of Vertical Velocity

this model too falls short of reproducing the non-Gaussian patchy nature of real turbulence. Figure 4b compares the artificially simulated gust field using the Gaussian model (with a Dryden spectrum) and real atmospheric turbulence. It may be observed that the intensity for the Gaussian model is nearly constant whereas measured ("real") turbulence exhibits a patchy nature or intensity bursts. Test pilots, when exposed to this model in a flight simulator, rated the realism fair to poor.(5,6)

Non-Gaussian Turbulence Model: Reference (6) presents a non-Gaussian turbulence model. Time histories are generated by multiplying two independent random variables, one to represent the turbulence within a patch and the other to represent the variation of intensity with time. Figure 5a shows two independent Gaussian white noise generators and linear filters, which produce Gaussian random variables, a(t) and b(t). These variables are then multiplied to produce gust time histories.

The non-Gaussian model proposed in Reference (5), a modification of the above, is shown in Figure 5b. Here a(t), b(t), and d(t) are independent Gaussian processes. The process c(t) is generated by multiplying a(t) and b(t). The resultant process, c(t), a modified Bessel process, is summed with d(t) to form the output, u(t). The most remarkable achievement of this model is that the patchy characteristic and several statistical parameters of the simulated turbulence field can be varied simultaneously by varying the standard deviation ratio ($R = \sigma_c/\sigma_d$). However, when R is varied to achieve one set of statistical properties, several other statistical parameters of

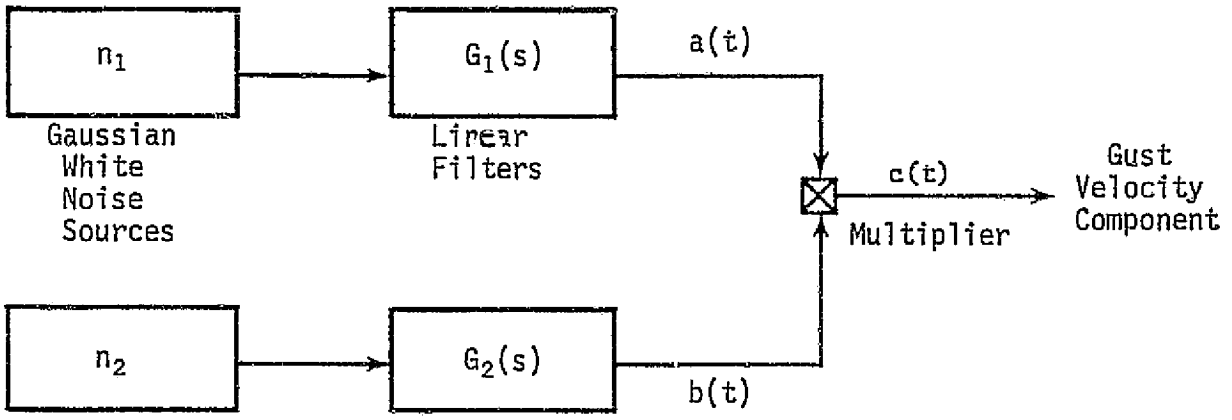

Figure 5a Non-Gaussian Turbulence Model (Reference 6)

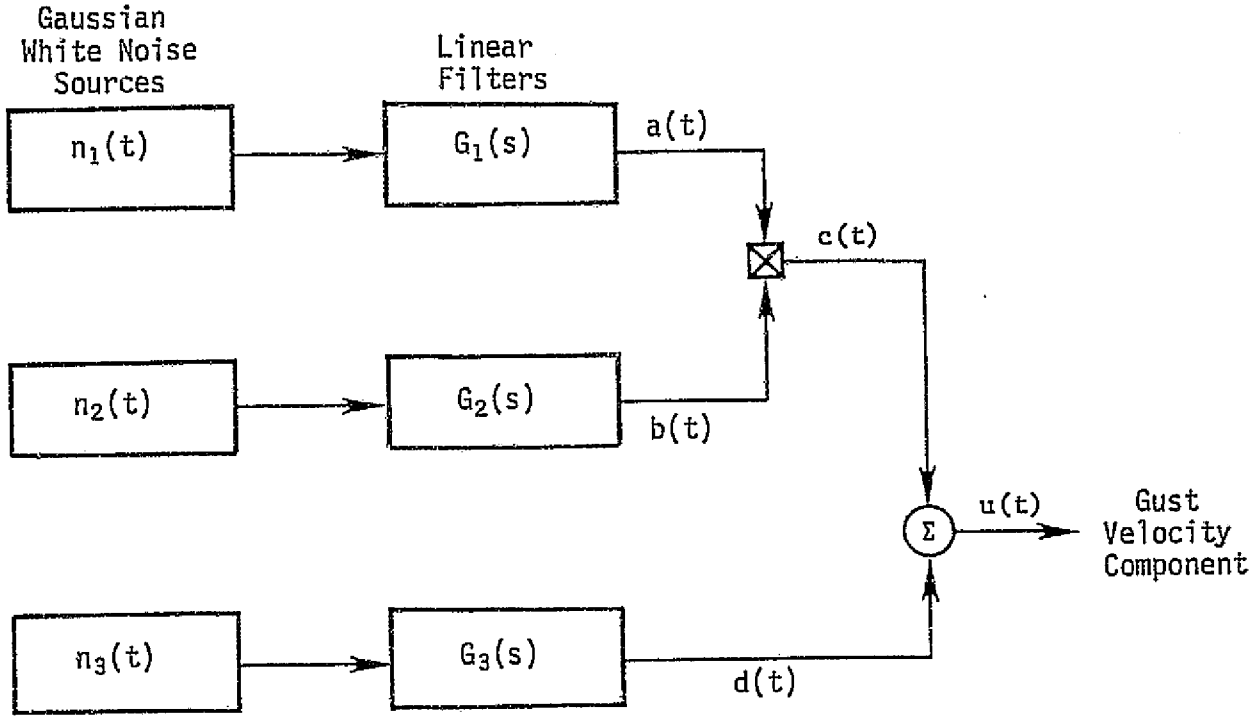

Figure 5b Non-Gaussian Turbulence Simulation (Reference 5)

interest do not match real turbulence. In addition, due to the mathematical complexity, the mechanization of this model on a flight simulator is complicated and expensive.

It can be observed from the review of presently-used simulation techniques that there is a need for a new model which adequately matches real atmospheric turbulence and is simple to implement in flight simulator studies. None of the preceding models have the flexibility of simulating various atmospheric conditions characterized by altitude, stability, and terrain. It is, therefore, necessary to introduce a new turbulence model which is realistic and can flexibly accommodate changes in atmospheric conditions and be easily implemented in flight simulator studies.

SECTION III

PROPOSED GUST MODELS

Of the simulation techniques described, the Gaussian turbulence model is the simplest to implement and least expensive computationally. The proposed turbulence models, modification of the Gaussian simulation technique, retain the simplicity of the Gaussian technique while adequately modelling the characteristics of real atmospheric turbulence. In this report three basic models are proposed:

1) Modified Gaussian Model

2) Rayleigh Model

3) Variable Length and Intensity (VLI) Turbulence Model.

3.1 Modified Gaussian Model

A block diagram of the modified Gaussian model is presented in Figure 6. Gaussian white noise, ϕ_0, is passed through a linear filter, $G_i(s)$ i = u, v, w, whose power spectrum is given by a Dryden model (e.g., Eqs. 2.1.4 to 2.1.6). The mathematical form of linear filter $G_i(s)$ is given as follows:

$$G_u(s) = \sigma_u \sqrt{\frac{2}{\pi\phi_0}\left(\frac{u_0}{L_u}\right)} \left[\frac{1}{S + v_0/L_u}\right] \tag{3.1.1}$$

$$G_v(s) = \sigma_v \sqrt{\frac{3}{\pi\phi_0}\left(\frac{u_0}{L_v}\right)} \left[\frac{S + \frac{1}{\sqrt{3}}\frac{u_0}{L_v}}{(S + v_0/L_v)^2}\right] \tag{3.1.2}$$

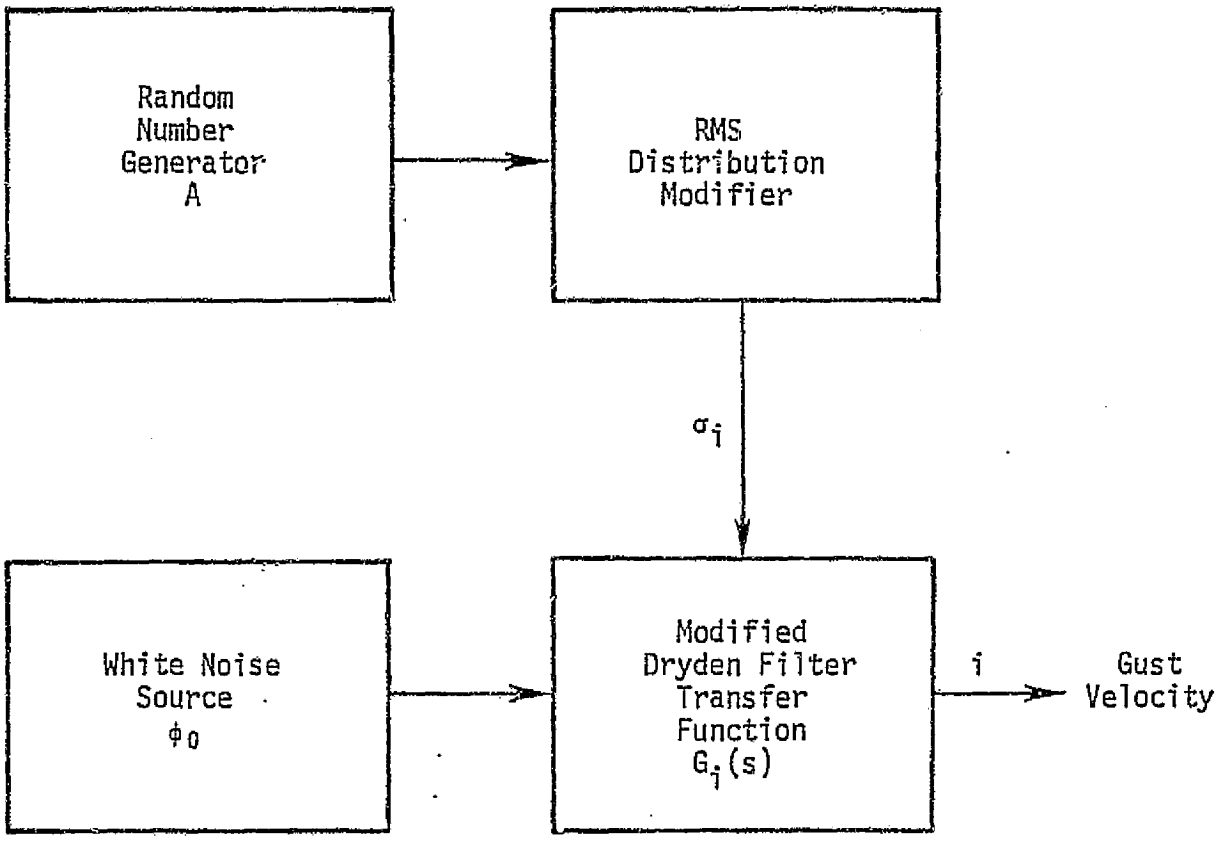

Figure 6 Modified Gaussian Turbulence Simulation

$$G_w(s) = \sigma_w \sqrt{\frac{3}{\pi\phi_0}\frac{u_0}{L_w}} \left[\frac{s + \frac{1}{\sqrt{3}}\left(\frac{u_0}{L_w}\right)}{(s + v_0/L_w)^2}\right] \qquad (3.1.3)$$

where ϕ_0 is the white noise power spectrum.

The linear filter, described above, is modified to include random variation of rms intensities. Random numbers generated by A are passed through a distribution modifier to generate rms intensities. Time histories are then generated by passing Gaussian white noise, ϕ_0, through the linear filter modified by the distribution modifier.

The patchy nature of atmospheric turbulence suggests that the turbulence field is composed of two components. One to represent variation of intensity within a patch and the other to represent variation of intensity with time (or from patch to patch). The distribution modifier in this model, essentially, represents the variation of intensity with time. The level of turbulence within each patch is controlled by the magnitude of the rms intensity.

The distribution modifier is the probability density function of the rms intensity. Analysis of several sets of atmospheric data characterized by various atmospheric conditions show that a truncated Gaussian distribution best fits the probability density of rms intensity. (1)

rms Distribution Modifier:

$$P(\sigma_i) = \frac{1}{S\sqrt{2\pi}} \exp\left[-\frac{1}{2}\left(\frac{\sigma_i - m}{S}\right)^2\right] \qquad (3.1.4)$$

where

P = probability density function

σ_i = rms intensity

S = root mean square of rms intensity

m = mean of rms intensity

i = u, v, w gust components.

Equation 3.1.4 is completely described by the mean, m, and the root mean square, S, of the rms intensity. These variables have been derived from the data presented in Reference (1) characterized by terrain, altitude, and atmospheric stability. Table 1 represents the distribution modifier for two sets of atmospheric conditions. Throughout this report, the turbulence generated by these two distribution modifiers will be referred to as Model 2 and 3 (Model 1 is Gaussian turbulence simulation).

The scale lengths for these models are given by the Dryden form:

$$L_u = L_v = h \qquad \text{for} \quad h \geq 1750 \text{ ft } (533.4 \text{ m}) \qquad (3.1.5)$$

$$L_u = L_v = 145\, h^{1/3} \qquad \text{for} \quad h < 1750 \text{ ft } (533.4 \text{ m}) \qquad (3.1.6)$$

$$L_w = h \qquad (3.1.7)$$

where h is the altitude.

3.2 Rayleigh Model

The Rayleigh model is derived from the modified Gaussian model by replacing the distribution modifier by a Rayleigh probability density function. The Rayleigh probability density function for rms vertical

TABLE 1

DISTRIBUTION MODIFIERS (rms INTENSITY)

		Mean	Variance
rms Distribution Modifier Model 2			
Altitude: 250 ft (76.2 m)	σ_u ft/sec (m/sec)	3.1 (0.94)	1.2 (0.37)
Atmospheric Stability: Unstable	σ_v ft/sec (m/sec)	3.2 (0.97)	1.2 (0.37)
Terrain: Plains	σ_w ft/sec (m/sec)	2.8 (0.85)	0.9 (0.27)
rms Distribution Modifier Model 3			
Altitude: 750 ft (228.6 m)	σ_u ft/sec (m/sec)	3.2 (0.97)	0.8 (0.24)
Atmospheric Stability: Unstable	σ_v ft/sec (m/sec)	3.5 (1.07)	1.0 (0.30)
Terrain: Mountain	σ_w ft/sec (m/sec)	4.1 (1.25)	0.9 (0.27)

turbulence intensity is, σ_w, is given by

$$P(\sigma_w) = \frac{\sigma_w}{C^2} \exp\left(-\frac{1}{2}\frac{\sigma_w^2}{C^2}\right) \tag{3.2.1}$$

where C^2 is one-half the expected value of σ_w^2.

Using Dryden spectrum models of real atmospheric turbulence, the value of C has been estimated in Reference (4) to be 2.3 ft/sec (0.70 m/sec).

The rms intensity of the longitudinal, u, and the lateral, v, gust components are obtained from the relation:

$$\frac{\sigma_u^2}{L_u} = \frac{\sigma_v^2}{L_v} = \frac{\sigma_w^2}{L_w} \tag{3.2.2}$$

The scale lengths are given by Equations 3.1.5 to 3.1.7. This will be referred to as Model 4.

3.3 Variable Length and Intensity (VLI) Turbulence Model

The VLI turbulence model includes, in addition to the rms distribution modifier, a scale length modifier. A block diagram of this model is presented in Figure 7. In addition to controlling the patchiness of the turbulence field, the time variations of scale length achieves numerical compatibility with the real atmosphere and further randomizes the simulation.

The scale length distribution modifier is derived from data collected in the LO-LO-CAT Program (1) for various combinations of

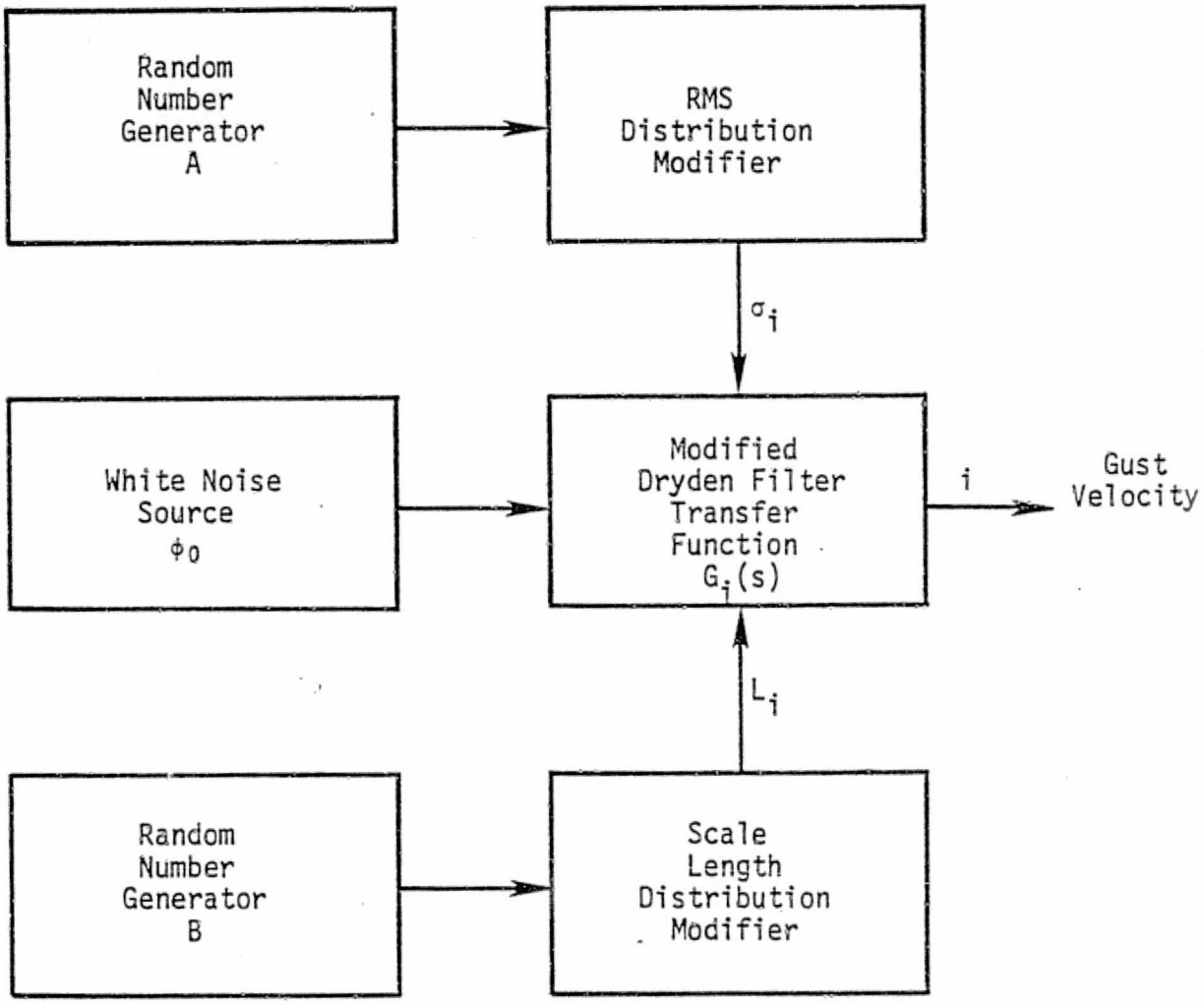

Figure 7 VLI Gust Model Turbulence Simulation

altitude, terrain, and atmospheric stability. Figures 8 and 9 show the fitted Gaussian distribution of scale length modifier for two sets of atmospheric conditions. The scale length distribution modifier is assumed to have the form

$$P(L_i) = \frac{1}{S\sqrt{2\pi}} \exp\left[-\frac{1}{2}\left(\frac{L_i - m}{S}\right)^2\right] \qquad (3.3.1)$$

where

P = probability density function

L_i = scale length of i^{th} component

S = root mean square of scale length

m = mean of scale length distribution

i = u, v, w gust components

Table 2 presents the root mean square and mean of scale length distribution along with the rms distribution modifier for specific atmospheric conditions. The turbulence signal generated by these two atmospheric conditions will be referred to as Models 5 and 6.

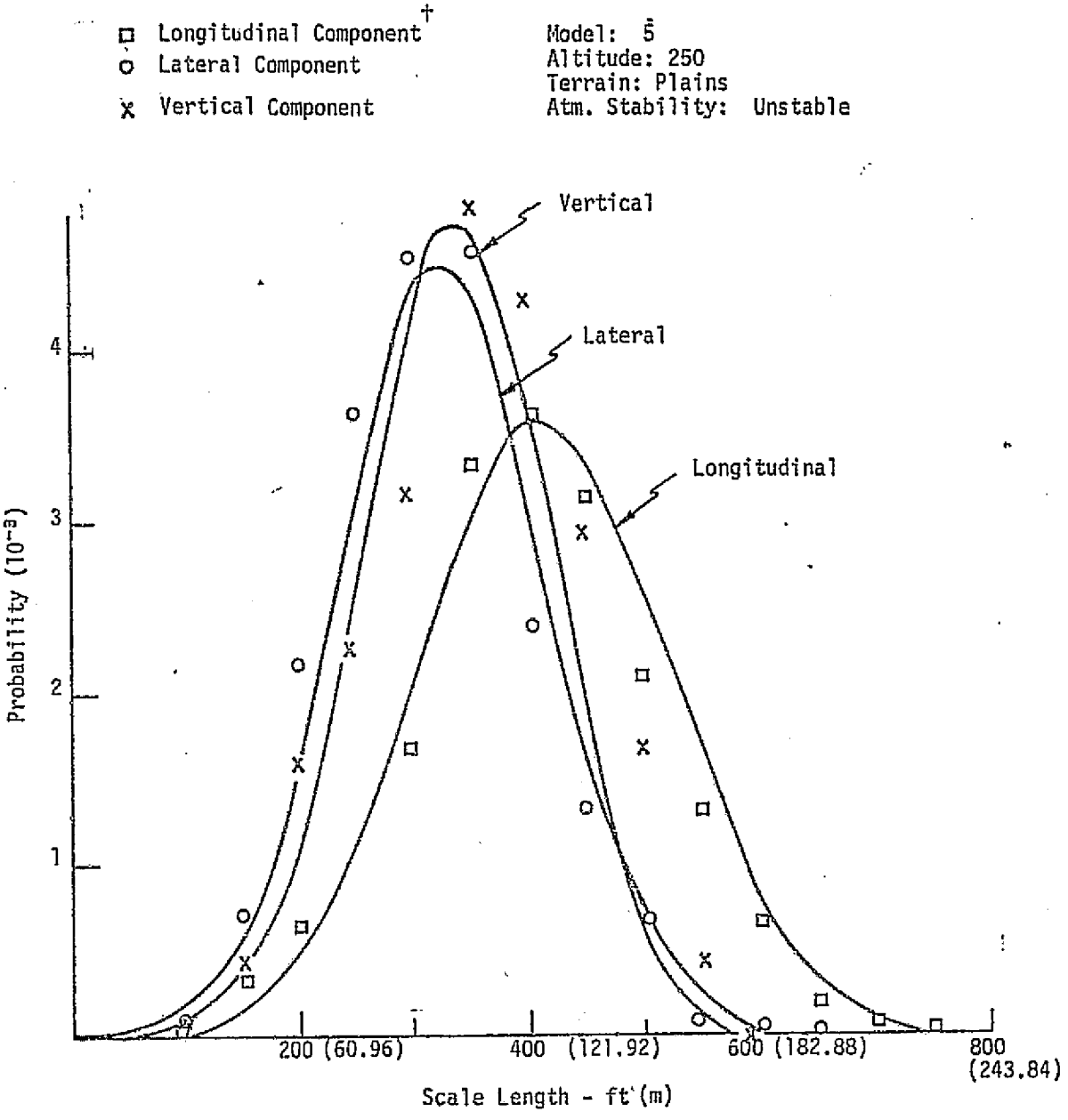

†Symbols represent empirical data.

Figure 8 Scale Length Distribution

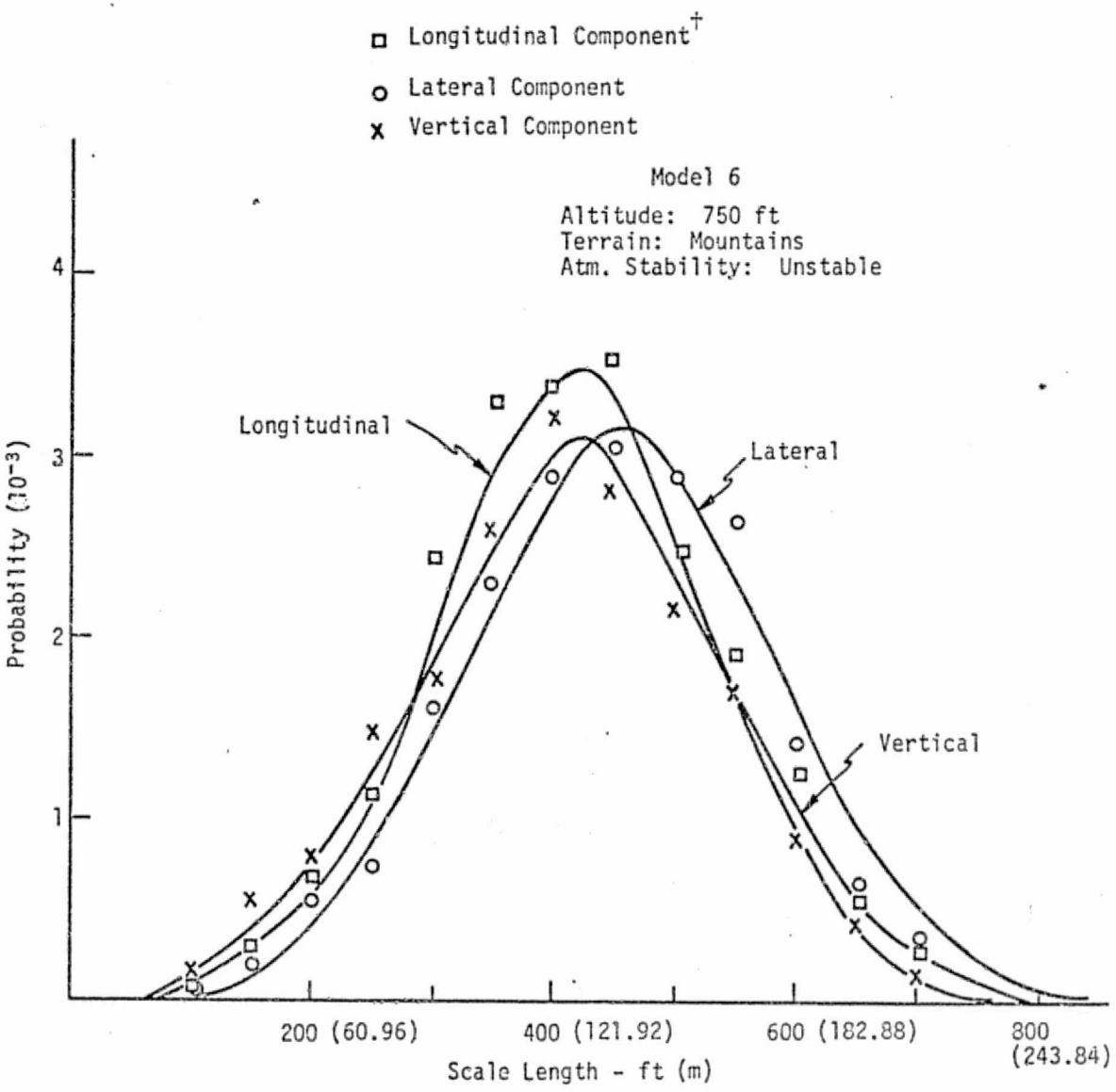

†Symbols represent empirical data.

Figure 9 Scale Length Distribution

TABLE 2

DISTRIBUTION MODIFIERS (SCALE LENGTH)

		Mean	Variance
rms Distribution Modifier Model 5			
Altitude: 250 ft (76.2 m)	σ_u ft/sec (m/sec)	3.1 (0.94)	1.2 (0.37)
Atmospheric Stability: Unstable	σ_v ft/sec (m/sec)	3.2 (0.97)	1.2 (0.37)
Terrain: Plains	σ_w ft/sec (m/sec)	2.8 (0.85)	0.9 (0.27)
Scale Length Modifier Model 5	L_u ft (m)	415 (126.4)	110 (33.5)
	L_v ft (m)	325 (99.1)	86.6 (26.4)
	L_w ft (m)	335 (102.1)	83.1 (25.3)
rms Distribution Modifier Model 6			
Altitude: 750 ft (228.6 m)	σ_u ft/sec (m/sec)	3.2 (0.97)	0.8 (0.24)
Atmospheric Stability: Unstable	σ_v ft/sec (m/sec)	3.5 (1.07)	1.0 (0.30)
Terrain: Mountains	σ_w ft/sec (m/sec)	4.1 (1.25)	0.9 (0.27)
Scale Length Modifier Model 6	L_u ft (m)	415 (126.4)	116.5 (35.5)
	L_v ft (m)	460 (140.2)	126.6 (38.6)
	L_w ft (m)	425 (129.5)	132.9 (40.5)

SECTION IV

THEORETICAL ANALYSIS OF PROPOSED MODELS

In this section results obtained by statistical analysis of the gust velocity components for each of the six models will be discussed and compared with the properties of real atmospheric turbulence where possible. The statistical results have been obtained in the form of:

1) mean and standard deviations
2) normalized fourth and sixth moments
3) probability density functions
4) power spectral densities
5) patchiness
6) frequency of element of surprise.

Table 3 tabulates the mean and standard deviation of gust components for each of the six models. It may be observed that the standard deviation varies from 2.6 to 5.2 ft/sec (0.79 to 1.58 m/sec) which is typical of low altitude clear air turbulence.

Fourth and sixth moment characteristics are tabulated in Table 4. Within the limits of experimental error these characteristics for the VLI models are in fairly good agreement with the real atmospheric data obtained in Reference (5).

Since the cumulative probability and the probability density function essentially contains identical information, only the probability density function will be analyzed. Figures 10 to 15 are plots of probability density functions for the simulated cases. In order to compare these with real atmospheric turbulence, a Gaussian

TABLE 3

MEAN AND STANDARD DEVIATION OF GUST COMPONENTS

(10-min. sample)

Model No.	Output Statistics	Gust Component u ft/sec (m/sec)	v ft/sec (m/sec)	w ft/sec (m/sec)	Simulation Technique
1	Mean	0.08 (0.02)	0.06 (0.02)	-0.03 (-0.009)	Gaussian
	St. Deviation	3.97 (1.21)	3.90 (1.18)	4.43 (1.35)	
2	Mean	0.83 (0.25)	-0.32 (-0.09)	-0.15 (-0.04)	Modified
	St. Deviation	3.90 (1.18)	3.50 (1.06)	2.60 (0.79	Gaussian
3	Mean	0.88 (0.27)	-0.40 (-0.12)	0.06 (0.02)	Modified
	St. Deviation	3.90 (1.18)	3.90 (1.18)	3.80 (1.15)	Gaussian
4	Mean	-0.36 (-0.11)	-0.16 (-0.049)	-0.22 (-0.06)	Rayleigh
	St. Deviation	5.19 (1.58)	4.84 (1.47)	4.48 (1.36)	Model
5	Mean	0.27 (0.08)	-0.36 (-0.11)	-0.20 (-0.06)	VLI
	St. Deviation	3.66 (1.11)	3.55 (1.08)	2.67 (0.81)	Model
6	Mean	0.20 (0.06)	-0.10 (-0.03)	-0.33 (-0.10)	VLI
	St. Deviation	3.67 (1.12)	3.90 (1.18)	3.81 (1.16)	Model

TABLE 4

NORMALIZED FOURTH AND SIXTH MOMENT DATA
OF REAL AND SIMULATED TURBULENCE FIELDS
(Over a 10-min. sample)

Model No.	Normalized Moment	Gust Velocity Component u	v	w	Simulation Technique
Real Atm.	Fourth	3.5	3.5	3.5	Real atmospheric turbulence data
	Sixth	21.7	21.7	21.7	
1	Fourth	3.0	3.0	3.0	Gaussian
	Sixth	15.0	15.0	15.0	
2	Fourth	5.9	3.5	3.2	Modified Gaussian
	Sixth	61.0	22.3	16.8	
3	Fourth	5.1	3.2	2.8	Modified Gaussian
	Sixth	46.7	18.9	11.9	
4	Fourth	3.7	3.2	3.3	Rayleigh Model
	Sixth	21.7	18.1	19.9	
5	Fourth	3.5	3.2	3.5	VLI Model
	Sixth	20.8	16.0	21.8	
6	Fourth	3.1	3.2	3.9	VLI Model
	Sixth	14.0	16.1	21.5	

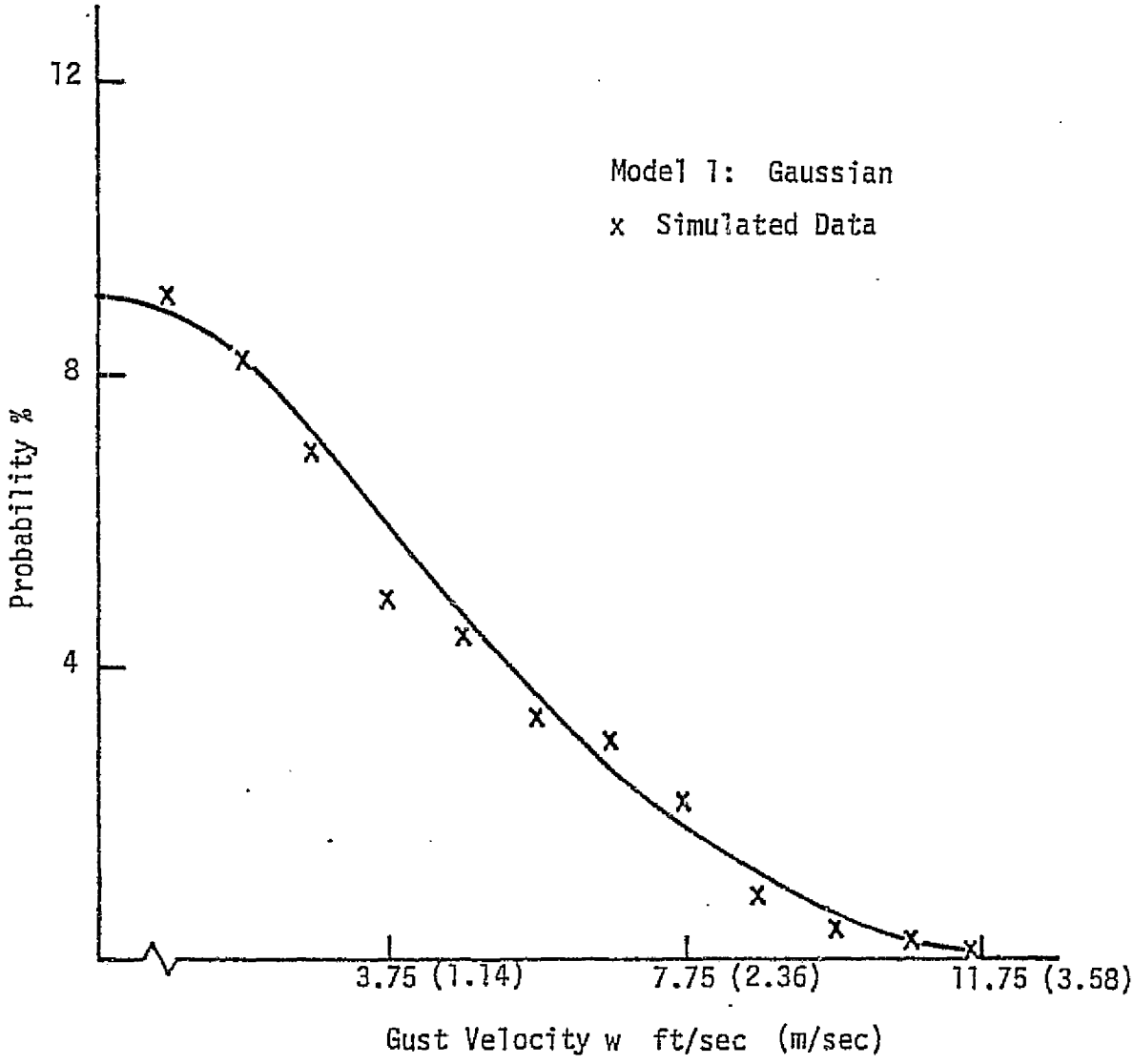

Figure 10 Probability Density of Simulated Field

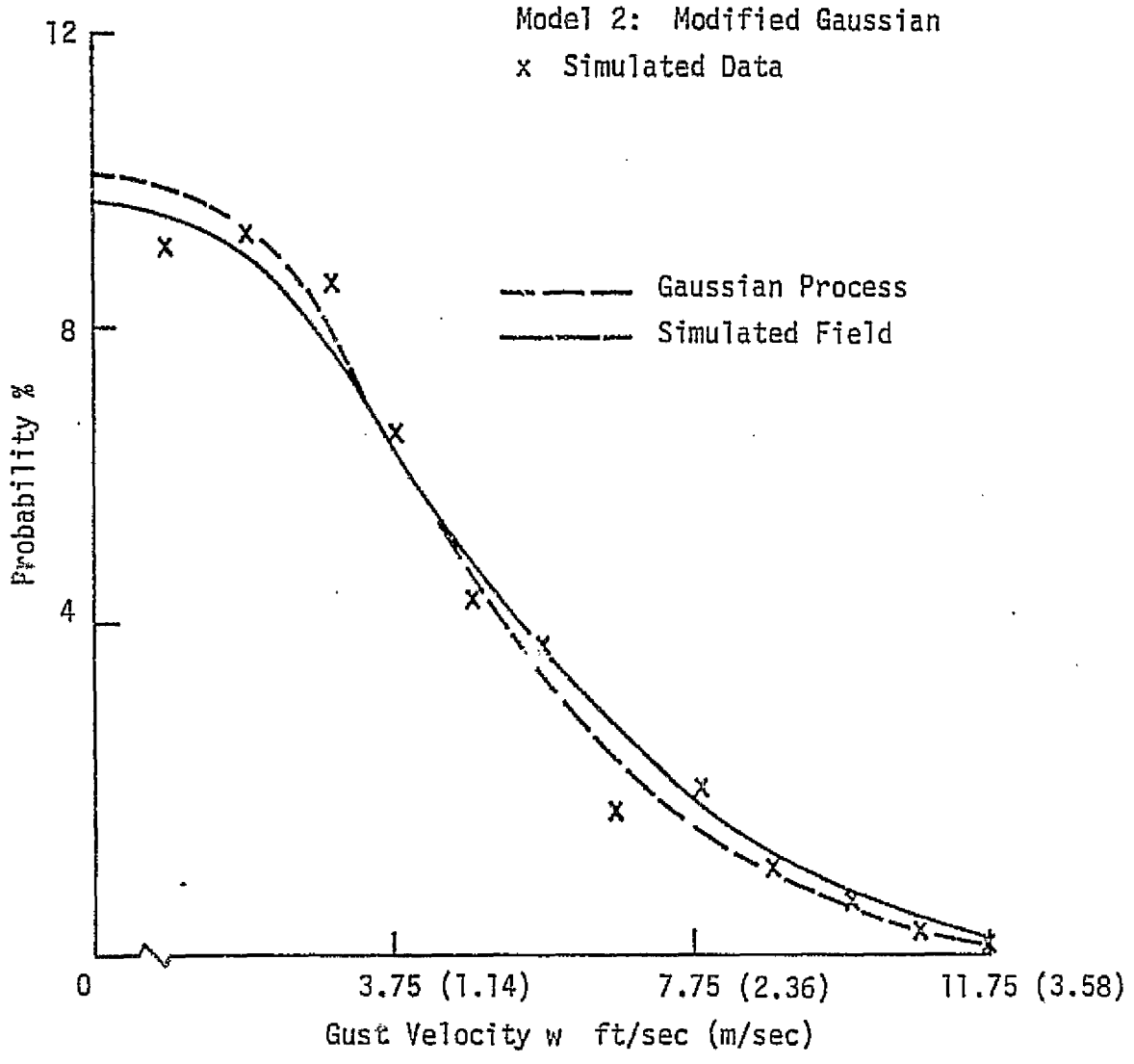

Figure 11 Probability Density of Simulated Field

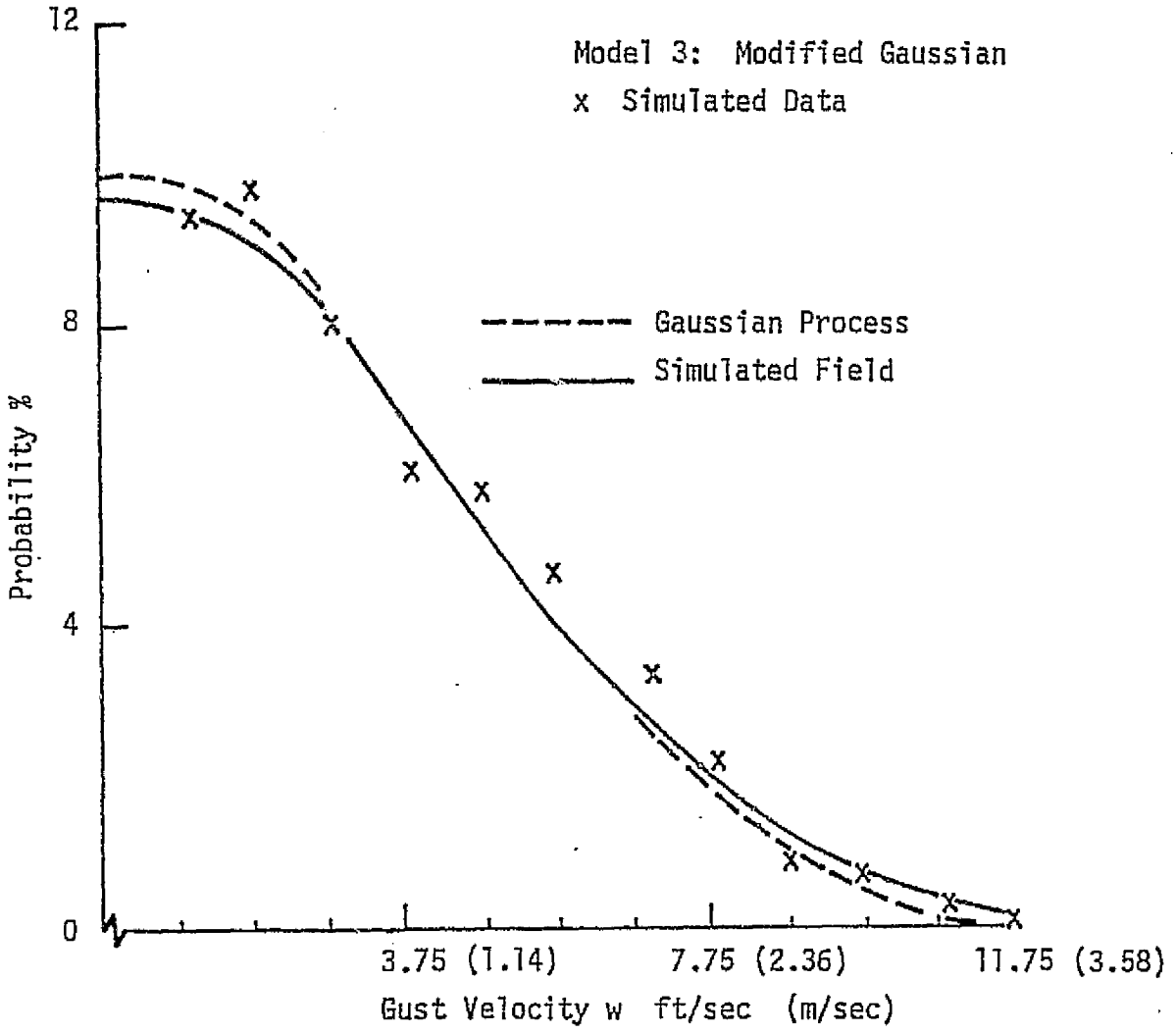

Figure 12 Probability Density of Simulated Field

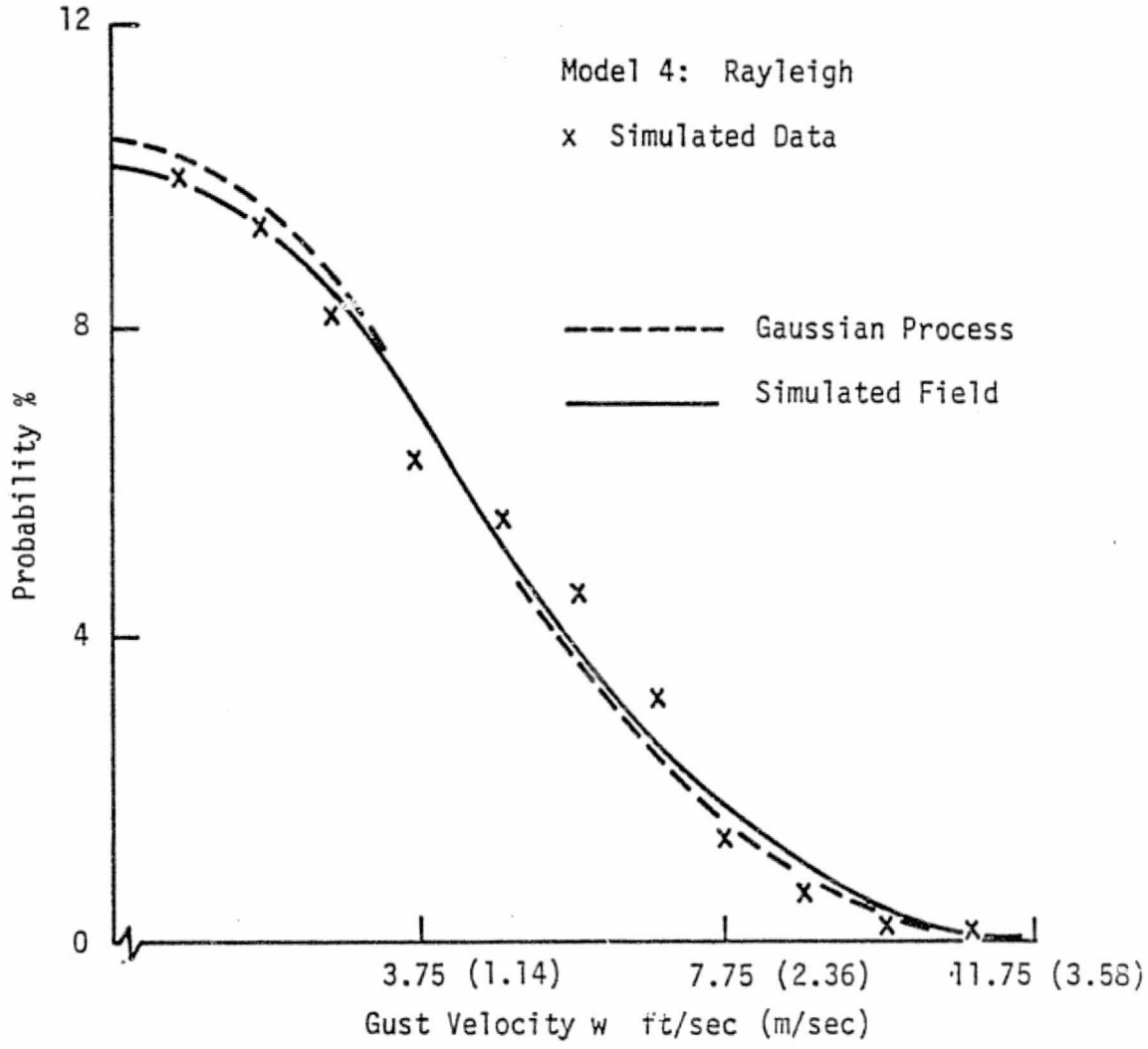

Figure 13 Probability Density of Simulated Field

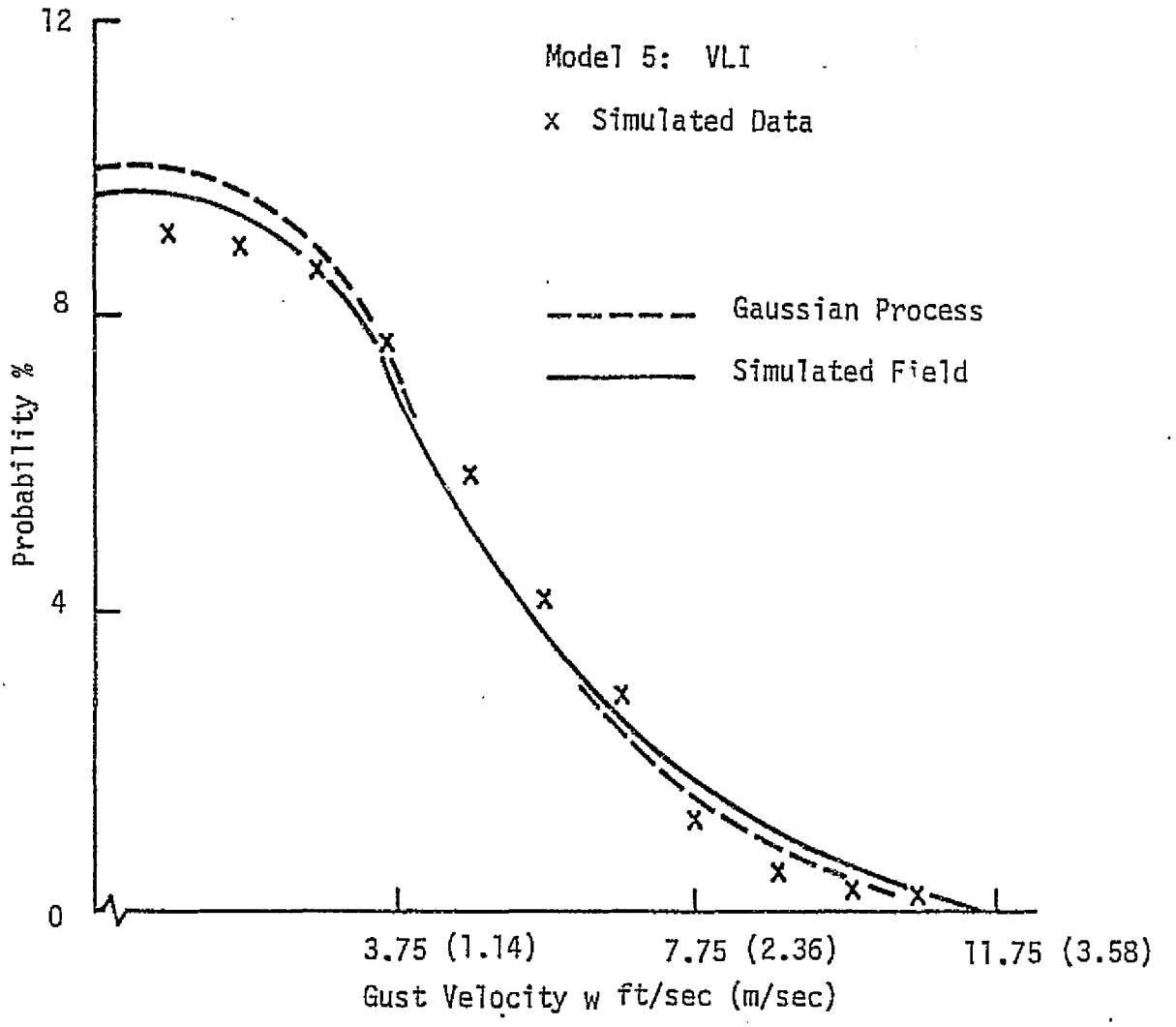

Figure 14 Probability Density of Simulated Field

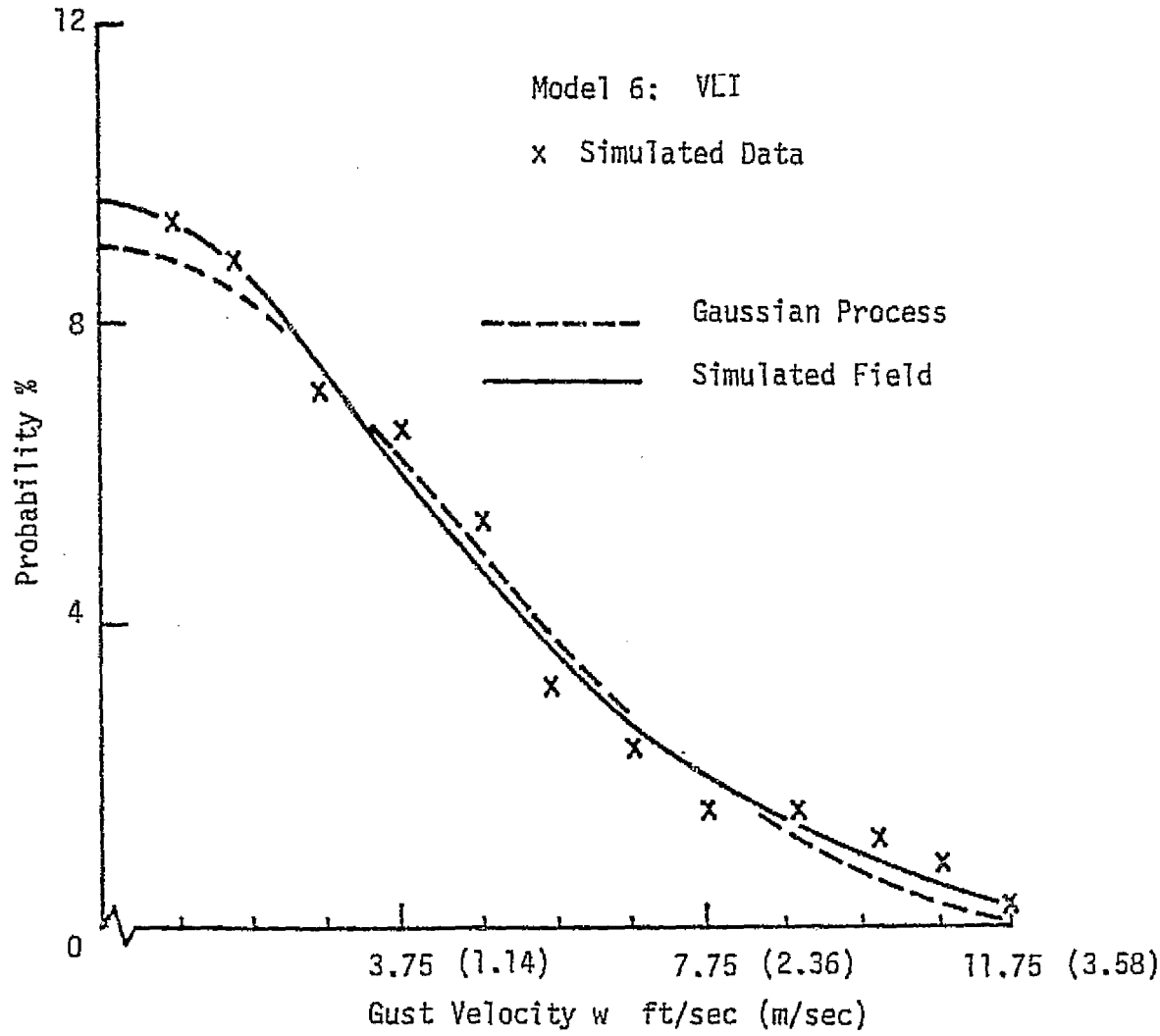

Figure 15 Probability Density of Simulated Field

distribution is plotted on the same scale. It has been established (5) that real atmospheric turbulence exhibits a higher probability of both smaller and larger gust velocities compared to a Gaussian distribution. A careful study of the probability density of the simulated field reveals a higher probability of larger gust velocities compared to a Gaussian distribution, however the distributions, with the exception of Model 6, do not show higher probability of lower gust velocities.

Power spectral densities of the simulated turbulence models are presented in Figures 16 to 21. The higher frequency components are compared with a line of slope -2 which is a characteristic of real atmospheric turbulence. The power spectrum in the entire frequency range within the limits of experimental error is in fairly good agreement with the assumed Dryden form (Equations 2.1.4 to 2.1.6).

The patchiness of each of the models is plotted in Figures 22 to 24. The derivative of vertical gust component is plotted illustrating a varying intensity of patchiness. Model 6 presents patchy characteristics which closely match real atmospheric turbulence.

Element of surprise is tabulated in Table 5. At present there is no criterion available to either quantitatively measure this phenomenon or to establish a basis of comparison. In this report, "sudden jump" in the velocity field is used to describe element of surprise.

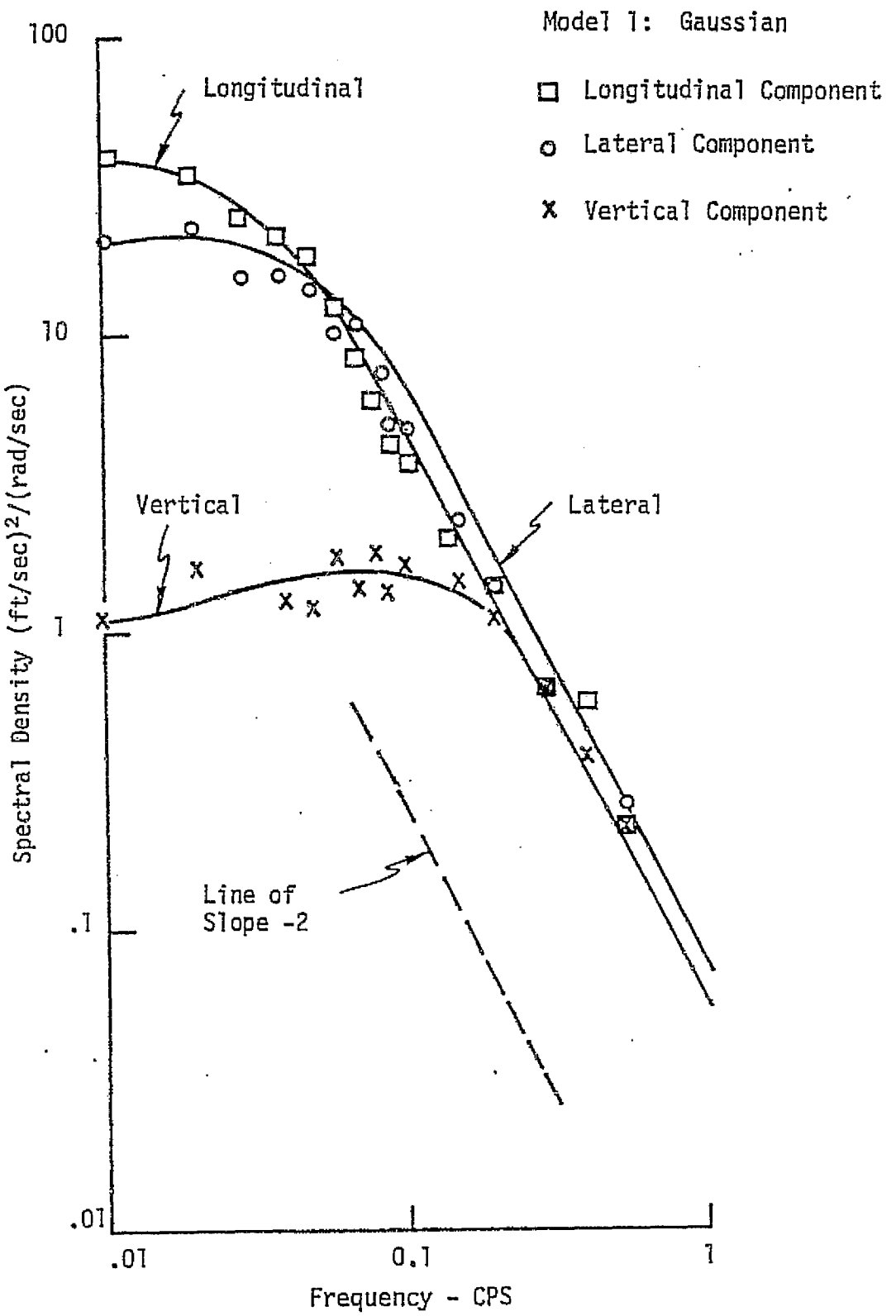

Figure 16 Power Spectral Density of the Simulated Field

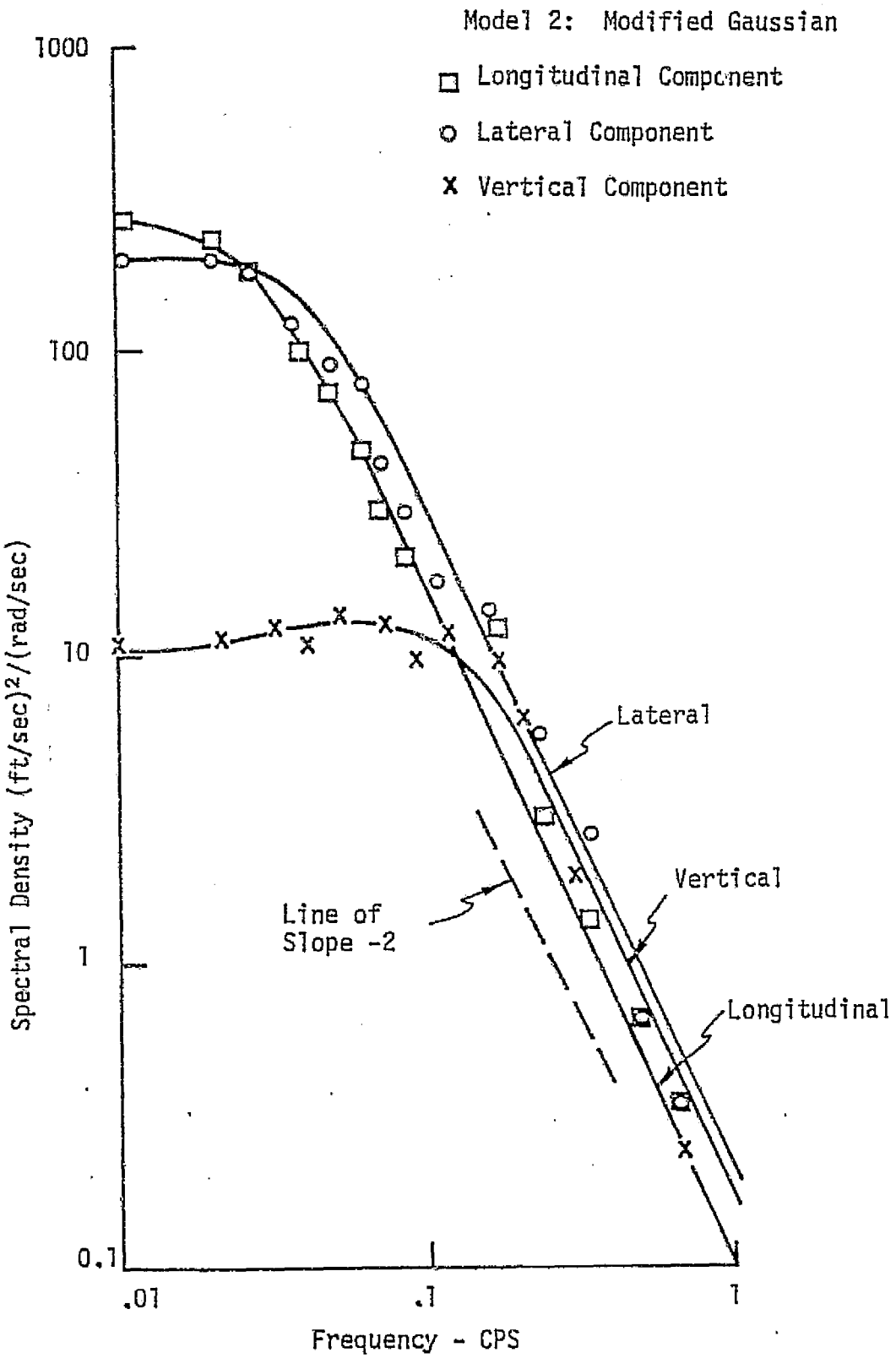

Figure 17 Power Spectral Density of Simulated Field

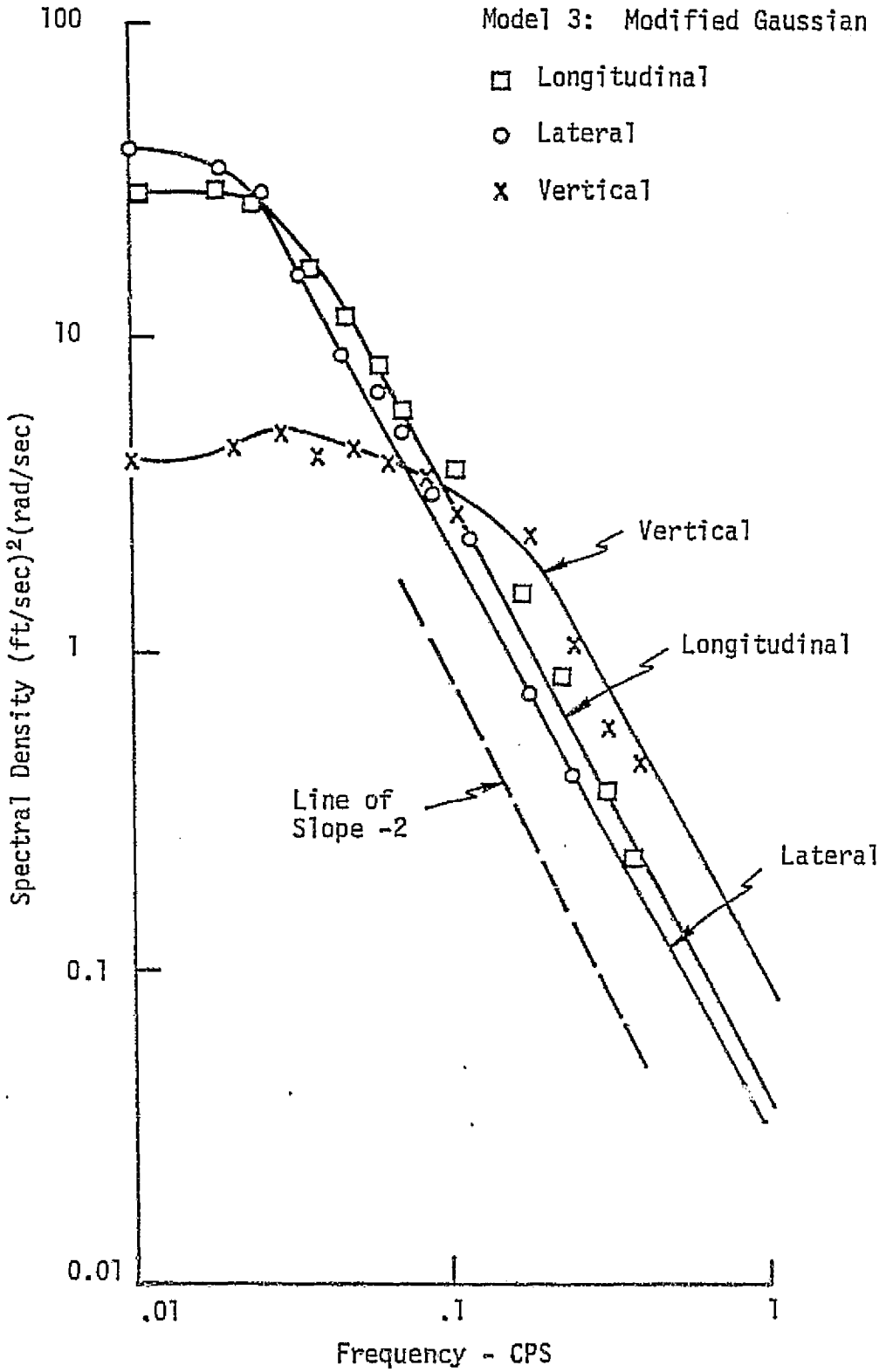

Figure 18 Power Spectral Density of Simulated Field

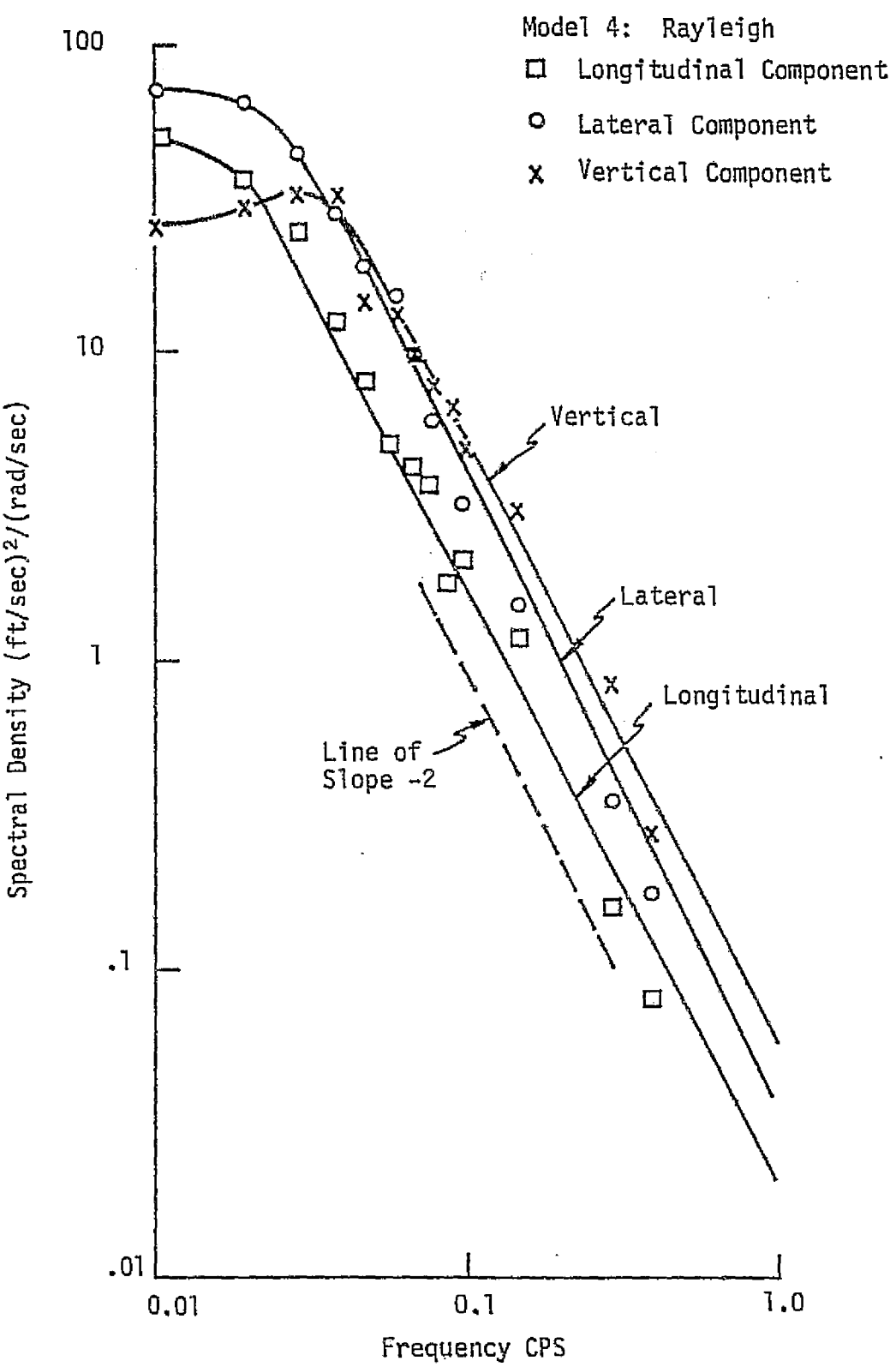

Figure 19 Power Spectral Density of Simulated Field

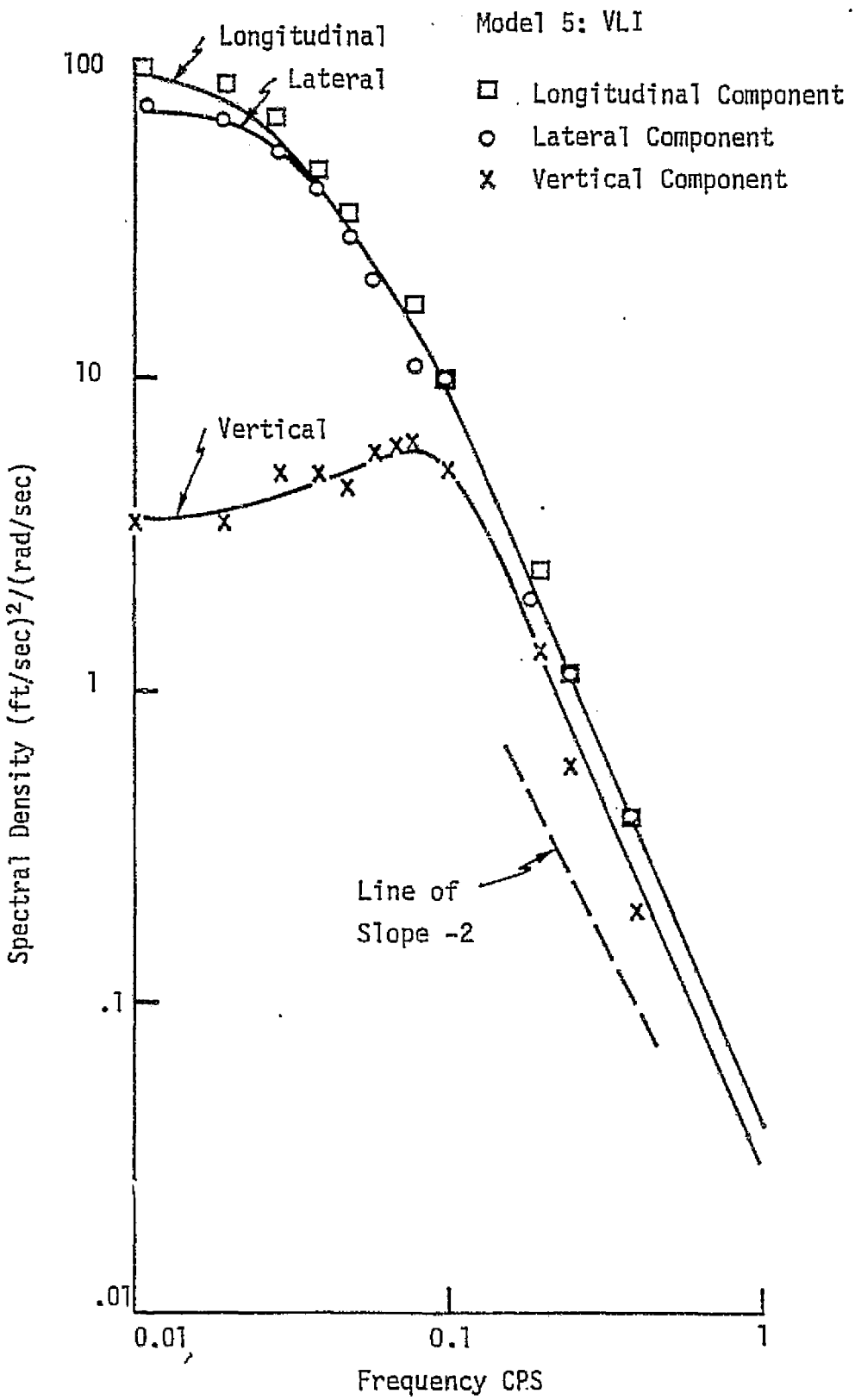

Figure 20 Power Spectral Density of the Simulated Field

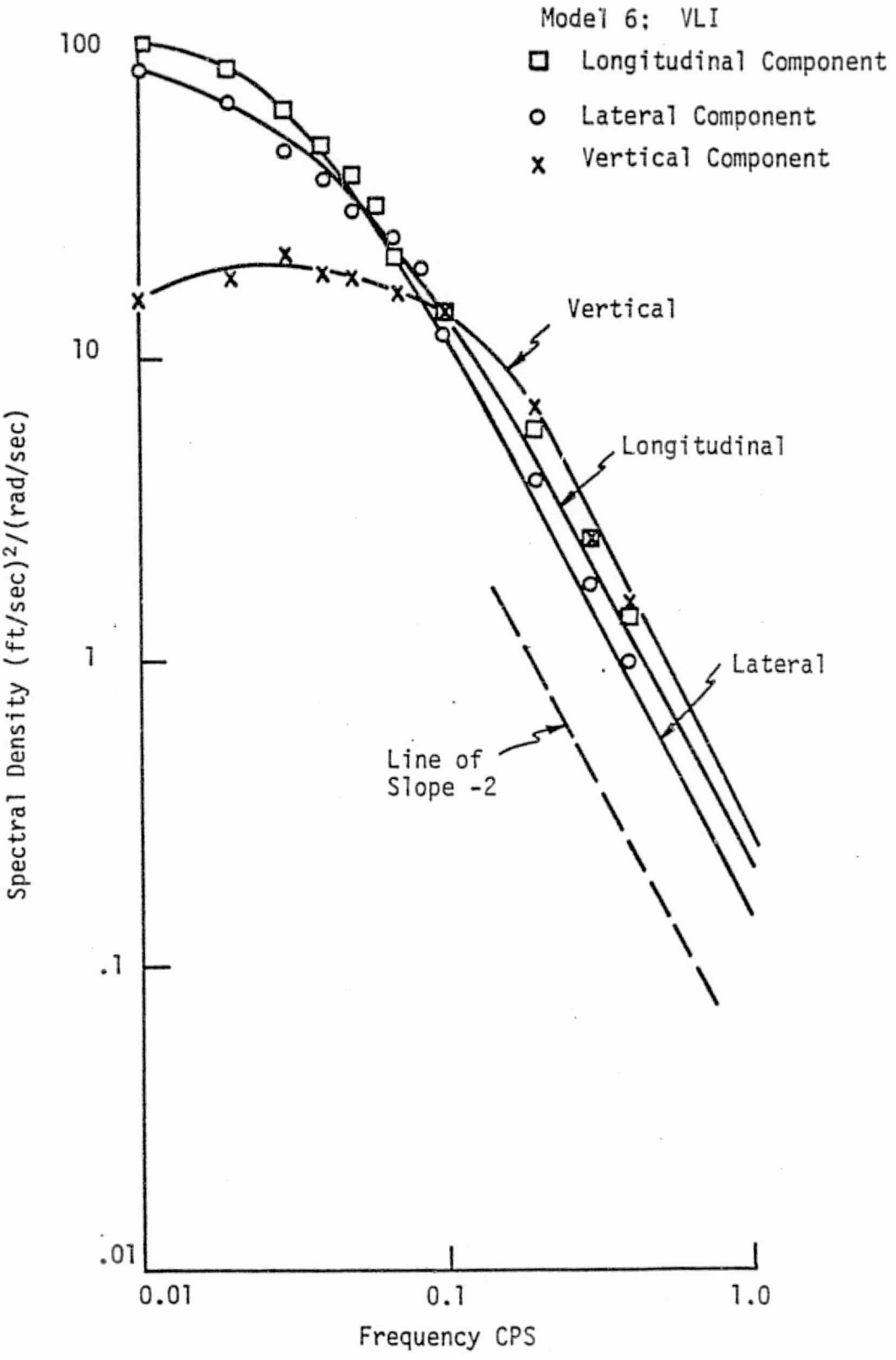

Figure 21 Power Spectral Density of Simulated Field

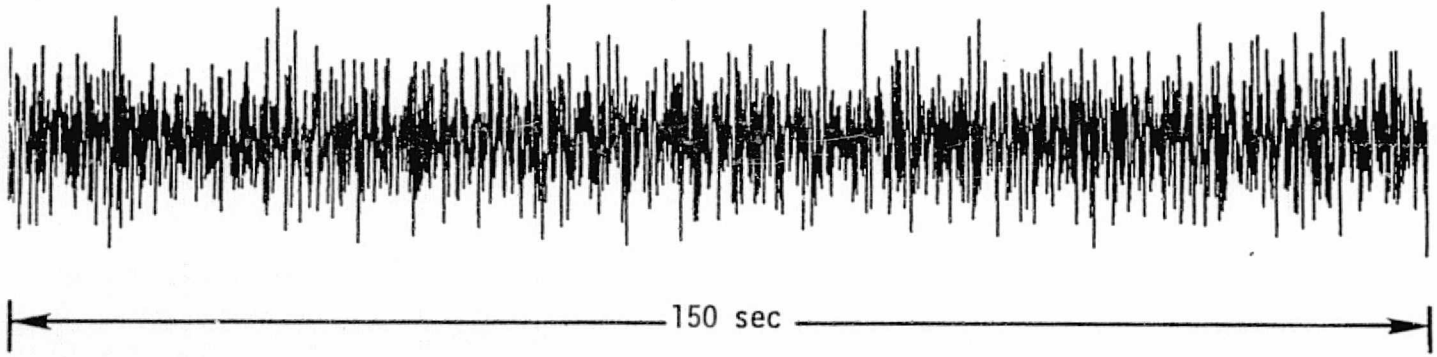

Model 1

Derivative of Vertical Gust Component vs Time

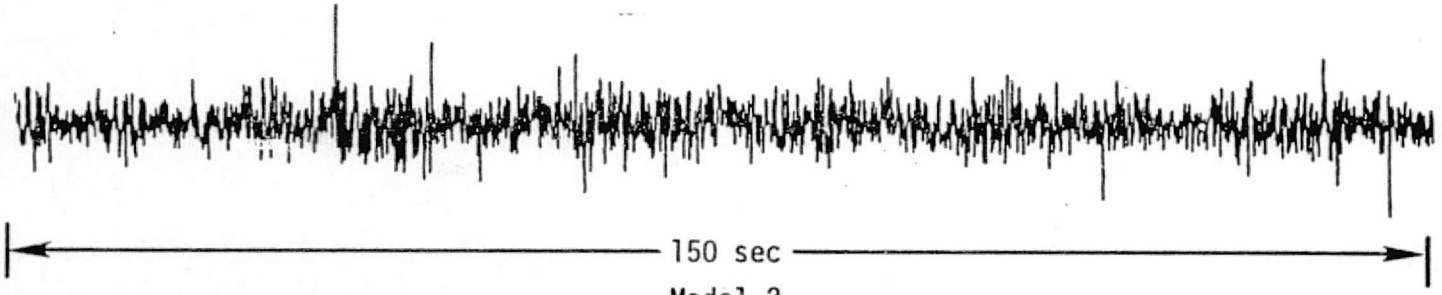

Model 2

Figure 22 Patchy Characteristics of Simulated Turbulence

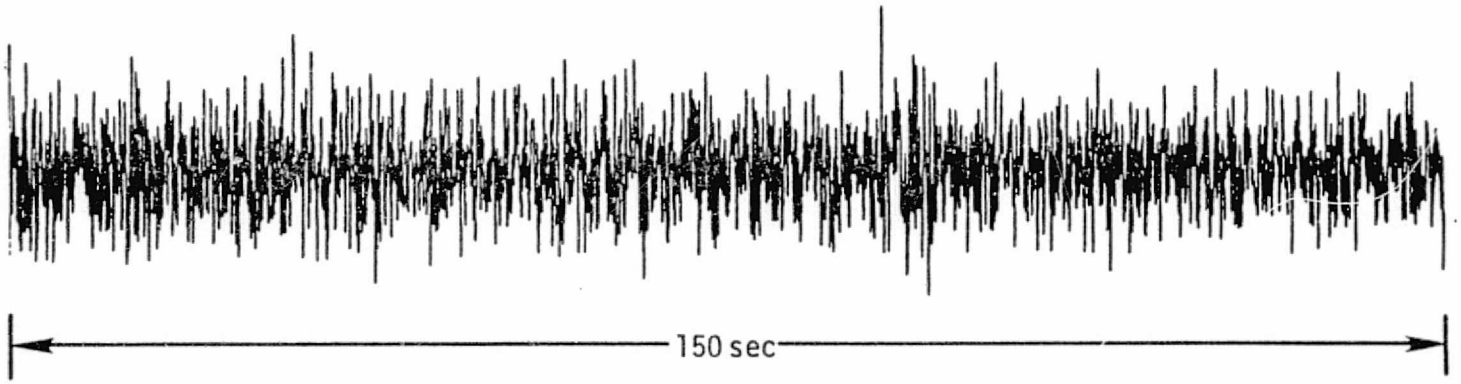

Model 3

Derivative of Vertical Gust Component vs Time

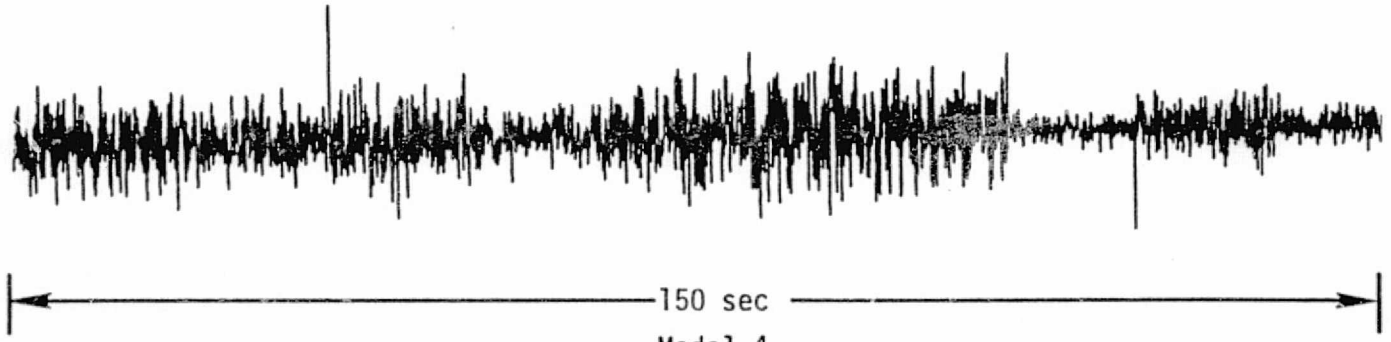

Model 4

Figure 23 Patchy Characteristics of Simulated Field

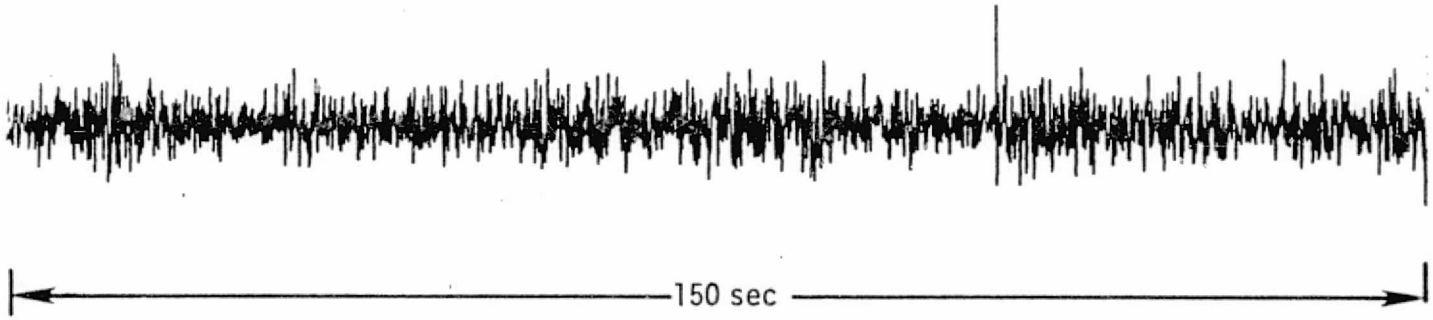

Model 5

Derivative of Vertical Gust Component vs Time

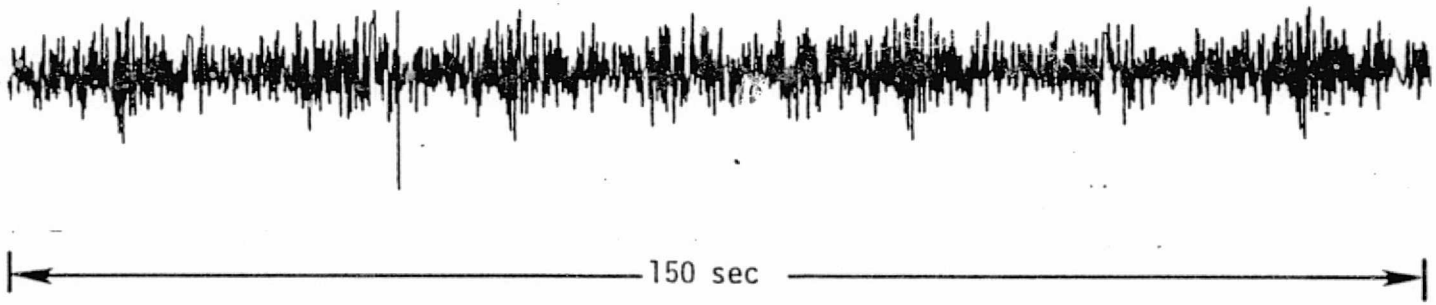

Model 6

Figure 24 Patchy Characteristics of Simulated Field

TABLE 5

FREQUENCY OF ELEMENT OF SURPRISE
OF SIMULATED FIELD *

Model	Frequency of Element of Surprise		
	u	v	w
1	0.03	0.0	0.0
2	0.07	0.07	0.0
3	0.03	0.00	0.0
4	0.0	0.0	0.23
5	0.03	0.03	0.0
6	0.27	0.40	0.0

*For a 3.5 ft/sec jump in velocity field).

SECTION V

TEST PROGRAM

This chapter describes the flight simulator experiment, including the details of the aircraft simulated, the flight simulator, and the pilot performance task.

5.1 Simulated Aircraft

The aircraft simulated is the Canadian deHavilland DHC-6 Twin Otter. This particular aircraft is chosen as representative of light-wing-loading STOL aircraft. In addition, there are pilots available with flying experience in the Twin Otter who can validate the simulation.

Aerodynamic and dynamic stability parameters are listed in References (5) and (8). A summary is given in Table 6.

5.2 Aircraft Simulator[1]

The Visual Motion Simulator (VMS) at the NASA Langley Research Center, a synergistic motion-base simulator with the basic interior and instrumentation of a jet transport cockpit (Figures 25), was employed in this study. A schematic diagram of the simulator, its control system, and its data output capabilities is presented in Figure 26 (8). A CDC-6600 digital computer, used exclusively to operate the real-time simulators, was programmed with the aircraft flight conditions, stability derivatives, six-degree-of-freedom differential equations of motion, and a simulator washout routine. The program

[1]This description has been adopted from Reference (8).

TABLE 6

AIRCRAFT PARAMETERS (REFERENCE 8)

$w = 11500$ lb (51152 N)	$I_x = 16900$ slug-ft^2 (22907 kg m^2)
$u_0 = 256.67$ ft/sec (78.2 m/sec)	$I_y = 27600$ slug-ft^2 (37411 kg m^2)
$C_T = 0.045$	$I_z = 40600$ slug-ft^2 (55031 kg m^2)
$\alpha_0 = -1.3^o$	$\bar{c} = 6.5$ ft (1.98 m)
$S = 420$ ft^2 (39.0 m^2)	$b = 65$ ft (19.8 m)

Longitudinal Stability Coefficients

$C_L = 0.3818$	$C_{D_\alpha} = 0$	$C_{x_\alpha} = C_L - C_{D_\alpha}$
$C_D = 0.045$	$C_{m_\alpha} = -5.9$	$C_{z_\alpha} = -C_{L_\alpha} - C_D$
$C_M = 0.035$	$C_{L_q} = 5.504$	$C_{x_{\dot{\alpha}}} = -C_{D_{\dot{\alpha}}}$
$C_{L_\alpha} = 5.7295$	$C_{D_q} = 0$	$C_{z_{\dot{\alpha}}} = -C_{L_{\dot{\alpha}}}$
$C_{D_\alpha} = 0.1432$	$C_{m_q} = -23.948$	$C_{x_q} = -C_{D_q}$
$C_{m_\alpha} = -1.9098$	$C_{x_u} = -2\,C_D$	$C_{z_q} = -C_{L_q}$
$C_{L_{\dot{\alpha}}} = 1.52$	$C_{z_u} = -2\,C_L$	

Lateral Derivatives

$C_{y_\beta} = -0.89$	$C_{y_p} = -0.1$	$C_{y_r} = 0.5$
$C_{\ell_\beta} = -0.12$	$C_{\ell_p} = -0.5488$	$C_{\ell_r} = 0.13$
$C_{n_\beta} = 0.1215$	$C_{n_p} = 0.006$	$C_{n_r} = -0.1855$

Control Derivatives

$C_{y_{\delta_r}} = 0.39$	$C_{\ell_{\delta_r}} = 0.0398$	$C_{m_{\delta_e}} = -1.79$
$C_{y_{\delta_a}} = 0.00348$	$C_{n_{\delta_r}} = -0.1$	$C_{L_{\delta_e}} = 0.45$
$C_{\ell_{\delta_a}} = 0.2055$	$C_{n_{\delta_a}} = -0.01$	

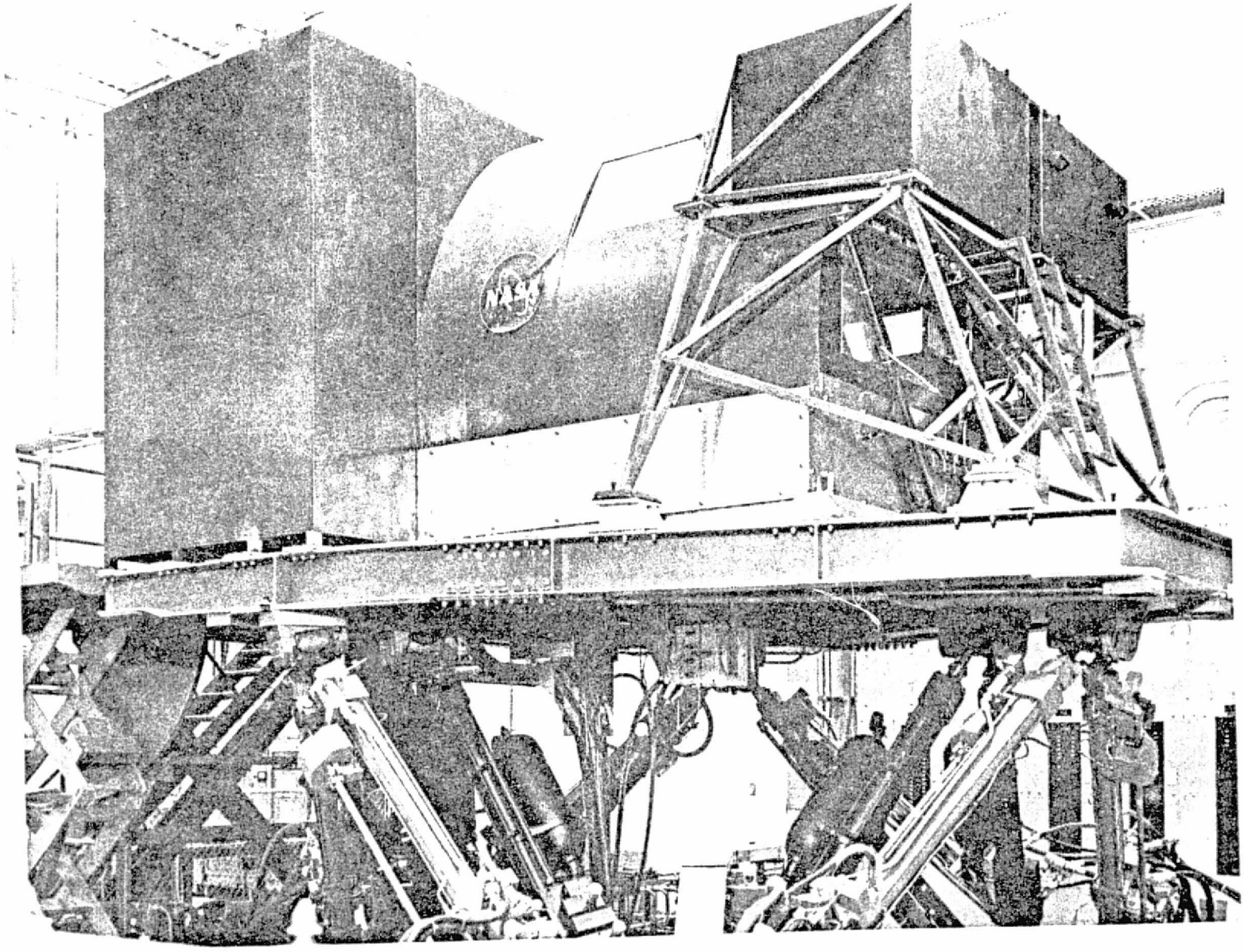

Figure 25 The Visual Motion Simulator (VMS) at the NASA Langley Research Center (Ref. 8)

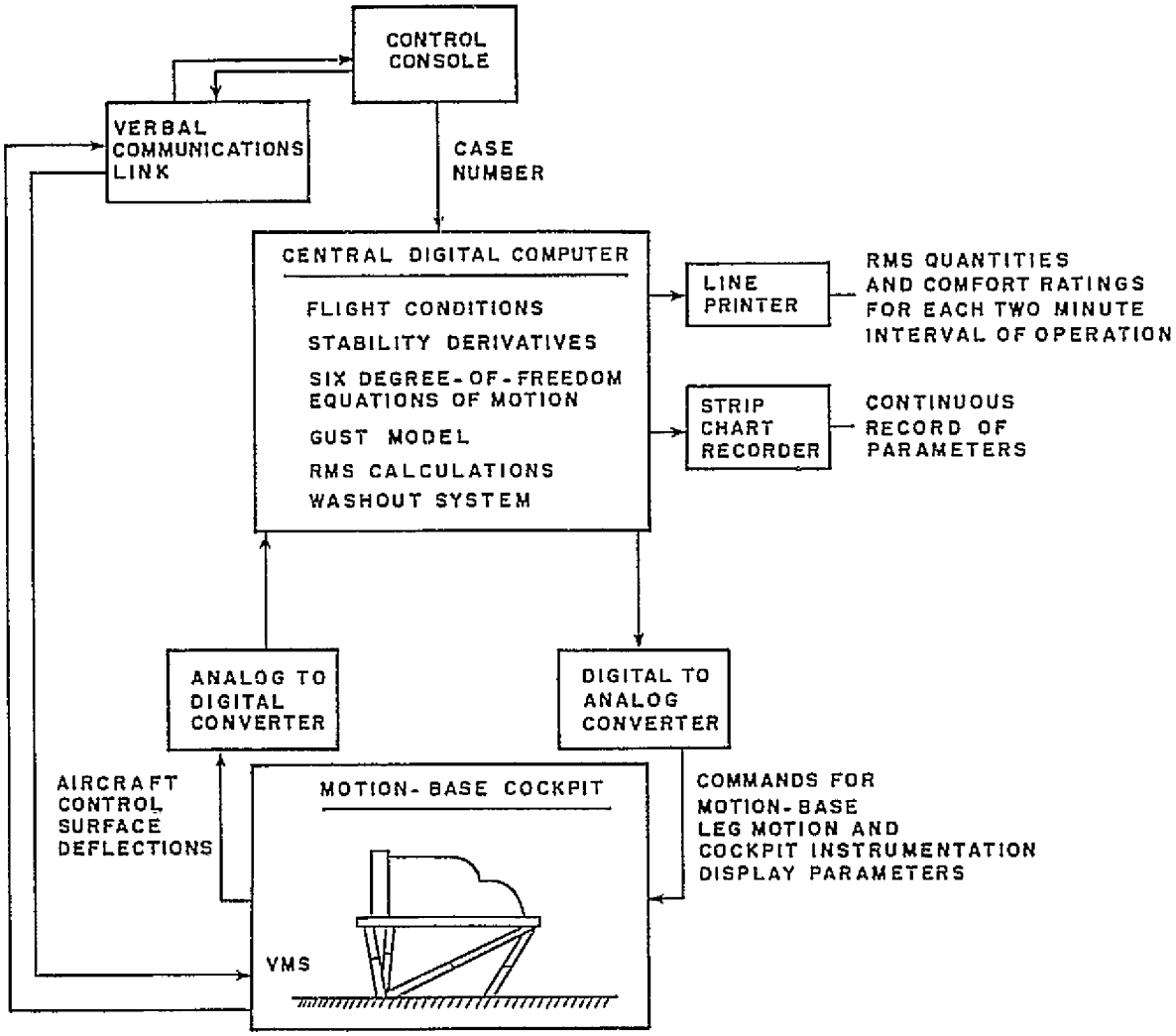

Figure 26 Block Diagram of Motion-Base Simulator Apparatus (Ref. 8)

integrates the equations of motion 32 times a second. These values are used by the simulator washout routine to determine the position of the simulator legs and the dynamic characteristics of the hydraulic actuators. Since the simulator is not capable of producing the magnitude and the duration of displacements, velocities, and acceleration of the real aircraft, the washout routine appropriately scales down the predicted motions of the real airplane to values that the simulator can produce without exceeding any of its design limitations. The washout routine also attempts to drive the simulator legs back to their neutral position following a disturbance from equilibrium in anticipation of a future disturbance. A detailed description of the physical dimensions and the performance specifications of the VMS may be found in References (9) and (10).

The simulator is equipped to provide two sets of landing conditions. In the first set of conditions the pilot is not given any external or "out the window" cue. In the second set the pilot is shown a visual display which generates a realistic landing scene. The aircraft motion signals, through a feed back loop, run a video camera on a scale model of the airfield and its surroundings (Figure 27). In addition, the simulator is equipped with ILS (Instrument Landing System) instrumentation which includes both a flight detector and raw data display. A 20° and 30° flap configuration is provided on the simulator for the landing approach. With the motion-base and all of the features described above, the simulator provides a realistic representation of a Twin Otter in a landing configuration.

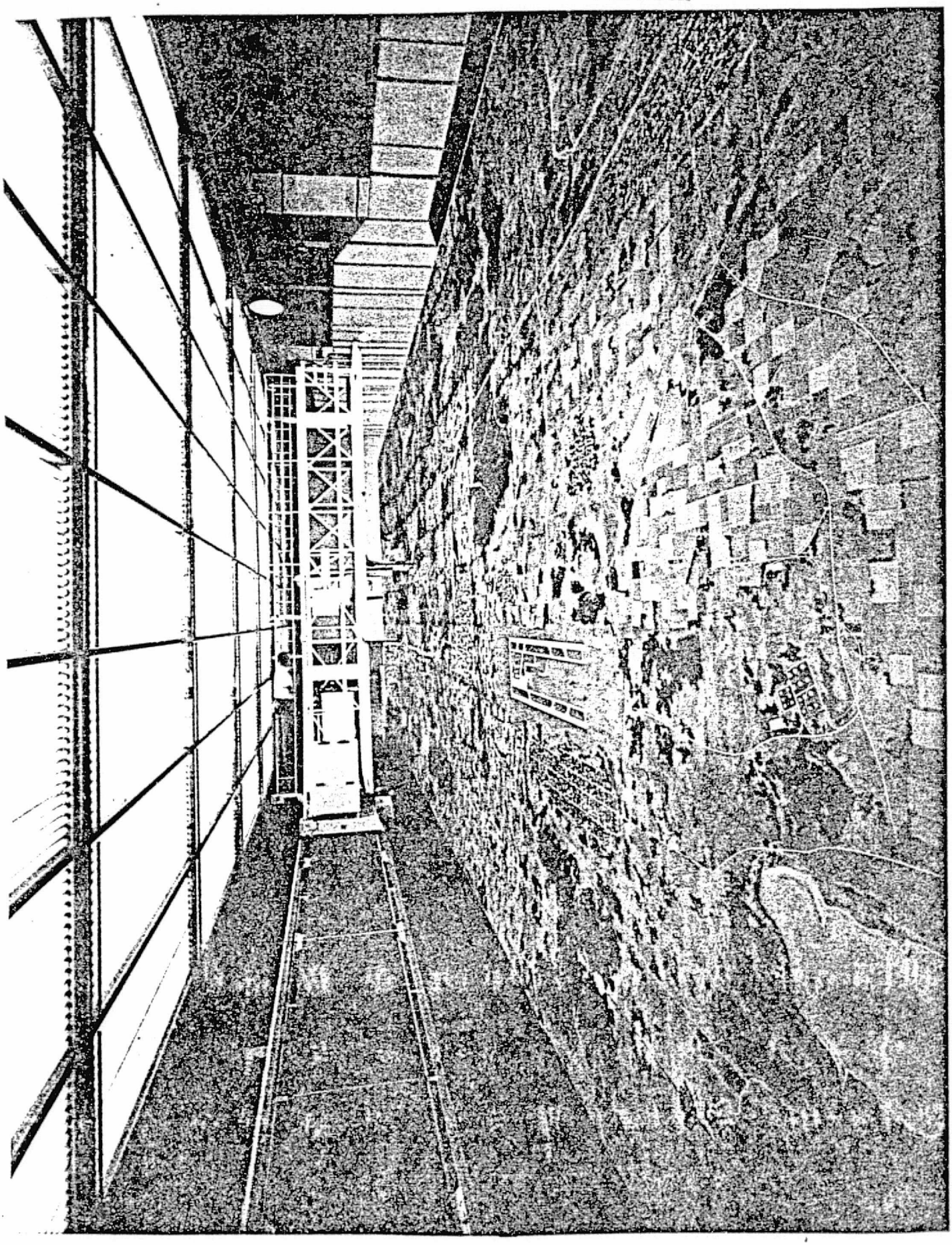

Figure 27 Landing Scene

5.3 Pilot Task Performance

Seven pilots experienced in civil, military and research flying were employed in the first part of the test program. Test runs, each of 8 to 10 minutes duration, for each of the six turbulence models were made in one pilot session. During separate sessions, some of the pilots repeated the models in random order. It was decided to have the pilots in a level flight, constant altitude tracking task with no visual or "out-of-window" cues in order not to introduce too many variables that might distract the pilots from their primary objective of trying to distinguish differences between various turbulence models. After each run, the pilot was asked for his comment on turbulence through the use of a flight questionnaire (see Appendix B).

In the final part, the landing approach test program, eleven pilots were employed to fly the VMS. Three of the eleven pilots each had experience of over 2,000 hours of flying in the Twin Otter. Test runs, each of 6 to 8 minutes duration, for each of the turbulence models, were made in one pilot session. During separate sessions, some of the pilots repeated the six models in random order. It was decided to have the pilots fly a constant altitude tracking task until the glide slope was intercepted. The pilots were then required to approach on a 6° glide slope using both the ILS and the visual display. The simulation is terminated at touch down. After each run, the pilot, through a flight questionnaire (see Appendix B) was asked to estimate the turbulence intensity, realism, relative amplitude of aircraft motions in each of the six degrees of freedom, patchiness, workload, and to give a Cooper-Harper handling quality rating (Figure 28) (11) for the airplane

turbulence interaction. Additional questions explored the bases for the pilot's judgments. In addition the pilots were also asked to estimate the altitude, terrain, and atmospheric stability in relation to their flying experience.

During each run, continuous strip-chart recordings were made displaying time histories of various aircraft parameters for later analysis. These include three linear accelerations, and three angular rates of the aircraft in body axes, elevator, aileron, and rudder deflections, throttle position, altitude, rate of climb and aircraft heading as well as the integral-squared error of the ILS track. A sample strip-chart is presented in Figures 29a and 29b. The rms intensities of the longitudinal, lateral and vertical gust fields are presented in Table 7.

In the following chapter these opinion ratings will be statistically analyzed to establish the most realistic turbulence model and to identify the variables that critically affect the handling quality of aircraft in turbulence.

HANDLING QUALITIES RATING SCALE

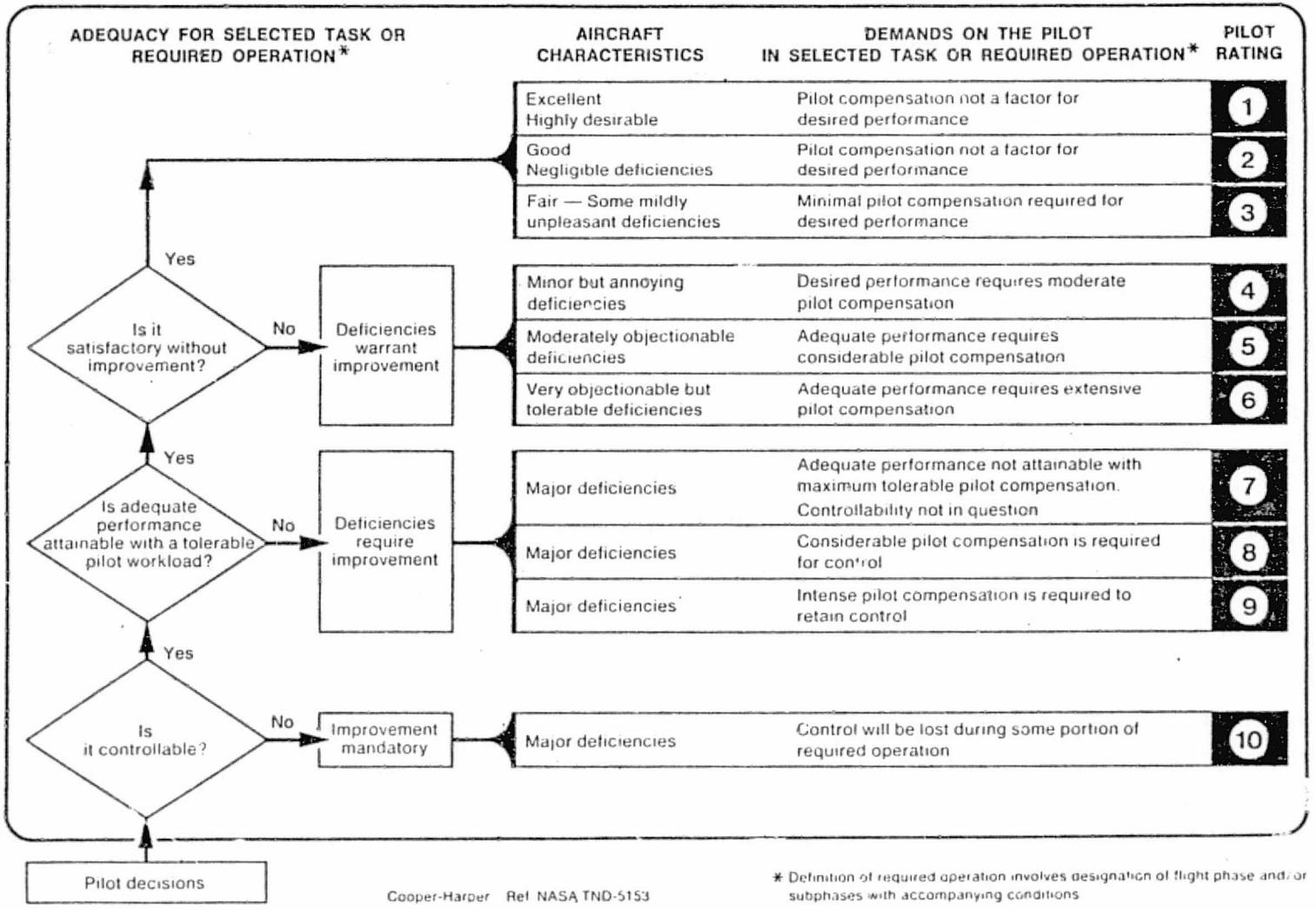

Figure 28 Cooper-Harper Pilot Rating Scale

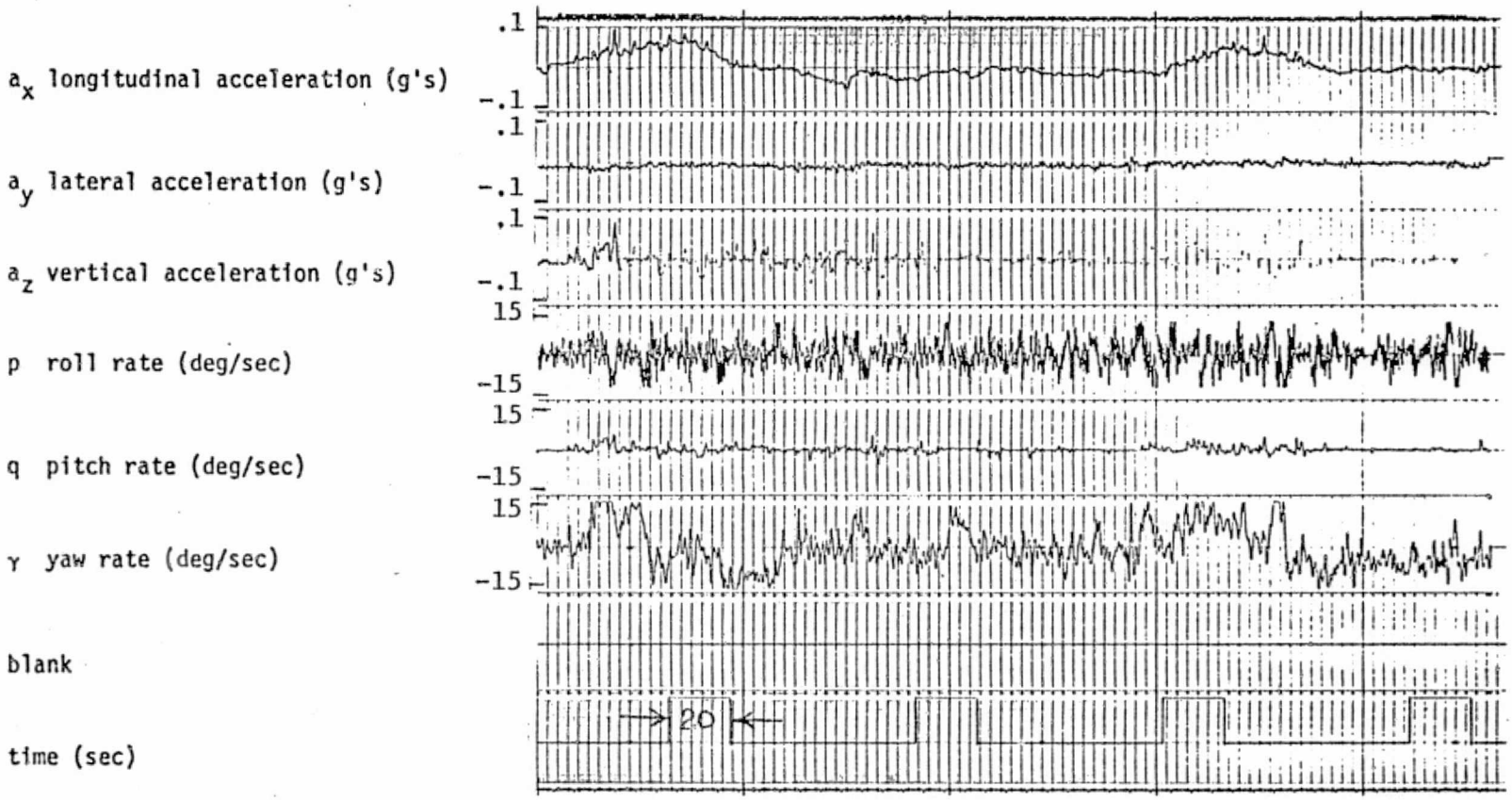

Figure 29a Typical Stip Chart Output of Flight Parameters

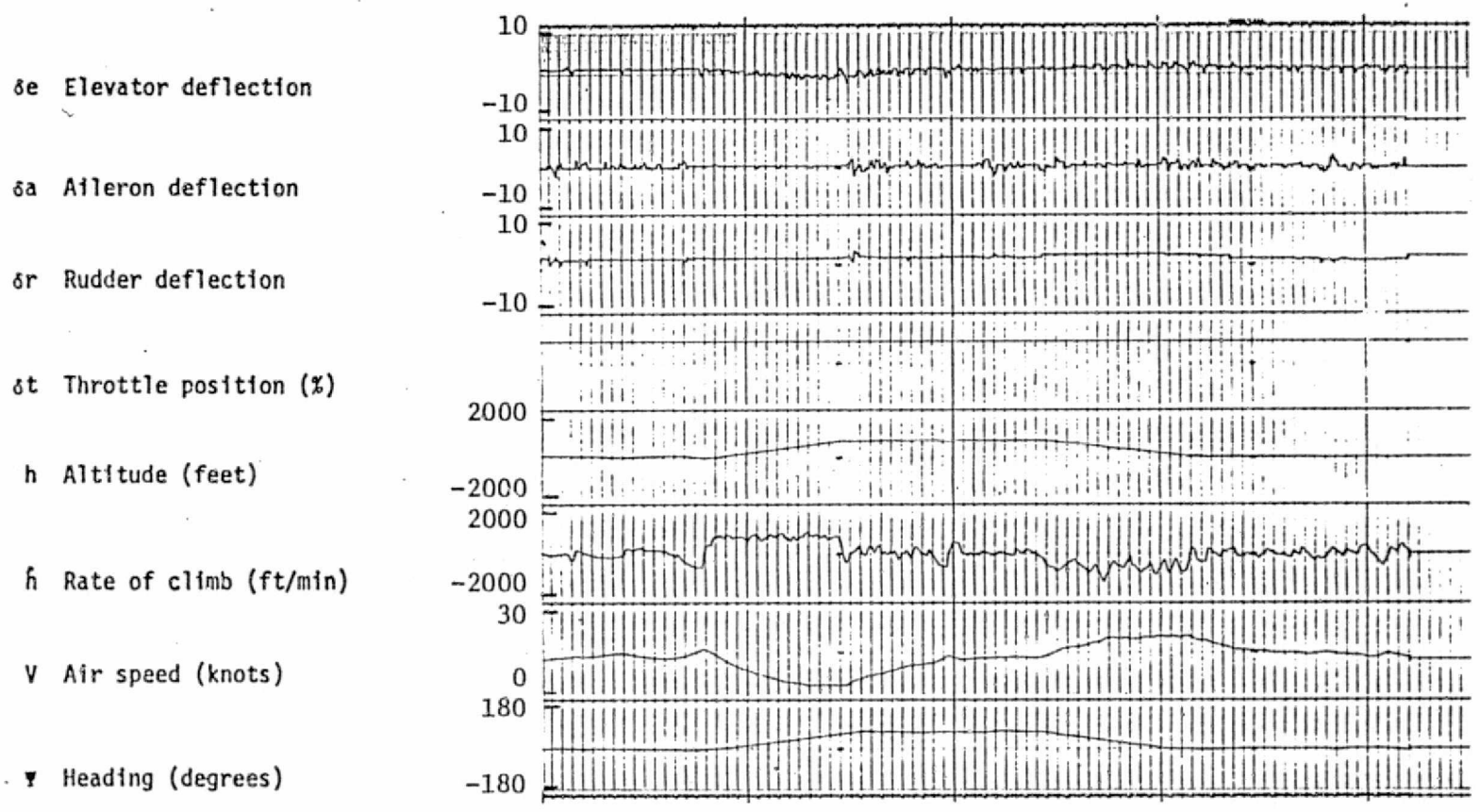

Figure 29b Typical Strip Chart Output of Flight Parameters

TABLE 7

INPUT-OUTPUT INTENSITIES

Model No.	Input rms ft/sec (m/sec) u	v	w	Output rms ft/sec (m/sec) u	v	w
1	4.0 (1.31)	4.0 (1.31)	4.5 (1.37)	3.97 (1.21)	3.90 (1.19)	4.43 (1.35)
2	m[1]= 3.1 (0.94)	m = 3.2 (0.97)	m = 2.8 (0.85)	3.92 (1.19)	3.53 (1.07)	2.6 (0.79)
	v[2]= 1.2 (0.37)	v = 1.3 (0.37)	v = 0.9 (0.27)			
3	m = 3.2 (0.97)	m = 3.5 (1.07)	m = 4.1 (1.25)	3.90 (1.19)	3.90 (1.19)	3.80 (1.16)
	v = 0.8 (0.24)	v = 1.0 (0.30)	v = 0.9 (0.27)			
4	m = 6.1 (1.86)	m = 6.1 (1.86)	m = 6.1 (1.86)	5.19 (1.58)	4.84 (1.47)	4.48 (1.36)
5	m = 3.1 (0.94)	m = 3.2 (0.97)	m = 2.8 (0.85)	3.60 (1.09)	3.5 (1.07)	2.60 (0.79)
	v = 1.2 (0.37)	v = 1.2 (0.37)	v = 0.9 (0.27)			
6	m = 3.2 (0.97)	m = 3.5 (1.07)	m = 4.1 (1.25)	3.60 (1.09)	3.92 (1.19)	3.82 (1.16)
	v = 0.8 (0.24)	v = 1.0 (0.30)	v = 0.9 (0.27)			

[1]m - mean

[2]v - variance

SECTION VI

RESULTS AND DISCUSSION OF SIMULATION

Data obtained during the flight test program consisted of pilot opinion ratings and commentary ralating to the simulated environment, aircraft handling quality and data relating to the physical environment to which the pilot was exposed. The pilot opinion rating, obtained through a questionnaire, were in the following form:

1. Realism of turbulence;
2. Correctness of relative amplitude of disturbances;
3. Patchy characteristics;
4. Frequency content;
5. Element of surprise;
6. Atmospheric conditions;
7. Handling quality ratings (Cooper-Harper); and
8. Pilot task performance error.

Since the flight experiment was conducted in two parts, the statistical analysis and other data will be presented separately. Figure and Table numbers with subscript A are the results of the constant altitude tracking task with no visual aid. In the same way subscript B denotes the results of the landing approach test program.

The pilot opinion ratings have been statistically analyzed and the results are presented in the following forms:

a) Mean and Standard Deviation: of pilot opinion ratings for each of the turbulences models (Figures 30A,B to 35A,B and 36A, 37A and 38B).

b) Correlation Matrix: Correlation among various physical

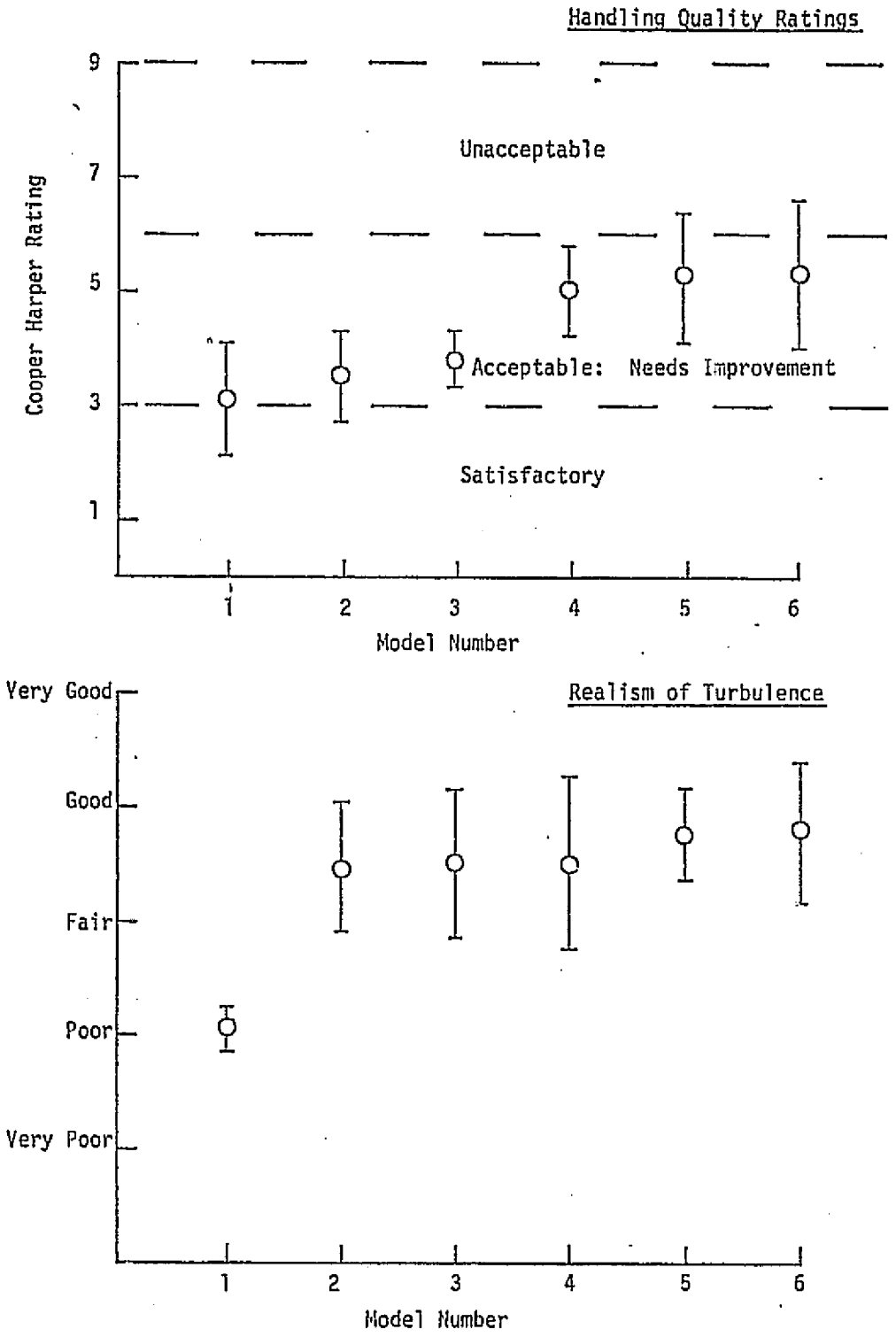

Figure 30A Pilot Opinion Ratings

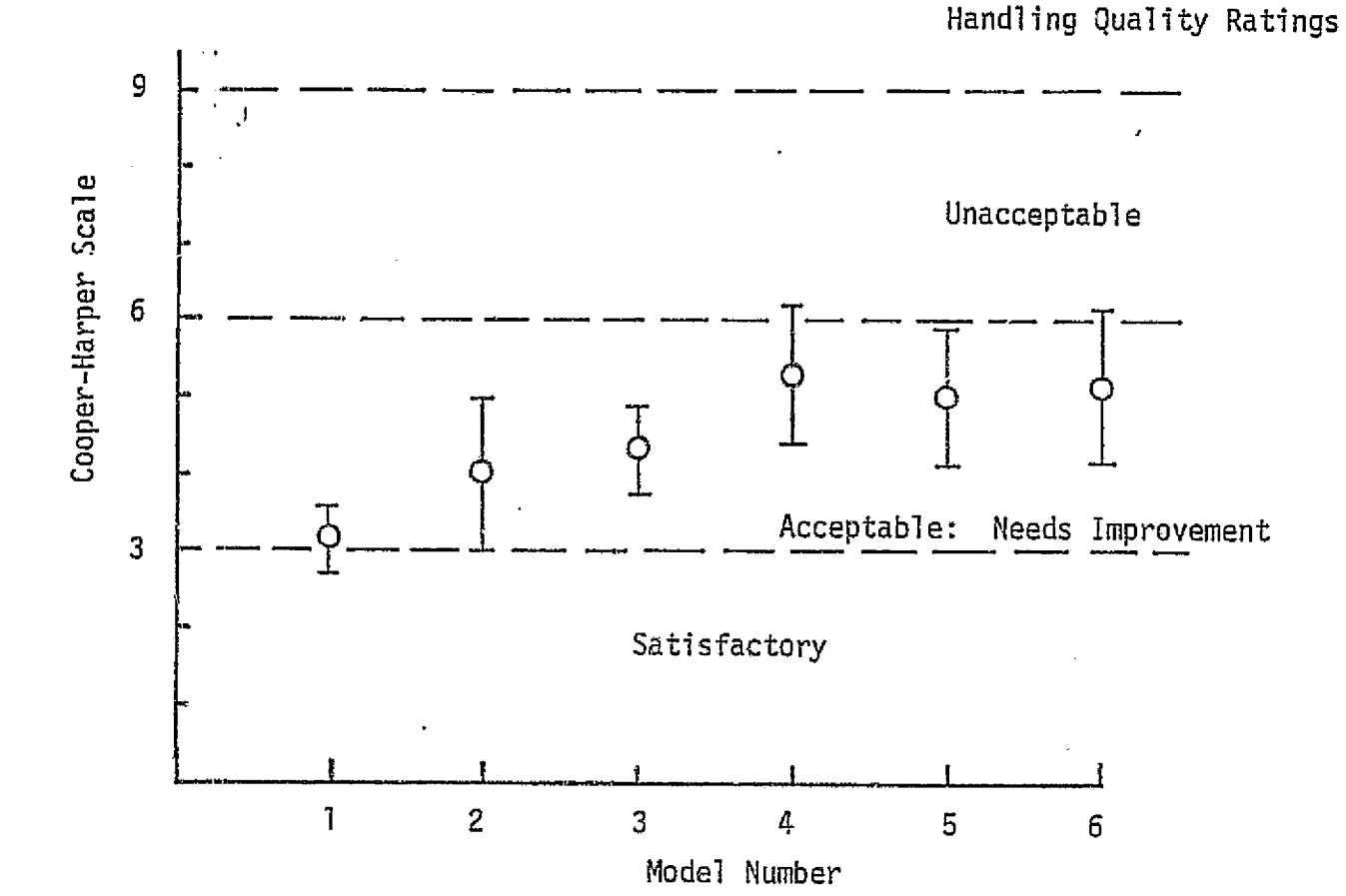

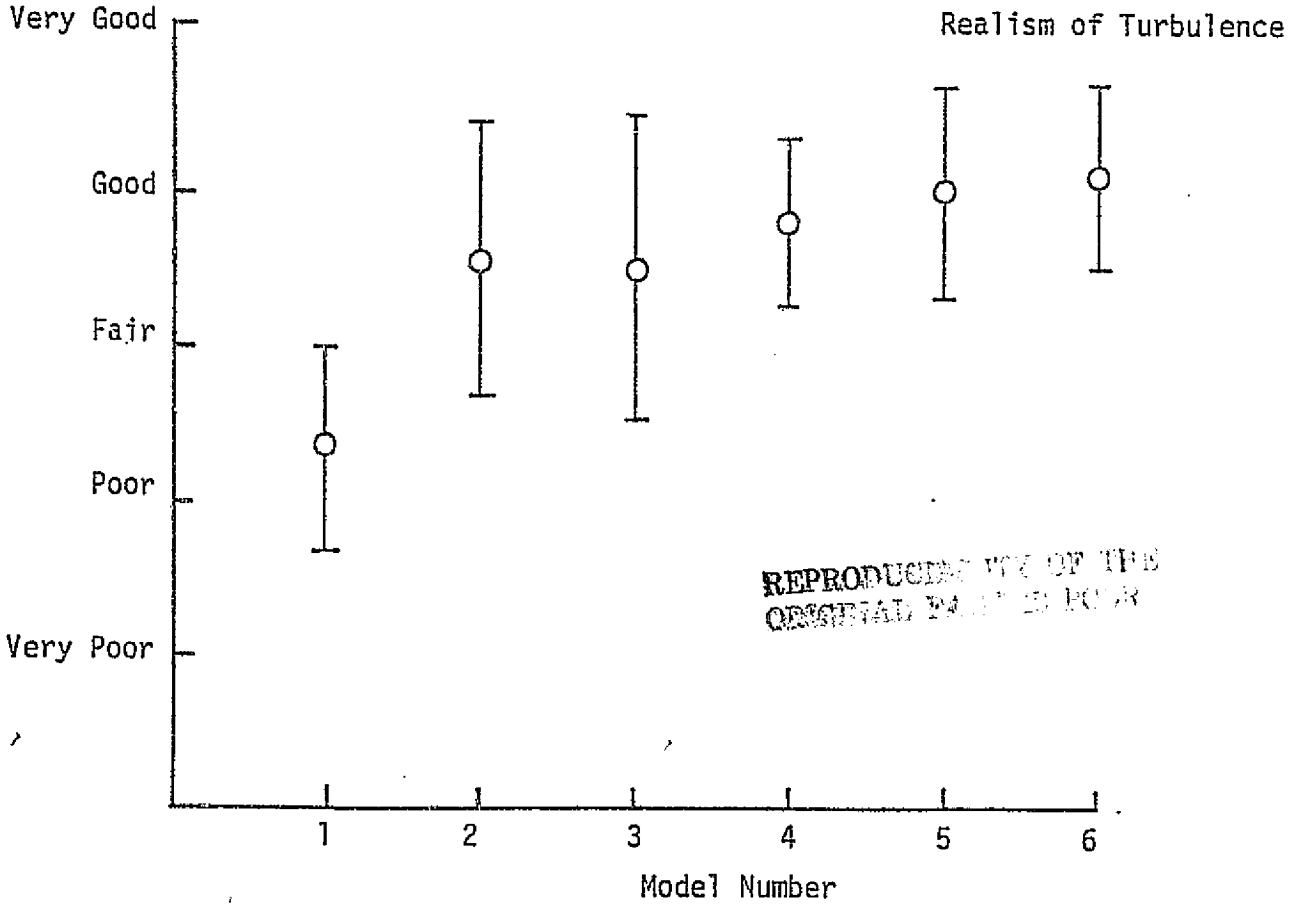

Figure 30B Pilot Opinion Ratings

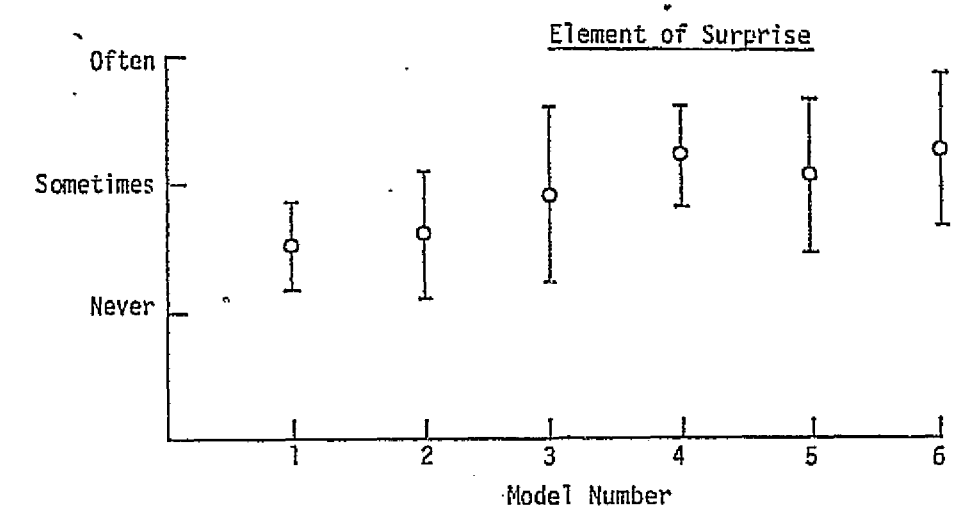

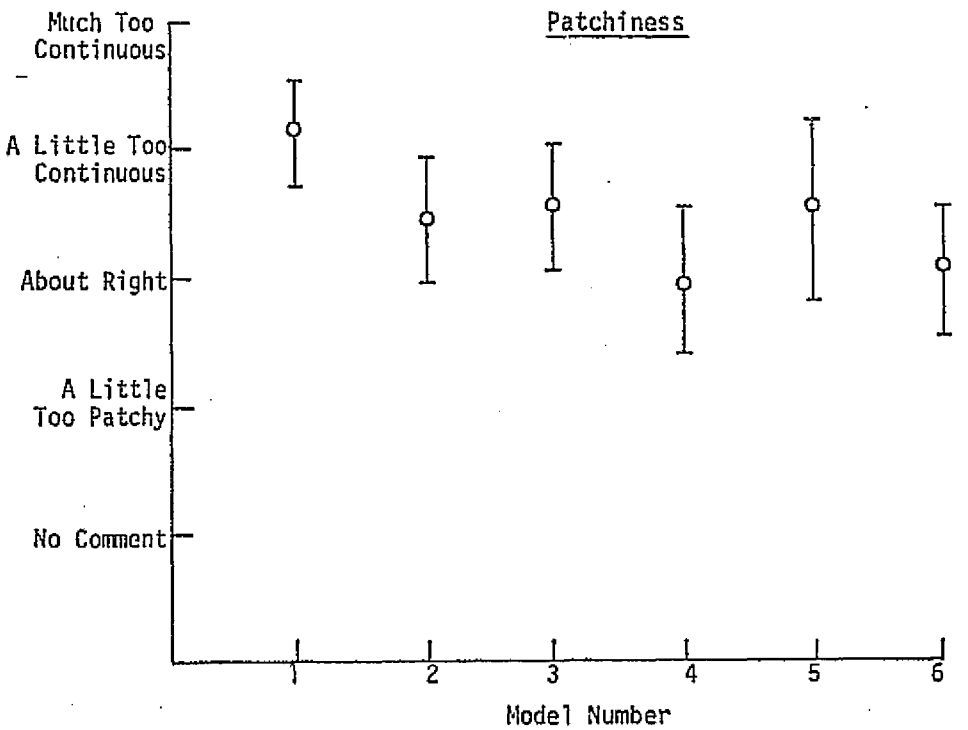

Figure 31A Pilot Opinion Ratings

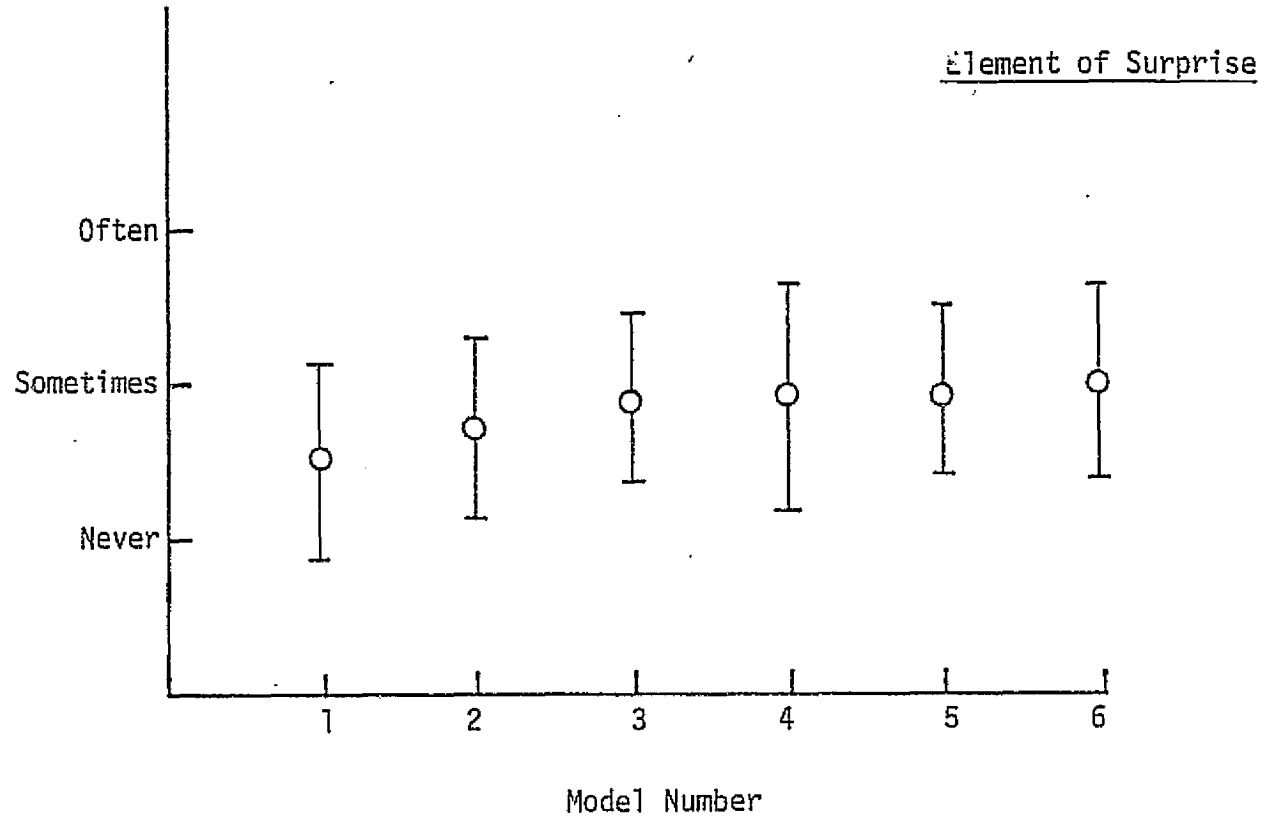

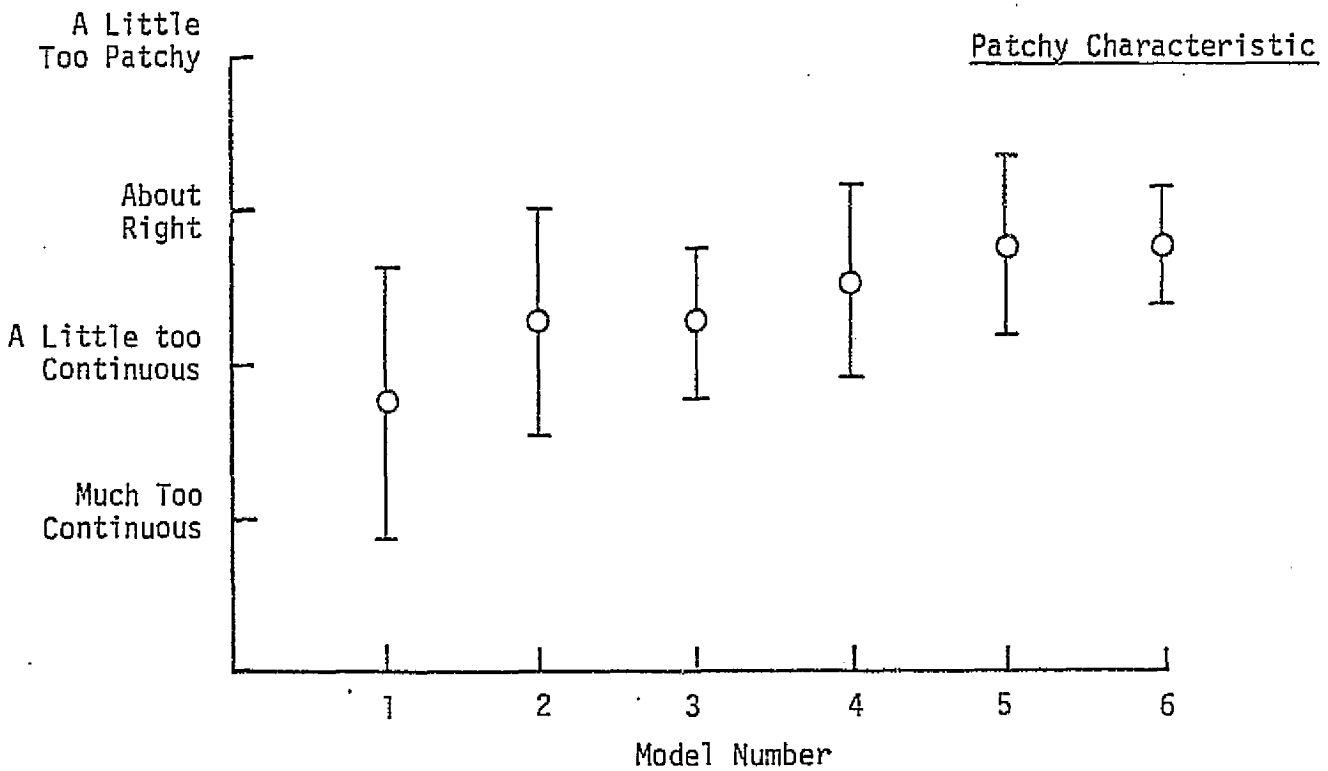

Figure 31B Pilot Opinion Rating

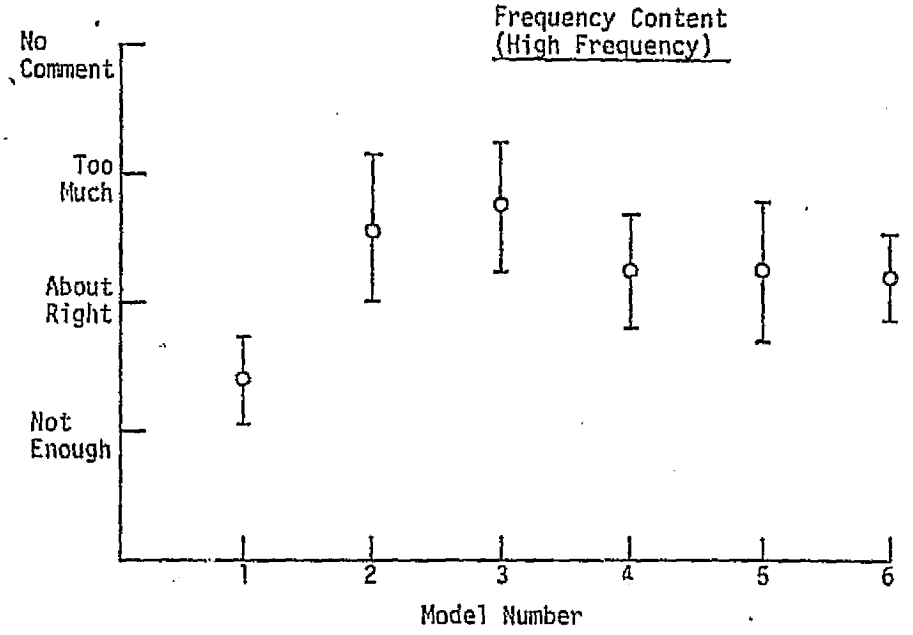

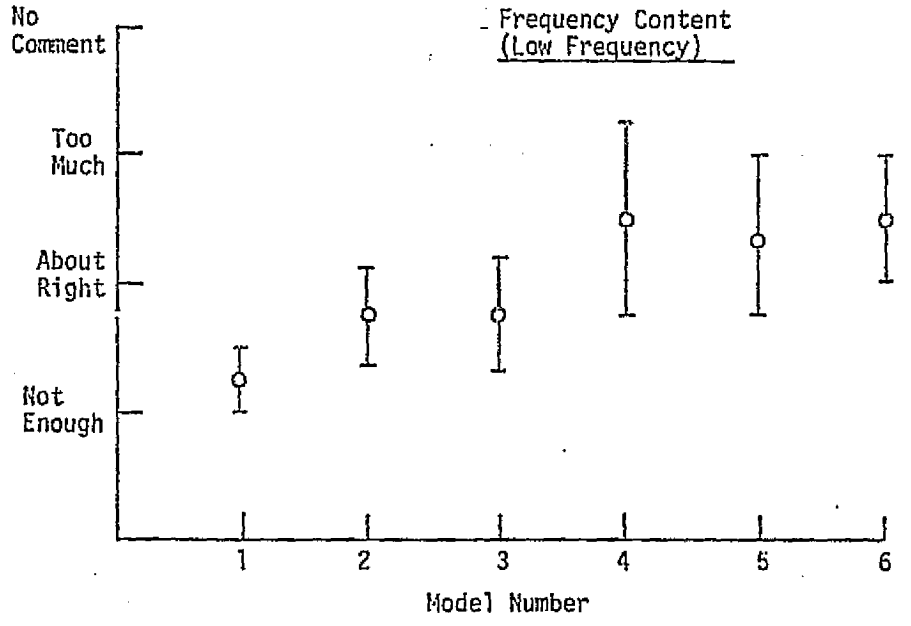

Figure 32A Pilot Opinion Ratings

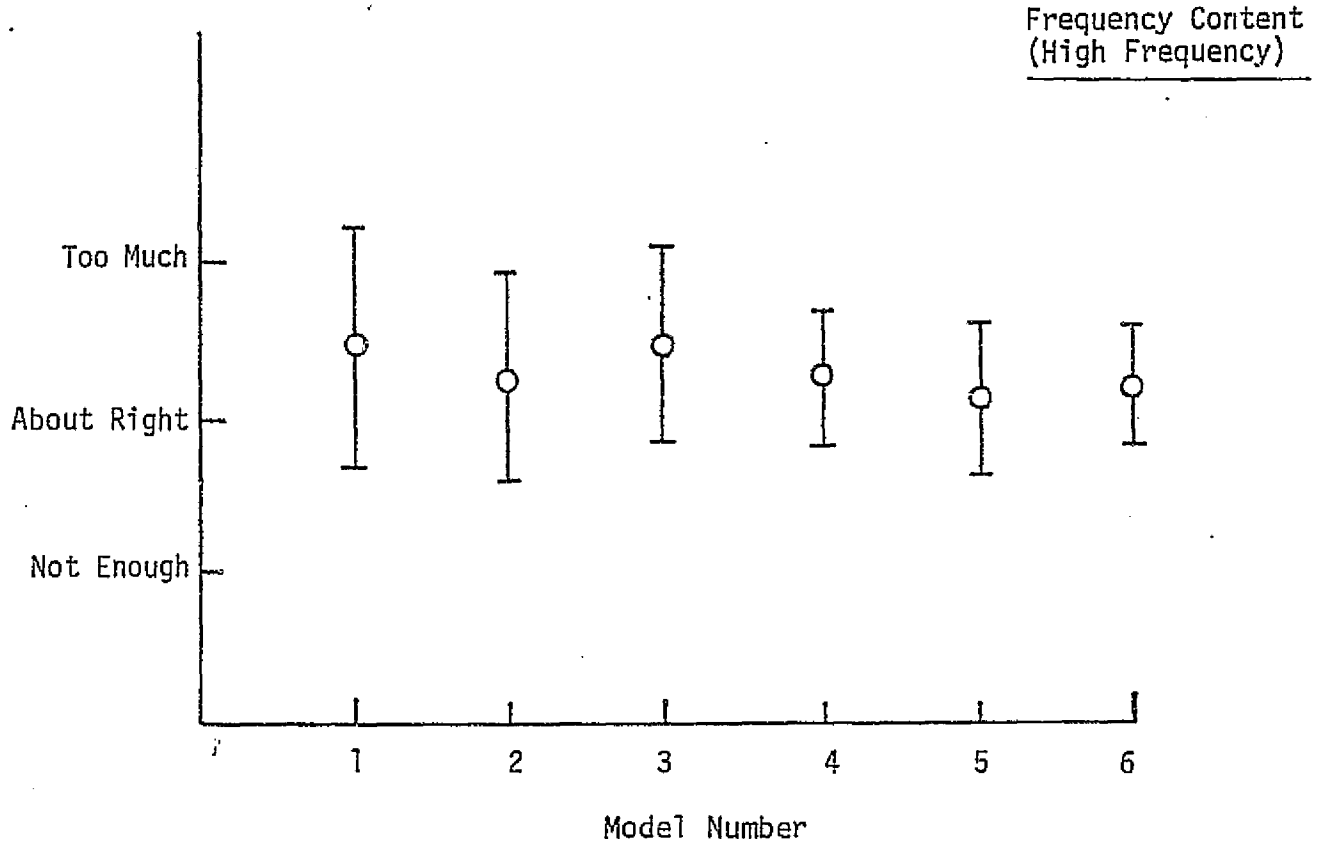

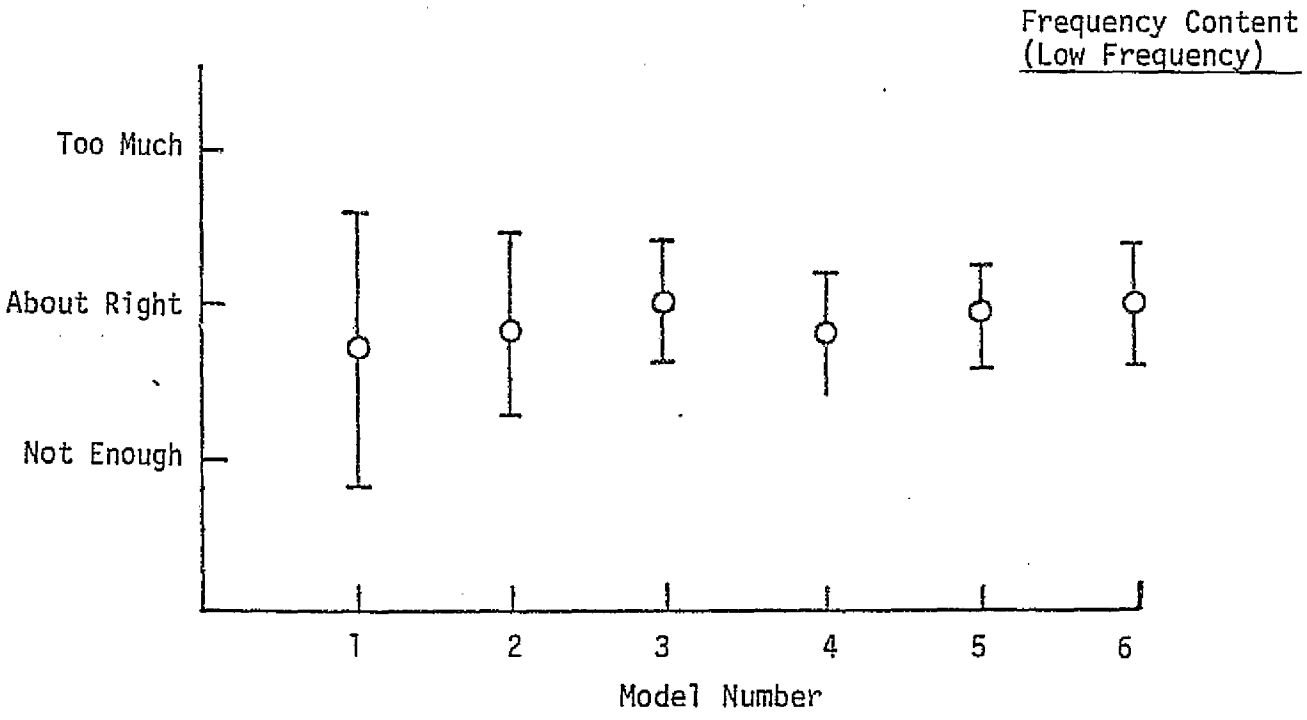

Figure 32B Pilot Opinion Ratings

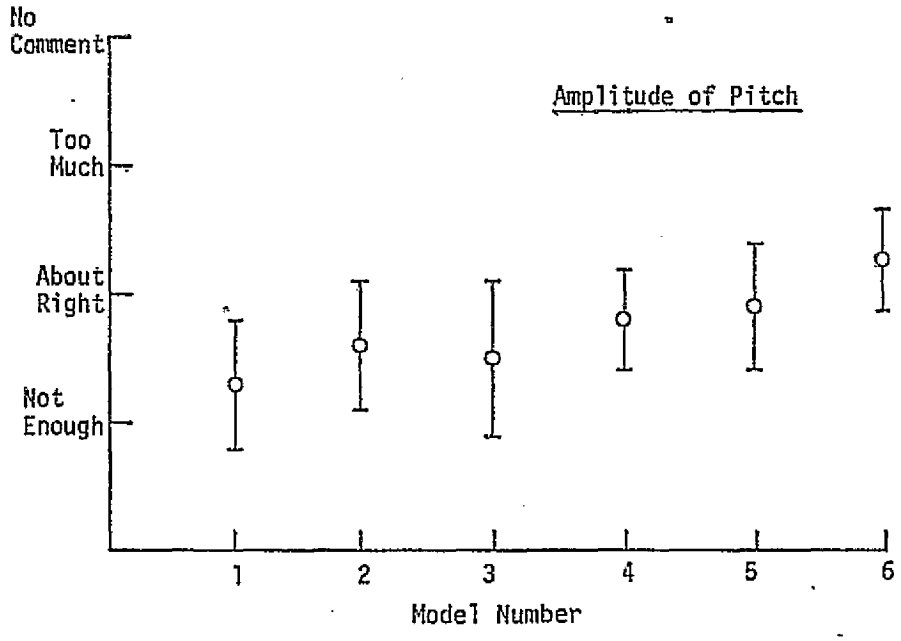

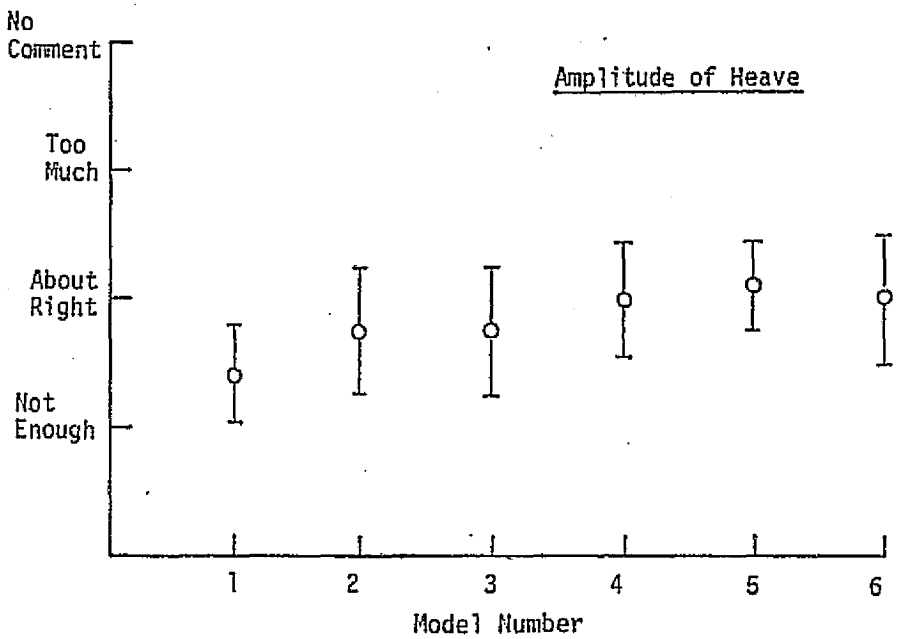

Figure 33A Pilot Opinion Ratings

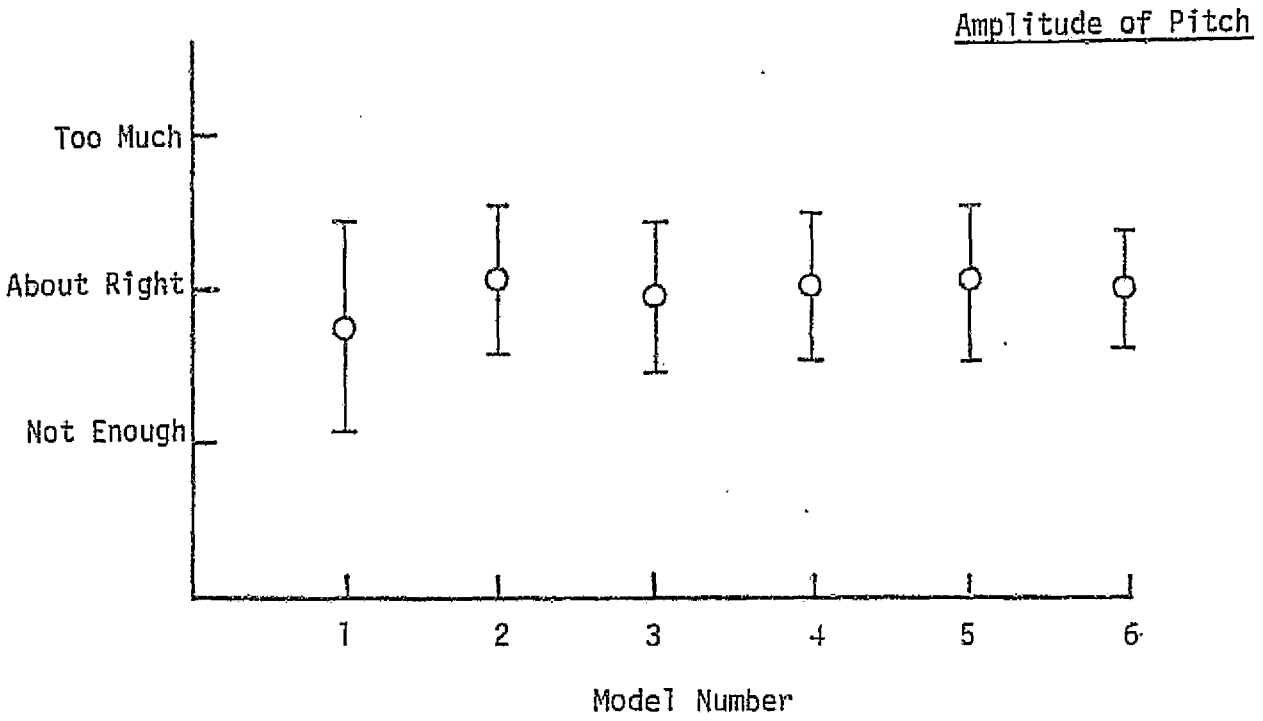

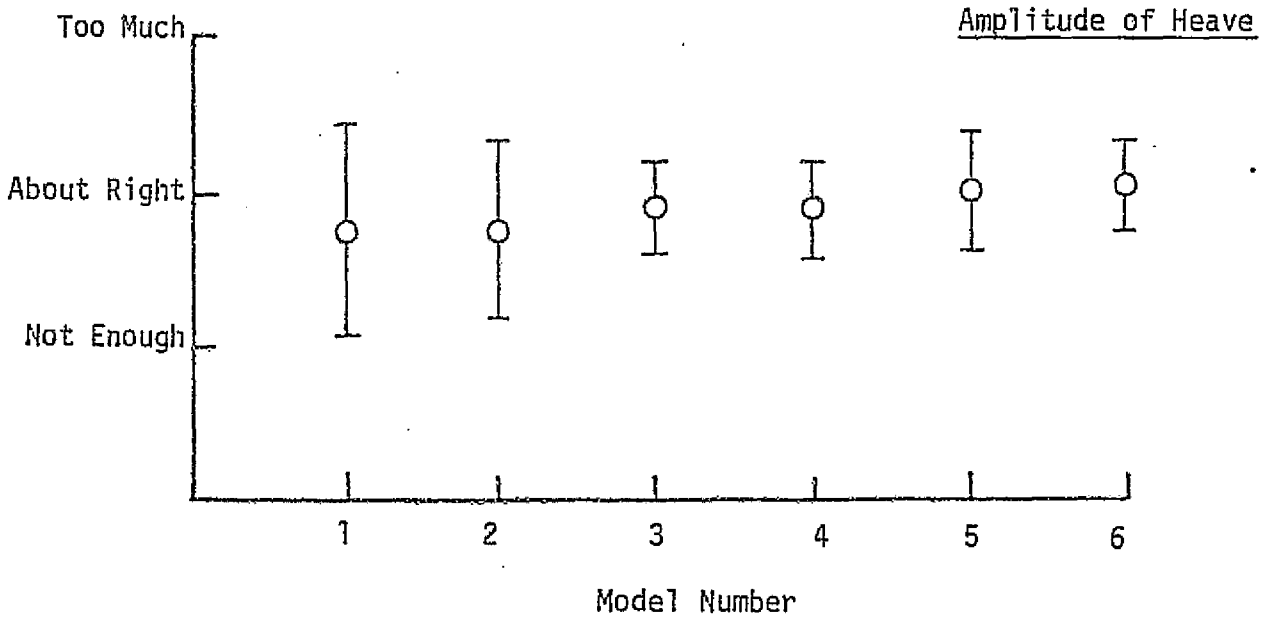

Figure 33B Pilot Opinion Ratings

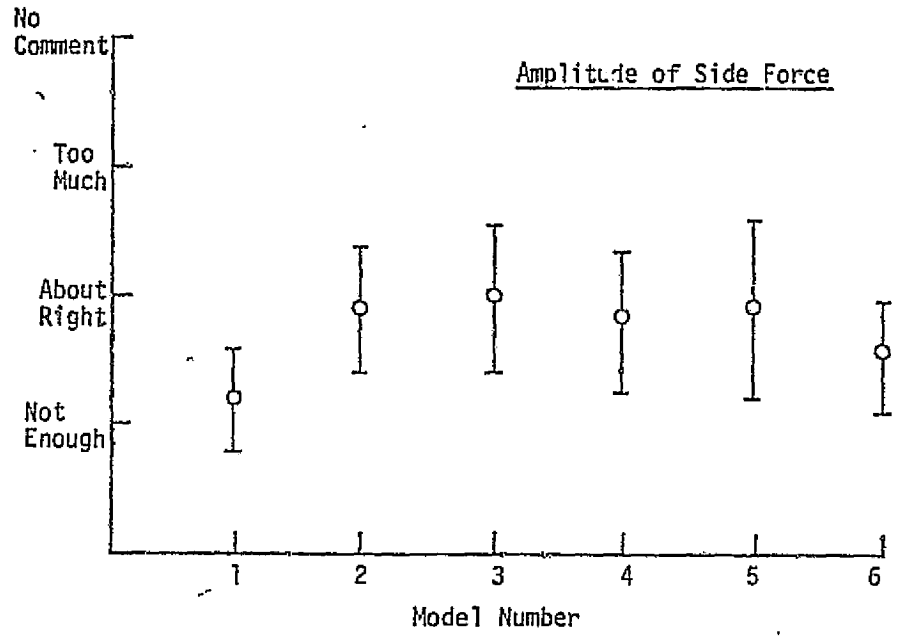

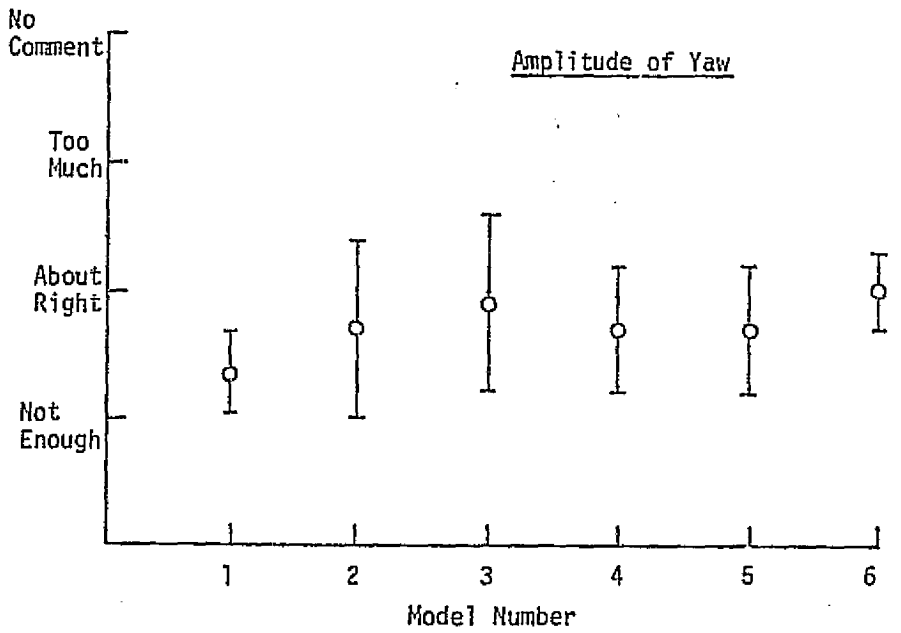

Figure 34A Pilot Opinion Ratings

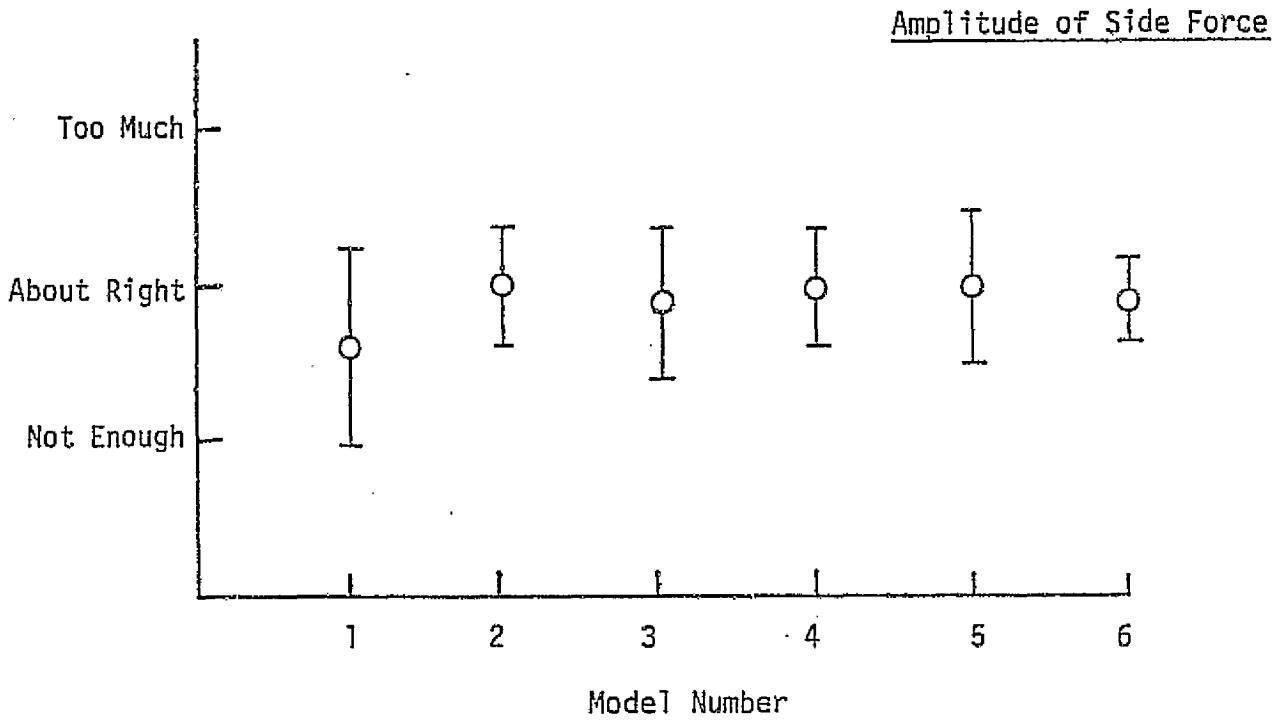

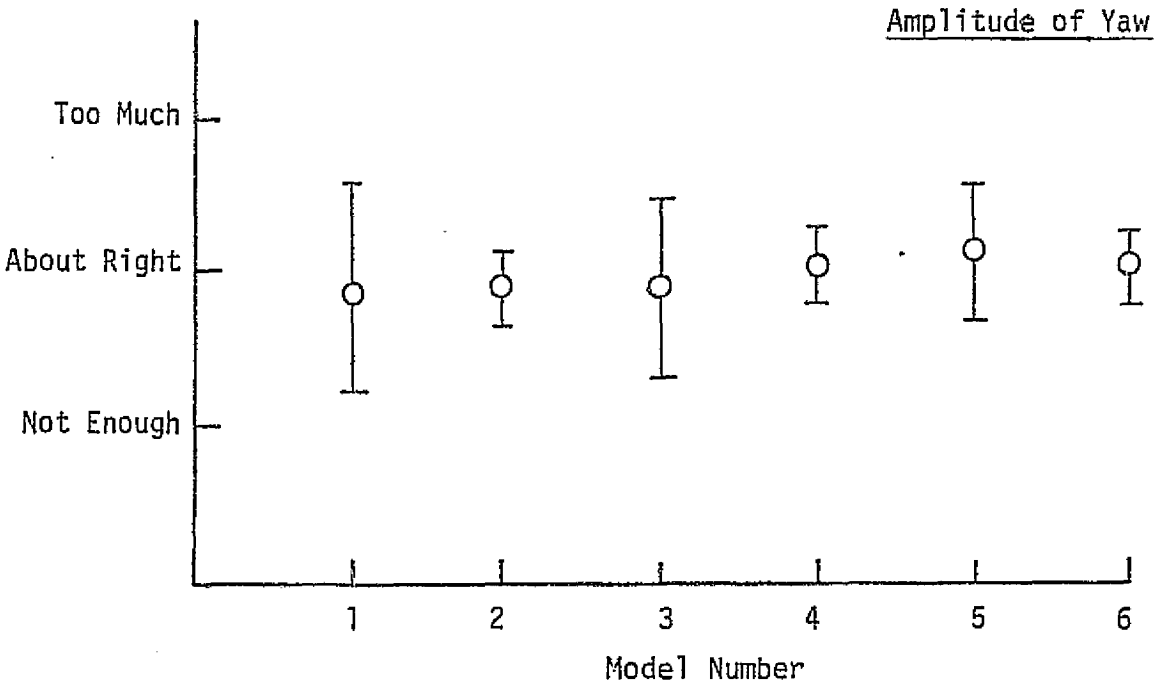

Figure 34B Pilot Opinion Ratings

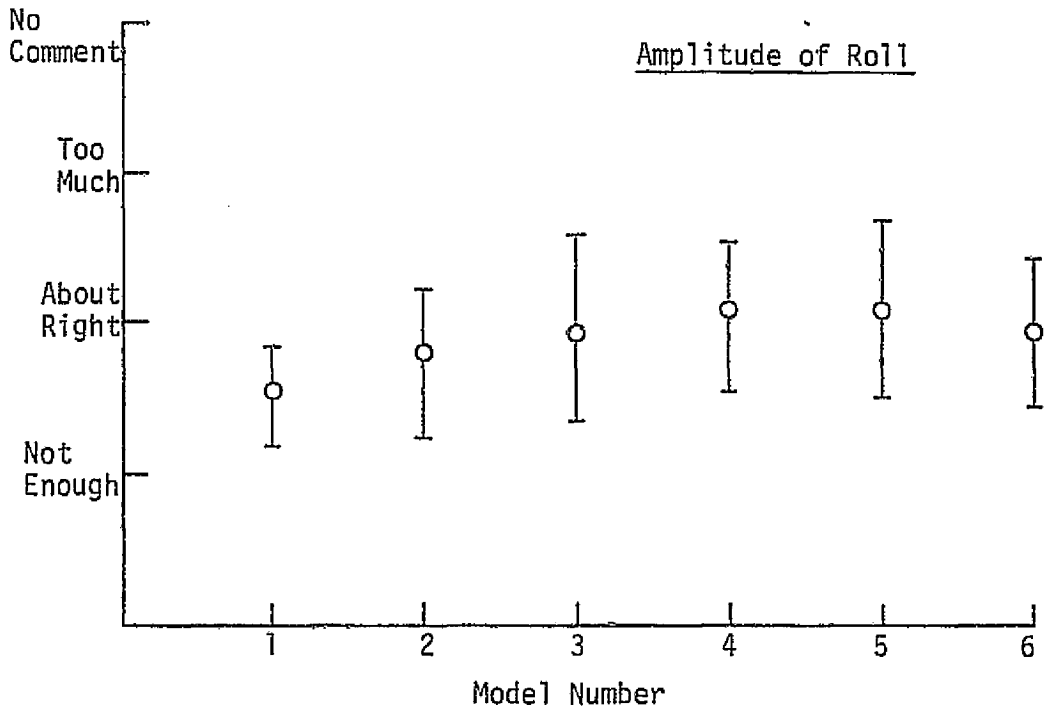

Figure 35A Pilot Opinion Ratings

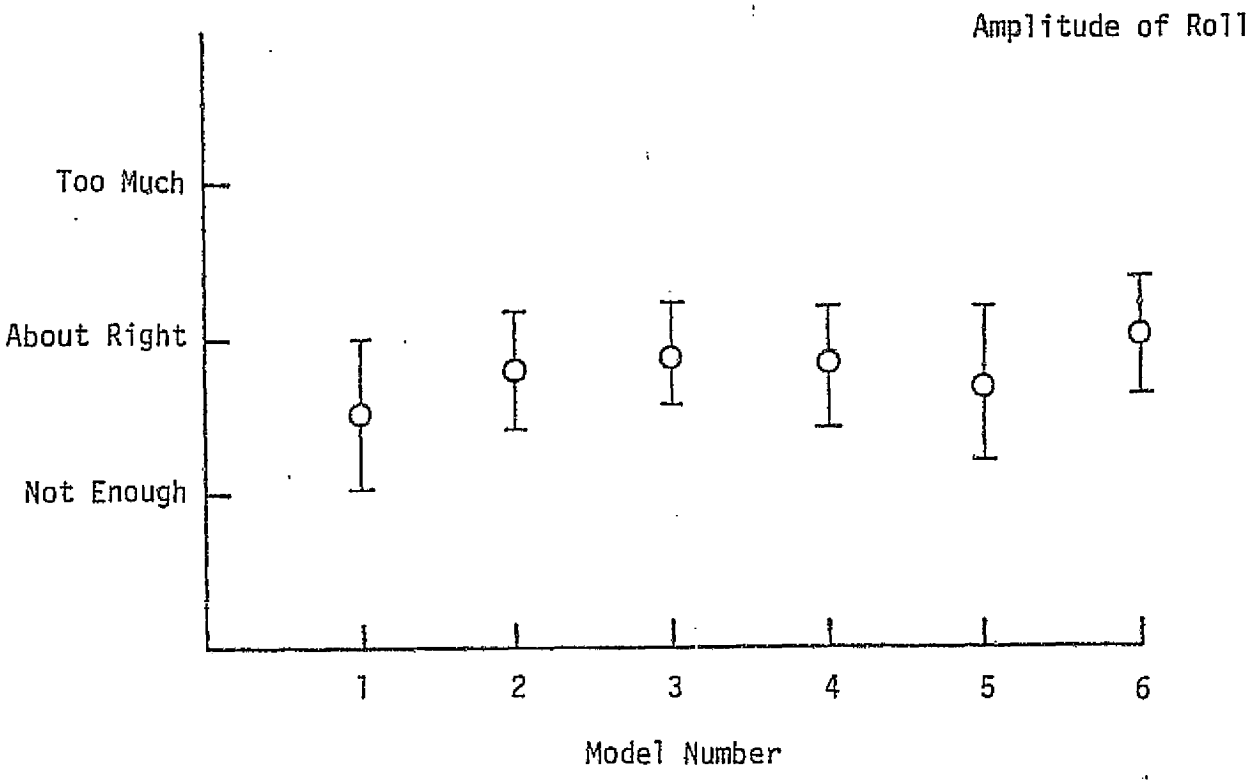

Figure 35B Pilot Opinion Ratings

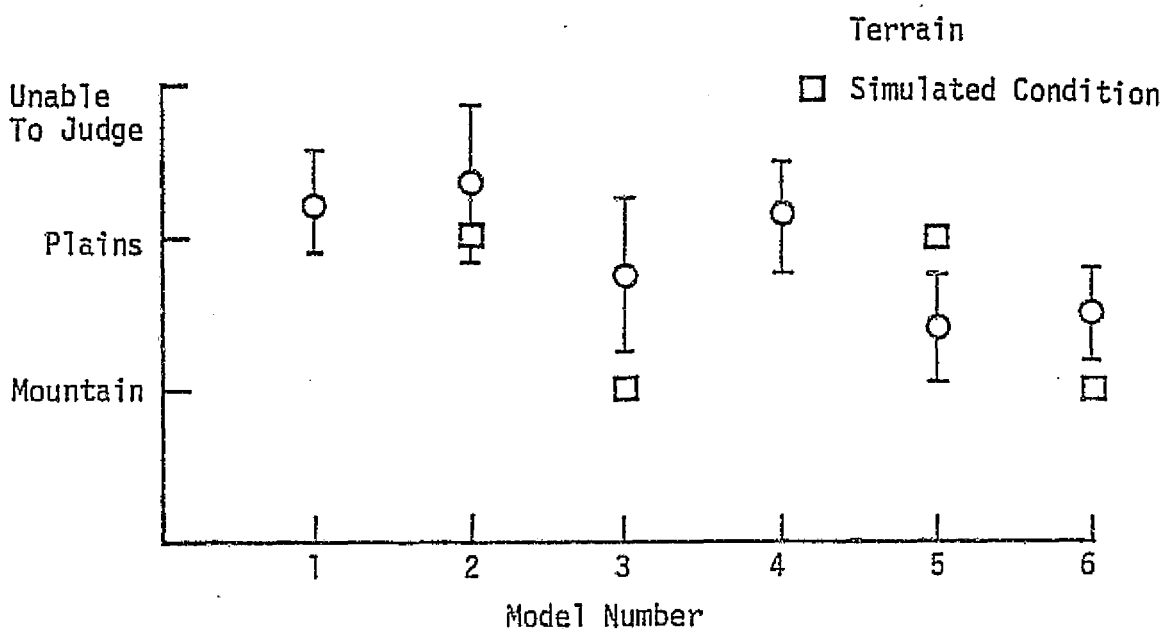

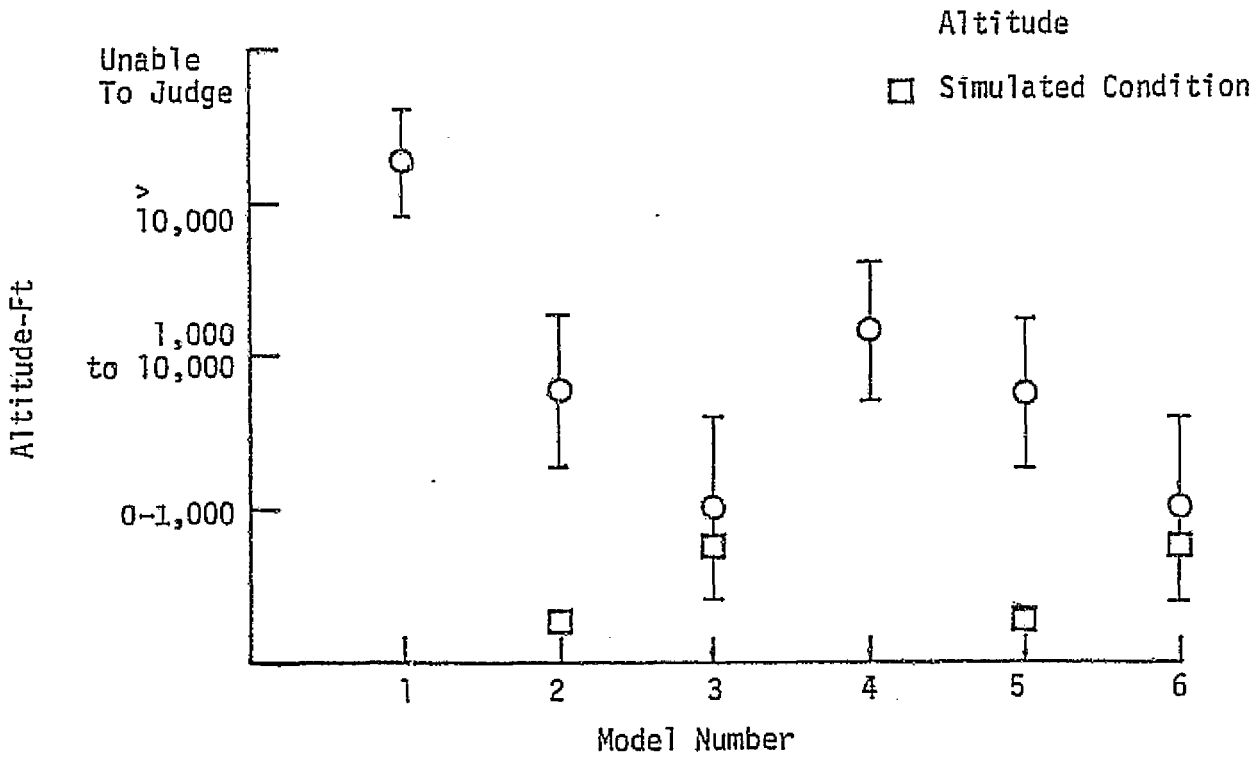

Figure 36A Atmospheric Condition

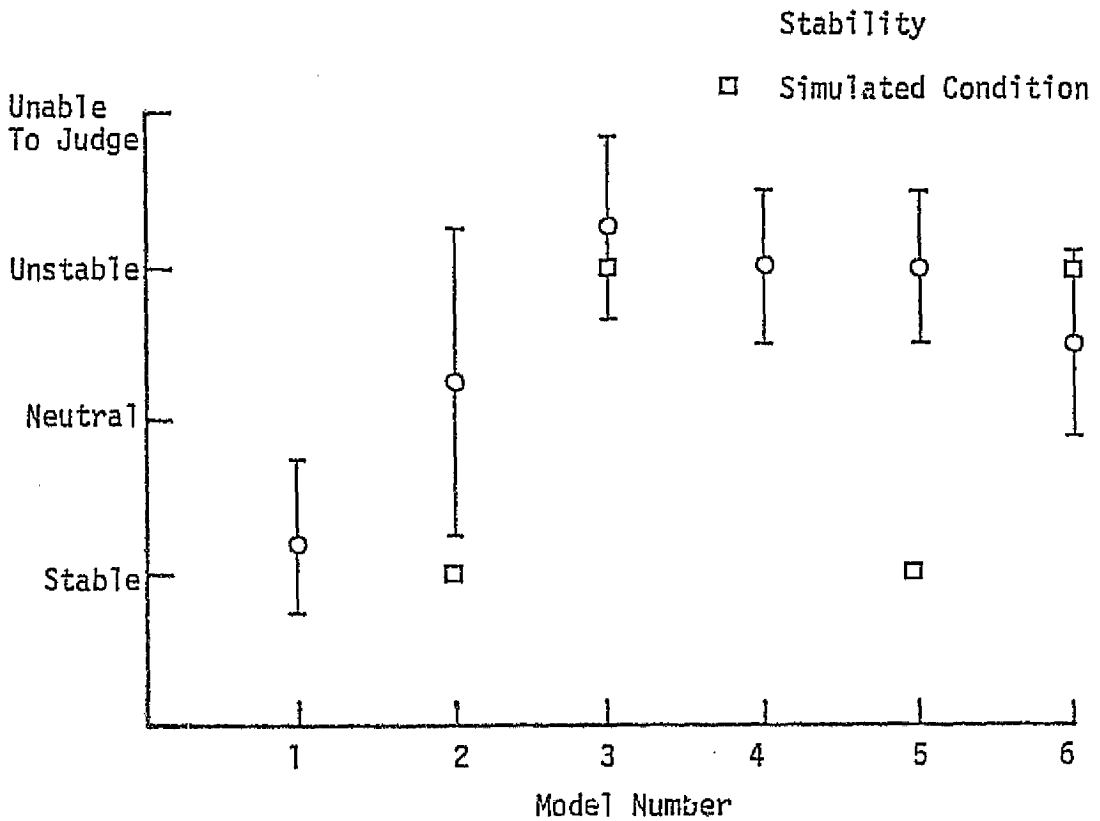

Figure 37A Atmospheric Condition

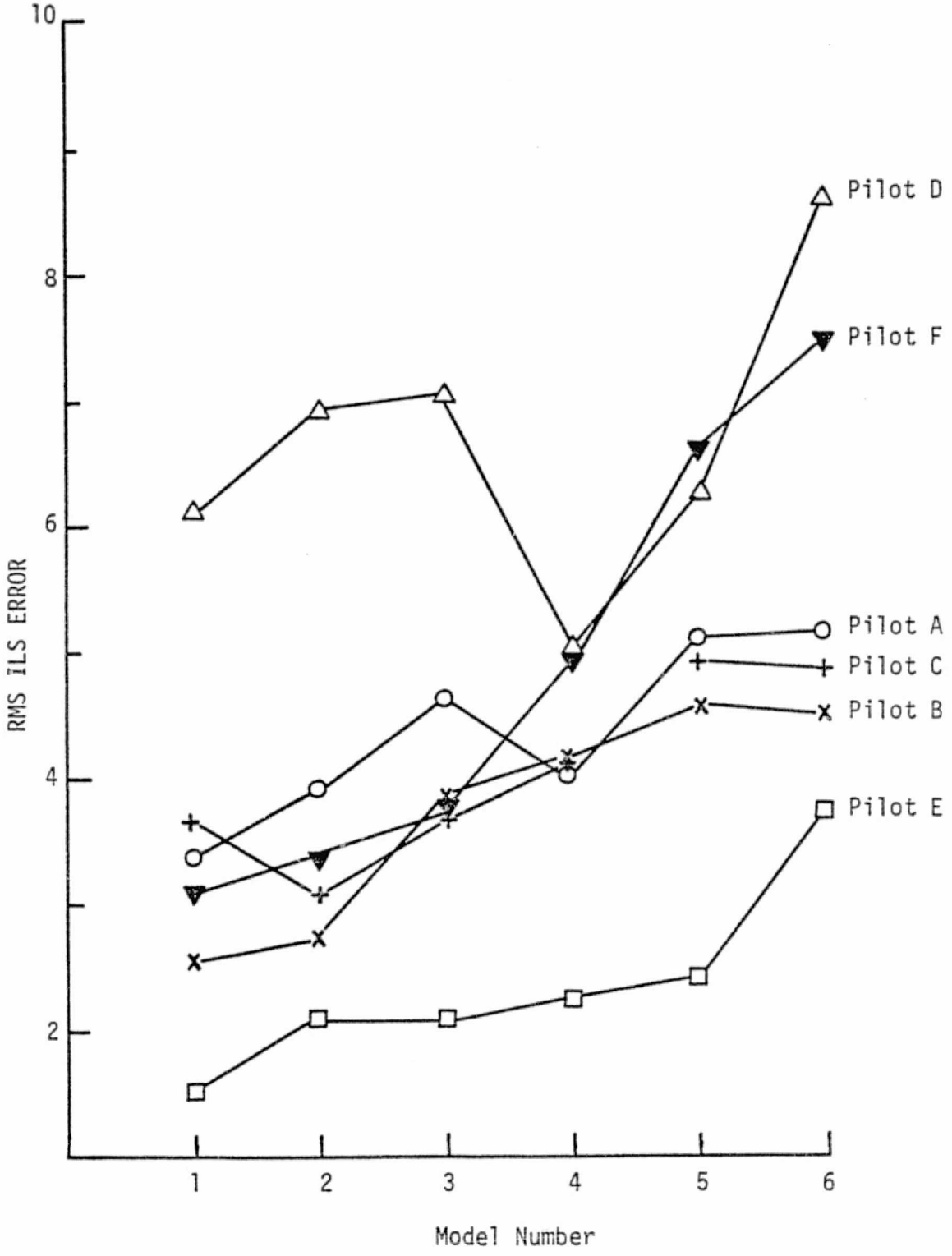

Figure 38B Pilot Error of Task Performance

characteristics of atmospheric turbulence is determined by

$$\gamma_{xy} = \frac{1}{n-1} \frac{\sum_{i=1}^{n} (x_i - \bar{x})(y_i - \bar{y})}{\sigma_x \sigma_y} \qquad (6.1.1)$$

where

γ_{xy} correlation between x and y

$\bar{x}, \bar{y}$ mean of x,y

σ_x, σ_y standard deviation of x,y

n number of observations.

The correlation matrices are presented in Table 8A and 8B.

The following observations can be made from the statistical analyses of pilot opinion ratings:

1. Figures 30A and 30B present the pilot opinion ratings of handling quality and the realism of turbulence. It may be observed that at approximately the same rms intensity (see Table 7) of turbulence, the handling quality ratings transit from the satisfactory level, for a simple Gaussian model, to an unacceptable level for the more realistic and compositely structured VLI turbulence model. By comparing Figures 30A and 30B it may be observed that visual display did not significantly alter the trend.

2. Figures 31A and 31B depict the element of surprise and the patchiness ratings. The Gaussian model (Model 1) was found to be a little too continuous by almost all the pilots under both experimental

conditions. On the other hand, the Rayleigh model (Model 4) was rated "about right" as was the VLI model (Model 6).

3. Figures 32A and 32B present the frequency content (low and high) ratings. The Gaussian Model (Model 1) was poorly rated whereas the mean ratings of the Rayleigh (Model 4) and VLI (Models 5 and 6) turbulence models were in the range of "about right". In addition, the spread (standard deviation) in the pilot opinion ratings is greater during the visual landing approach task.

4. Figures 32A,B to 35A,B present amplitude of disturbances as perceived by the pilots. The ratings show a progressive improvement as the pilots are exposed to more sophisticated models (see Models 4, 5 and 6).

5. Figures 36A and 37A present the atmospheric condition observations in the form of terrain, altitude, and atmospheric stability. The primary purpose of evaluating these was to determine how sensitive the pilots were to changes in atmospheric condition. Most pilots, when exposed to the six turbulance models, thought they were flying over level plains. On the altitude rating, the pilots flying the Gaussian model felt this turbulence was typical of altitude greater than 10,000 feet whereas they consistently rated the other models as typical low altitude turbulence.

6. Figure 38B presents pilot estimates of task performance. This is a measure of how well a pilot performed in tracking the ILS. Here we observe that the pilots had a greater difficulty in tracking the ILS for the VLI models than the simple Gaussian model.

7. Table 8A and 8B present the correlation matrix for various

turbulence properties and aircraft handling qualities. Several important observations can be made from these symmetric matrices. From Table 8A (Level flight), the realism of turbulence is highly correlated with patchiness (0.58), element of surprise (-0.63), and frequency content (0.52). This shows that in the opinion of pilots, the realism of a turbulence model is closely linked to the physical properties of real atmosphere. In addition, the high correlation between handling qualities and realism (0.74) indicates that the handling qualities are considerably worse for more realistic turbulence models. The low correlation between the patchiness characteristics and the intensity of turbulence (0.07) shows that the non-Gaussian patchiness characteristics cannot be induced by simply chosing a higher level of intensity (rms). On the other hand patchiness is correlated to frequency content (0.45) and handling quality. Table 8B (the second part of the experiment) shows the same trend. Here pilot error is highly correlated with handling quality, and patchiness.

TABLE 8A

CORRELATION MATRIX

	Turbulence Intensity	Realism	Patchiness	Frequency Content	Element of Surprise	Handling Quality
Turbulence Intensity	1.0	0.36	0.07	-0.16	0.54	0.27
Realism	0.36	1.0	0.58	0.52	-0.63	0.74
Patchiness	0.07	0.58	1.0	0.45	0.39	0.50
Frequency Content	-0.16	0.52	0.45	1.0	0.23	0.63
Element of Surprise	0.54	-0.63	0.39	0.23	1.0	-0.02
Handling Quality	0.27	0.74	0.50	0.63	-0.02	1.0

TABLE 8B

CORRELATION MATRIX

	Turbulence Intensity	Realism	Patchiness	Frequency Content	Element of Surprise	Handling Quality	Pilot Error
Turbulence Intensity	1.0	0.41	0.21	0.18	0.27	0.31	.43
Realism	0.41	1.0	0.60	0.49	0.36	0.70	.38
Patchiness	0.21	0.60	1.0	0.46	0.38	0.47	.54
Frequency Content	0.18	0.49	0.46	1.0	0.31	0.66	0.11
Element of Surprise	0.27	0.36	0.38	.31	1.0	0.31	0.16
Handling Quality	0.31	0.70	0.47	.66	0.31	1.0	.68
Pilot Error	0.43	0.38	0.54	.11	0.16	0.68	1.0

SECTION VII

CONCLUSIONS

This report has described several proposed turbulence models for producing artificial turbulence time histories which match the desired statistical properties of real atmosphere better than the presently-used simulation techniques. The use of these models gives improved realism and accuracy in piloted simulator studies of handling qualities as affected by atmospheric turbulence.

From the analytical study of the time histories generated by these models, and their comparison with real atmospheric turbulence, the following conclusions can be drawn:

a) Turbulence simulated by the VLI gust models adequately matches the probability distribution (fourth and sixth normalized moments, probability density, and cumulative probability) of real atmospheric turbulence; and hence, presents an improved representation of atmospheric turbulence.

b) Frequency content and the patchy characteristics of real turbulence can be closely matched.

c) The proposed turbulence models (VLI) can flexibly accommodate changes in atmospheric conditions characterized by terrain, altitude, and atmospheric stability. This flexibility is not provided by any of the presently-used techniques.

d) The mechanization of the proposed models on a motion-base simulator is easy and inexpensive computationally because these models utilize only three linear filters for the entire simulation.

The time histories derived from turbulence models and the commonly used Gaussian model, were employed in a flight simulator experiment to determine the extent of pilot sensitivity to realism of various turbulence models and to evaluate the effects of turbulence on aircraft handling qualities. The principal conclusions drawn from the flight simulator study are:

a) As expected from the analytical study, the pilot opinion ratings show a considerable improvement of turbulence properties (realism, patchiness, frequency content, etc.) over the most commonly used Gaussian turbulence model.

b) Aircraft handling quality and pilot task performance are critically affected by low altitude clear air turbulence. Realistic turbulence models present greater difficulty in controlling the aircraft than simple Gaussian model.

c) The correlation coefficient between the handling quality and the realism of turbulence is 0.74. This high correlation indicates that the handling qualities are considerably worse for more realistic turbulence models.

d) From the flight test results of this program, it is apparent that the pilot's ability to handle the airplane in a turbulent environment not only depends on the rms intensity, but also the composition and the structure of turbulence. Pilots rated handling qualities in the

satisfactory range while flying in a turbulence environment simulated by a simple Gaussian model; whereas the handling quality ratings degraded while flying in a turbulence environment simulated by the VLI turbulence model of approximately the same intensity. In fact, the handling quality ratings monotonically degrade as the pilots encountered more complex and realistic turbulence models. It may be concluded, therefore, that handling quality studies, using motion-base simulators, are critically affected by the suitable choice of a realistic turbulence model in addition to the appropriate rms intensities of turbulence.

The tests were conducted in a simulated environment of a light general aviation STOL airplane. Caution should, therefore, be exercised in applying and extending the results to a general aircraft configuration.

REFERENCES

1. Gunter, D. E.; Jones, J. W.; and Monson, K. R.: Low Altitude Atmospheric Turbulence LO-LO-CAT Phases I and II. AST-TR-69-12, The Boeing Company, February 1969.

2. Atnip, F. K.: Turbulence at Low Altitude, Summary of the Results of LO-CO-CAT Phases I and II. Proceedings of Symposium on CAT and Its Detection, Plenum Press, 1969.

3. Elderkin, C. E.: Experimental Investigation of the Turbulence Structure in Lower Atmosphere. Battelle-Northwest Report 329, December 1966.

4. Chalk, C. R., et al.: Background Information and User Guide for MIL-F-8785B(ASG), Military Specification Flying Qualities of Piloted Airplanes. Technical Report AFFDL-TR-69-72, Air Force Flight Dynamics Laboratory, Air Force Systems Command, Wright Patterson Air Force Base, Ohio, August 1969.

5. Reeves, P. M., et al.: Development and Application of a Non Gaussian Atmosphere Turbulence Model for Use in Flight Simulators. NASA CR-2451, September 1974.

6. Kurkowski, R. L., et al.: Development of Turbulence and Wind Shear Models for Simulator Application. NASA SP-270, May 4-6, 1971.

7. Dutton, J. A., et al.: Statistical Properties of Turbulence at Kennedy Space Center for Aerospace Vehicles Design. NASA CR-1889, August 1971.

8. Jones, C. R.; and Jacobson, I. D.: Effects of Aircraft Design on STOL Ride Quality. STOL Program Technical Report 4035-103-75, University of Virginia, May 1975.

9. Parrish, Russell V., et al.: Motion Software for a Synergistic Six-degree of Freedom Motion Base. NASA TN-D-7350, December 1973.

10. Parrish, Russell V., et al.: Compensation Based on Linearized Analysis for a Six-degree of Freedom Motion Simulator. NASA TN-D-7349, November 1973.

11. Cooper, G. E.; and Harper, R. P., Jr.: The Use of Pilot Rating in the Evaluation of Aircraft Handling Qualities. NASA TN-D-5153, April 1969.

APPENDIX A

REVIEW OF BASIC DEFINITIONS (5)

Stationarity: A random process is stationary if its statistical properties are not dependent on the time of their measurement. One could, for example, collect an infinite number of time histories, called an ensemble, which are representative of the process. If one takes an average across the ensemble, and if these averages are not a function of time, the process is stationary.

Homogeneity: A random process is homogeneous if its statistical properties are independent of position.

Ergodicity: In turbulence measurements it is impossible to obtain an ensemble from atmospheric measurements. Thus it is necessary to use time averages to get statistical information. If such a time average yields the same statistical properties as the ensemble average, the process is called ergodic.

Mean Value: The mean value of a random variable, u, of an ergodic random process is given by

$$\overline{u} = \underset{T\to\infty}{\text{Lim}} \frac{1}{2T} \int_{-T}^{T} u(t)dt \qquad (A.1)$$

In practice the limit is not required and $\overline{u}$ can be approximated by

$$u \simeq \frac{1}{T} \int_{0}^{T} u(t)dt, \text{ for T large.} \qquad (A.2)$$

This approximate representation is especially useful for processes such

as turbulence. However, the time interval T must be large enough so that the average approaches the asymptotic value one would obtain for a stationary process.

Variance: The variance of u is defined as

$$\sigma_u^2 = \underset{T\to\infty}{\text{Lim}} \frac{1}{2T} \int_{-T}^{T} [(u(t) - \bar{u})^2]dt. \qquad (A.3)$$

As before in practical applications the variance can be approximated by

$$\sigma_u^2 \approx \frac{1}{T} \int_0^T [u(t) - \bar{u}]^2 dt, \text{ for sufficiently large T.} \qquad (A.4)$$

Standard Deviation (Root Mean Square): The standard deviation is defined as the square root of the variance.

Normalized Central Moment: The n^{th} normalized central moment, M_n, of a random process, u(t), is

$$M_n = \underset{T\to\infty}{\text{Lim}} \frac{1}{2T} \int_{-T}^{T} \left[\frac{u(t) - \bar{u}}{\sigma_u}\right]^n dt \qquad n = 1,2,3... \qquad (A.5)$$

which can be approximated by

$$M_n \approx \frac{1}{T} \int_0^T \left[\frac{u(t) - \bar{u}}{\sigma_u}\right]^n dt \qquad n = 1,2,3... \qquad (A.6)$$

Cumulative Probability Distribution: The cumulative probability distribution of u(t), $P_u(x)$ is defined as the probability that $u \leq x$.

Probability Density Distribution: Probability density distribution of $u(t)$, $P_u(x)$ is defined as the probability that

$$x < u \leq x + dx.$$

Gaussian Probability Density Distribution: If a random variable, $u(t)$, is Gaussian distributed its probability density is given by

$$P_u(x) = \frac{1}{\sigma_u \sqrt{2\pi}} \exp \left[- \frac{1}{2} \left(\frac{x - \bar{u}}{\sigma_u} \right)^2 \right] \tag{A.7}$$

Rayleigh Distribution: Another probability density of interest is the Rayleigh distribution defined as follows:

$$P(x) = \frac{x}{c^2} \exp \left(- \frac{1}{2} \frac{x^2}{c^2} \right) \tag{A.8}$$

where c^2 is one half the expected value of the random variable x or

$$c^2 = \frac{1}{2} E(x) = \frac{1}{2} \int_0^\infty x P_x(x) dx \tag{A.9}$$

Cross Correlation Function: The cross correlation function of two random processes $u(t)$, $w(t)$ is defined as

$$R_{uw}(\tau) = \lim_{T \to \infty} \frac{1}{2T} \int_{-T}^{T} u(t) w(t + \tau) dt \tag{A.10}$$

correlations are the measures of the predictability of a signal at some future time $(t + \tau)$ based on the knowledge of a signal at time t.

Autocorrelation Function: The autocorrelation function is a special case of the cross correlation function defined above in which $w(t) = u(t)$, such that,

$$R_{uu}(\tau) = \underset{T\to\infty}{\text{Lim}} \frac{1}{2T} \int_{-T}^{T} u(t)u(t+\tau)dt. \tag{A.11}$$

Integral Scale Length: A statistical parameter of special importance in atmospheric turbulence is the integral scale length,

$$L_u = \frac{u_0}{\sigma_u^2} \int_{-\infty}^{\infty} R_{uu}(\tau)d\tau, \tag{A.12}$$

where u_0 is the reference steady state flight speed of the aircraft flying through turbulence. Scale length is an approximate measure of the distance an aircraft flies through turbulence.

Cross Spectral Density: The cross spectral density of two random processes $u(t)$ and $w(t)$ is defined as the Fourier transform of their cross correlation

$$\Phi_{uw}(f) = \int_{-\infty}^{\infty} R_{uw}(\tau)\exp(-i2\pi f\tau)d\tau \ , \tag{A.13}$$

where f is frequency.

Power Spectral Density: The power spectral density, PSD, of a random process is the Fourier transform of its autocorrelation function, or

$$\phi_u(f) = \int_{-\infty}^{\infty} R_{uu}(\tau)\exp(i2\pi f\tau)d\tau. \qquad (A.14)$$

The PSD can be interpreted physically as the average contribution to the variable σ_u^2 from the frequency component f. Thus,

$$\sigma_u^2 = \int_{-\infty}^{\infty} \phi_u(f)df. \qquad (A.15)$$

White Noise: White noise is a random process for which the PSD is a constant independent of frequency. That is,

$$\phi_u(f) = \phi_0 = \text{constant}. \qquad (A.16)$$

APPENDIX B

FLIGHT QUESTIONNAIRE

Flight Number _____ Date _____

Pilot: _____

1. Turbulence Intensity:

   Light ____ Moderate ____ Severe ____ Extreme ____

2. Realism of Turbulence:

   Very Good ____ Good ____ Fair ____ Poor ____ Very Poor ____

3. Correctness of Relative Amplitude of Disturbances:

	Not Enough	About Right	Too Much	No Comments
Roll	____	____	____	____
Pitch	____	____	____	____
Yaw	____	____	____	____
Heave	____	____	____	____
Side Force	____	____	____	____

4. Patchy Characteristics (Variation of Intensity Bursts)

   Much Too Continuous ___ A Little Too Continuous ___ About Right ___

   A Little Too Patchy ___ No Comments ___

5. Frequency Contents of Turbulence:

	Not Enough	About Right	Too Much	No Comments
Low FRQ:	____	____	____	____
High FRQ:	____	____	____	____

6. Element of Surprise in the Simulated Turbulence Field:

   a. Quite Often ____ Sometimes ____ Never ____

   b. Realism of 6a:

      Very Good ____ Good ____ Fair ____ Poor ____ Very Poor ____

7. Atmospheric Conditions:

   a. Altitude: 0 - 1,000 Ft ____ 1,000 - 10,000 Ft ____

      Over 10,000 Ft ____ Unable to Judge ____

   b. Atmospheric Stability: Stable ____ Unstable ____

      Neutral ____ Unable to Judge ____

   c. Terrain: Mountains ____ Plains ____ Unable to Judge ____

8. Pilot Estimate of the Work Load:

   Very Easy ____ Easy ____ Average ____ Difficult ____ Very Difficult ____

9. Pilot Estimate of Task Performance: (Integral Squared Error for ILS Tracking Task)

   Very Good ____ Good ____ Average ____ Poor ____ Very Poor ____

10. Realism of This Model Compared to Previously Flown Model:

    Very Good ____ Good ____ About the Same ____ Poor ____ Very Poor ____

11. Did You Observe a Repetitive Pattern in the Turbulence Field?

    Yes ____ No ____

12. Cooper-Harper Rating: _____

13. Additional Comments About Realism of Turbulence and Aircraft Simulation:

_____

_____

_____

_____

APPENDIX B
(Cont.)

PILOT EXPERIENCE

1. Name _____ Date _____

2. What Type of Flying Experience Have You Had?

   Military _____ Civil _____

3. Main Types of Aircrafts Flown: _____

   _____

4. Total Number of Hours Flown: _____

5. Hours of Instrument Flying: _____

6. Hours in Simulators: _____

7. Hours in VMS: _____

8. Hours in Twin Otter: _____

9. a. Estimate the % of Time Flown in Turbulence: _____

   b. Of This Time What % Was Flown in

Light Turbulence	Moderate Turbulence	Severe Turbulence	Extreme Turbulence
_____	_____	_____	_____

10. What Characteristic of Turbulence Interferes Most with Your Ability to Control the Aircraft? _____

    _____

11. Describe the Most Critical Case of Turbulence Encountered During Your Flying Experience:

    a. Day _____ Night _____

    b. Terrain: _____ Altitude: _____

c. Atmospheric Stability:

Stable _____ Neutral _____ Unstable _____ Unable to Judge _____

d. What Was the Task You Were Attempting Before Turbulence Was Encountered:

(e.g. ILS Approach, Cruise, etc.)_____

e. Any Additional Comments: _____